

**The Effect of Artificial Aging (*LTD*) on The Mechanical and
Optical Properties of Conventional and Translucent Zirconia
for Fixed Prosthodontics**

Aziz Ghanim Aziz Aziz

Submitted in accordance with the requirements for the degree of
Doctor of Philosophy

The University of Leeds
School of Dentistry

February 2018

© 2018 The University of Leeds and Aziz Ghanim Aziz Aziz

The candidate confirms that the work submitted is his own and that appropriate credit has been given where reference has been made to the work of others.

This copy has been supplied on the understanding that it is copyright material and that no quotation from the thesis may be published without proper acknowledgement

Acknowledgements

I would like to take this opportunity to express my endless gratitude to my primary supervisor Professor **David Wood**. He was not only the supervisor of my research, he was a great mentor who supported me throughout my PhD journey which was not an easy one due to the circumstances that I had during my study including the war back home in Iraq. I would like to thank him for encouraging my research and for allowing me to grow as a research scientist and for supporting me every time I presented my work in international conferences. I would have never ever asked about a supervisor better than him and I owe him a lot to the end of my life.

I would like to thank Dr's **Nigel Bubb** and **Paul Hyde** for supervising my research alongside Professor Wood. A special thanks go to Dr **Peter Rhodes** in the School of Design, University of Leeds for his generous contribution to my research and his endless support. My deep thanks to Dr **Neil Thomson** and **Ashley Stammers** in the School of Physics, University of Leeds for their help in using atomic force microscopy.

My brother **Ali Marie**, you are not just a friend you are a real brother without your support this work wouldn't be completed. I wish you all the best in your PhD journey.

This work is dedicated with a big thanks to my wife, **Semaa**, who kept me supported throughout this journey in spite of her illness. This wouldn't happen without you being here with me, looking after me and our kids.

To my mother and father who burnt their life to light ours; me and my siblings. No words can express the amount of love and respect that I have for both of you. I know how proud you will be of me after finishing this journey. To my lovely children **Sana** and **Zaid**, you are my strength and many thanks for being patient with me during this journey. I love you to the moon and back.

I would like to thank my colleagues in the School of Dentistry who were my second family. I would like to thank Dr **Asma Al-Taie** for her support. Many thanks to my dear friend Dr **Yasir Al-Anii** for his graphic designs which have enriched my thesis.

Abstract

In the last decade, zirconia has been of a great interest to dentists due to its superb mechanical and optical properties. At first, the use of zirconia was limited to fabrication of cores replacing the metal in crown construction. Nowadays, there is an increase in the trend of using monolithic 'full contour' translucent zirconia to overcome the problem of chipping of porcelain veneers and to overcome the limitation of using lithium disilicate in long span replacement. This has brought zirconia in direct contact with saliva and oral fluids and introduced the possibility of the material undergoing low temperature degradation.

This study aimed to investigate the effect of accelerated hydrothermal aging on the mechanical and optical properties of two conventional core and two full contour translucent zirconia materials, expected to be used by 90% of zirconia manufacturers globally.

Hydrothermal aging was carried out using an autoclave to simulate *in vivo* aging, using a specific protocol proposed by ISO 13356:2015 mimicking 15-20 years of clinical service of the material. Each of the four materials were tested before and after aging, including structural analysis which was carried out using XRD, SEM, FIB-SEM and AFM. Mechanical property investigations were carried out by measuring BFS and Vickers hardness. Optical properties were thoroughly investigated through measuring a range of translucency parameters and changes in colour before and after aging.

The results of this study showed that conventional core materials were less affected by hydrothermal aging in comparison to full contour translucent zirconia in terms of optical properties. All of the used materials showed clear colour changes after aging, however none of them showed significant changes in the mechanical properties even with more than 20% of t → m phase transformation in one of the translucent zirconia materials.

Within the limitation of this *in vitro* study, it can be concluded that full contour translucent zirconia can be used clinically with no concern about its mechanical and optical properties, however, further studies on the perception and acceptability for changes in the optical properties would be highly recommended.

Table of Contents

Acknowledgements	i
Abstract	ii
Table of Contents	iii
List of Tables	vii
List of Figures	viii
List of Abbreviations	xi
Chapter 1 Introduction	1
Chapter 2 Literature Review	4
2.1 Ceramic	4
2.2 Ceramics in Dentistry.....	4
2.3 Classification of dental ceramics.....	5
2.3.1 Glass Matrix Ceramics	6
2.3.1.1 Feldspathic	6
2.3.1.2 Synthetic	6
2.3.1.3 Glass infiltrated	7
2.3.2 Resin-Matrix Ceramics	8
2.3.2.1 Resin nanoceramic	8
2.3.2.2 Glass ceramic in a resin interpenetrating matrix	8
2.3.2.3 Zirconia-silica ceramic in a resin interpenetrating matrix	8
2.3.3 Polycrystalline ceramics	8
2.3.3.1 Alumina.....	9
2.3.3.2 Zirconia-toughened alumina and alumina-toughened zirconia	9
2.3.3.3 Stabilised zirconia	9
2.4 Zirconia.....	10
2.5 Crystallographic structure of zirconia.....	10
2.6 Zirconia for Medical purposes.....	11
2.7 Zirconia in dentistry.....	12
2.8 Challenges facing dental zirconia	13
2.9 Proposed Solutions for Delamination.....	14
2.10 Full Contour Zirconia (monolithic zirconia).....	16
2.11 Low Temperature Degradation (<i>LTD</i>)	19
2.12 Transformation toughening of zirconia.....	22

2.13 Mechanical Properties of Zirconia.....	22
2.13.1 Chemical composition	22
2.13.1.1 Colouring agents.....	22
2.13.1.2 Y ₂ O ₃	23
2.13.1.3 Al ₂ O ₃	23
2.13.2 Processing Methods.....	23
2.13.3 Test Methods.....	25
2.14 Colour and Translucency.....	26
2.15 Retention of Ceramic Restorations	33
2.16 Aim of the study	34
2.17 Null hypothesis	34
2.18 Objectives of the study	35
2.18.1 Mechanical properties	35
2.18.2 Structural analysis	35
2.18.3 Optical properties	35
Chapter 3 Materials and Methods	36
3.1 Materials	36
3.2 Sample Preparation	37
3.2.1 Uniaxial Press	37
3.2.2 Cold Isostatic Press.....	38
3.2.3 Sintering	39
3.2.4 Hydrothermal Artificial Aging	40
3.3 Physical and Mechanical Properties	40
3.3.1 Shrinkage and Density	40
3.3.2 Flexural Strength	41
3.3.2.1 Weibull Analysis.....	45
3.3.3 Hardness	47
3.3.3.1 Knoop Hardness	47
3.3.3.2 Vickers Hardness.....	48
3.4 Structural Analysis	49
3.4.1 Scanning Electron Microscope (SEM).....	49
3.4.2 Grain Size Measurement.....	51
3.4.3 Focused Ion Beam/Scanning electron Microscope	51
3.4.4 X-Ray diffraction.....	54
3.4.5 Surface Roughness Measurement	57

3.5	Optical Properties	61
3.5.1	Colorimeter.....	61
3.5.2	Spectrophotometers	62
3.5.2.1	45°/0° -0°/45° spectrophotometers.....	63
3.5.2.2	Sphere Spectrophotometers	63
3.5.3	Spectroradiometer	65
3.5.4	Transmission, Contrast ratio, Translucency Parameters	66
3.5.5	Colour Measurement.....	67
3.5.6	Irradiance measurements.....	68
Chapter 4 Mechanical Properties and Structural Analysis: Results and Discussion		70
4.1.1	Shrinkage and Density	70
4.1.2	Biaxial Flexural Strength Result	71
4.1.3	Hardness Results	77
4.1.4	XRD.....	78
4.1.4.1	Starting Powders.....	78
4.1.4.2	Post-sintering.....	79
4.1.4.3	Post-aging.....	79
4.1.5	SEM.....	81
4.1.6	Grain size results.....	89
4.1.7	FIB-SEM.....	91
4.1.8	Surface Roughness Results	96
Chapter 5 Optical Properties: Results and Discussion		102
5.1	Effect of thickness.....	102
5.1.1	Translucency parameter.....	102
5.1.2	Transmittance.....	105
5.1.3	Contrast Ratio	107
5.2	Effect of aging on the translucency.....	111
5.2.1	Translucency parameter.....	112
5.2.2	Transmission	113
5.2.3	Contrast Ratio	114
5.3	Effect of material on translucency.....	114
5.3.1	Translucency Parameter	115
5.3.2	Transmission	116
5.3.3	Contrast Ratio	117
5.4	Colour Stability after Aging	120

5.4.1 Chroma.....	123
5.5 Effect of thickness and aging on light irradiance.....	126
Chapter 6 General discussion.....	130
Chapter 7 Conclusions	133
Chapter 8 Future Works.....	135
Chapter 9 References	136

List of Tables

Table 3-1 Composition of powder materials	36
Table 4-1 Green and Sintered Density.....	70
Table 4-2 Mean Values of Biaxial Flexural Strength (BFS), Weibull modulus , characteristic strength and Hardness (HVF)	75
Table 4-3 Bar Chart showing Hardness before and after aging.	78
Table 4-4 Grain size result before and after aging.	89
Table 4-5 Mean and Standard deviation for surface roughness before and after hydrothermal aging.....	96
Table 5-1 Mean, SD and R² of Translucency parameter	103
Table 5-2 Mean, SD and R² of Transmission %.....	106
Table 5-3 Mean, SD and R² of Contrast ratio (CR)	108

List of Figures

Figure 2-1 Polymorphic transformation of ZrO ₂	11
Figure 2-2 Schematic representation of aging process.....	20
Figure 2-3 schematic representation of crack induced transformation.....	21
Figure 2-4 The Munsell colour system	27
Figure 2-5 Representation of CIEL* a* b* space	29
Figure 3-1 schematic illustration of Uniaxial press and pressure distribution within the sample.	38
Figure 3-2 schematic illustration of Cold Isostatic press and pressure distribution.	39
Figure 3-3 (a) Three Point Bending Test (b) Four Point Bending Test .	43
Figure 3-4 Biaxial Flexural Test.....	44
Figure 3-5 FIB-SEM setup used.....	53
Figure 3-6 Stages of FIB-SEM sample preparation and Imaging	54
Figure 3-7 Classic Bragg-Brentano XRD setup	56
Figure 3-8 A schematic representation of the AFM instrument.	59
Figure 3-9 Elements of visual process.....	61
Figure 3-10 Geometry of 45°/0° spectrophotometer.....	63
Figure 3-11 Geometry of sphere spectrophotometer.....	64
Figure 3-12 Geometry of Multi-Angle spectrophotometer	65
Figure 3-13 SP64 Spectrophotometer, X-Rite™	66
Figure 4-1 Percentage Shrinkage of all materials after sintering.....	70
Figure 4-2 Bar Chart showing the <i>BFS</i> before (BA) and after aging(AA).....	71
Figure 4-3 Weibull probability plot for <i>BFS</i> data of 3YE_BA and 3YE_AA.	74
Figure 4-4 Weibull probability plot for <i>BFS</i> data of 3YBE_BA and 3YBE_AA.	74
Figure 4-5 Weibull probability plot for <i>BFS</i> data of Zpex_BA and Zpex_AA.	76
Figure 4-6 Weibull probability plot for <i>BFS</i> data of ZpexS_BA and ZpexS_AA.	76
Figure 4-7 XRD pattern and Rietveld analysis for powders of all tested groups.	79
Figure 4-8 XRD pattern and Rietveld analysis for all tested groups showing the transformation after aging.....	80
Figure 4-9 SEM images showing the surface topography of 3YE.....	83

Figure 4-10 SEM images showing the surface topography of 3YBE. ..	84
Figure 4-11 SEM images showing the surface topography of Zpex. ...	85
Figure 4-12 SEM images showing the surface topography of ZpexS..	86
Figure 4-13 SEM images of the fractured surface of 3YE before (A) and after (B)Aging.....	87
Figure 4-14 SEM images of the fractured surface of 3YBE before (A) and after (B)Aging.....	87
Figure 4-15 SEM images of the fractured surface of Zpex before (A) and after(B)Aging.....	88
Figure 4-16 SEM images of the fractured surface of ZpexS before (A) and after(B)Aging.....	88
Figure 4-17 Bar chart showing the mean and standard deviation of the grain size before and after aging.....	89
Figure 4-18 Ion beam images and SEM images for FIB prepared section for 3YE.....	91
Figure 4-19 Ion beam images and SEM images for FIB prepared section for 3YBE.	92
Figure 4-20 Ion beam images and SEM images for FIB prepared section for Zpex.	93
Figure 4-21 Ion beam images and SEM images for FIB prepared section for ZpexS.....	95
Figure 4-22 AFM for 3YE before and After aging. (a) height sensor BA (b) amplitude view BA (c) 3D view BA (d,e,f After aging).	97
Figure 4-23 AFM for 3YBE before and After aging. (a) height sensor BA (b) amplitude view BA (c) 3D view BA (d,e,f After aging).	98
Figure 4-24 AFM for Zpex before and After aging. (a) height sensor BA (b) amplitude view BA (c) 3D view BA (d,e,f After aging).	99
Figure 4-25 AFM for ZpexS before and After aging. (a) height sensor BA (b) amplitude view BA (c) 3D view BA (d,e,f After aging).	100
Figure 5-1 Effect of thickness on Translucency Parameter (TP).	102
Figure 5-2 Plot of the thickness against translucency parameter (TP) of all groups before aging.	104
Figure 5-3 Effect of thickness on Transmittance (Tt%).....	105
Figure 5-4 Plot of the thickness and Transmittance (Tt%) of all groups before aging.	107
Figure 5-5 Effect of thickness on Contrast Ratio(CR).....	107
Figure 5-6 Plot of the thickness and contrast ratio (CR) of all groups before aging.....	108
Figure 5-7 Effect of aging on Translucency Parameter(TP).	112
Figure 5-8 Effect of aging on Transmission %.	113

Figure 5-9 Effect of aging on Contrast ratio (CR).....	114
Figure 5-10 The difference in the translucency, 0.75mm thickness. ..	115
Figure 5-11 TP of the four tested groups.	115
Figure 5-12 Total transmittance of the four tested groups.....	116
Figure 5-13 CR of the four tested groups.....	117
Figure 5-14 Mean +SD of ΔE^*ab for all groups.	121
Figure 5-15 ΔE^*ab Mean +SD of 1.00 mm thickness of all tested groups.....	121
Figure 5-16 L^* mean values+ SD before and after aging.....	122
Figure 5-17 a^* mean values+ SD before and after aging.....	122
Figure 5-18 b^* mean values+ SD before and after aging.....	123
Figure 5-19 Chroma mean values \pmSD before and after aging.....	123
Figure 5-20 Difference in colour before and after aging.	125
Figure 5-21 Mean light irradiance for all tested materials before aging at various thicknesses.	126
Figure 5-22 Mean light irradiance for all tested materials after aging at various thicknesses.....	128
Figure 5-23 Total irradiant energy for all tested groups zirconia brands at different thicknesses and 10 s curing time.....	128
Figure 5-24 Effect of hydrothermal aging on the irradiance of all tested materials.....	129

List of Abbreviations

°C-	degrees Centigrade
ADA-	American Dental Association
ADS-	Automatic divergence slits
AFM-	Atomic Force Microscope
ATZ-	Alumina-toughened zirconia
BFS-	Biaxial Flexural Strength
CAD-	Computer Aided Design
CAM-	Computer Aided Manufacturing
CIE-	Commission International de l'Eclairage
CR-	Contrast ratio
FDP-	Fixed dental Prosthesis
FESEM-	Field emission scanning electron microscopy
FIB-	Focused Ion Beam
FPD-	Fixed Partial Denture
FSZ-	Fully stabilised zirconia
ISO-	International Organization for Standardization
LTD-	Low temperature degradation
MA-	Multi Angle
PSZ-	Partially stabilised zirconia
RS-	Raman Spectroscopy
SEM-	Scanning Electron Microscope
T%-	transmission
Td%-	Direct transmittance
TP-	Translucency Parameter
Tt%-	Total transmittance
UV-	Ultra Violet
XRD-	X-ray diffraction
Y-TZP-	Yttria stabilised tetragonal zirconia
ZTA-	Zirconia toughened alumina

Chapter 1 Introduction

There is no single factor governing the success or failure of any dental material. The story starts from selecting the right restoration for the right patient using the right material that suits the exact requirement for each single case. Both clinical and technical procedures are crucial to achieve the best possible restoration. Technically, this includes many factors; material properties, long term resistance to the aging process in the mouth, different processing steps and techniques, all have a direct impact on the behaviour of any material.

Failure of a material clinically is not just limited to a processing or a mechanical deficiency only. For example, a material can have excellent mechanical properties but may be deficient in aesthetics. Therefore, aesthetic requirements have a great impact on the selection of any dental material and remain as one of the main drivers for developing new dental materials, trying to satisfy patient expectation to obtain a restoration that can mimic the natural teeth. Unhappiness with tooth colour is among the main aesthetic concerns for patients (Tin-Oo et al., 2011).

In the last decade there has been a tremendous research effort employed to take metal out of prosthetic dentistry (Manicone et al., 2007) and to improve the aesthetics of restorations. This has resulted in establishing all-ceramic fixed dental prostheses (FDPs) as an alternative to metal-ceramic FDPs in daily clinical life. The use of all-ceramics as an alternative was driven by their more favourable aesthetic properties (Edelhoff and Brix, 2011) as they have the ability to mimic the optical properties of natural teeth (Sailer et al., 2015). In addition, the increase in the cost of precious metals such as gold played a clear role in supporting the use of all-ceramics (Walton, 2014). However the use of the first introduced all-ceramic restorations such as feldspathic porcelain, was limited to a single unit in the anterior region due to the limitations and instability of its mechanical properties (Pjetursson et al., 2007; Sailer et al., 2015). Therefore, looking for a restorative material that satisfied the need for aesthetic and mechanical properties at the same time can be

regarded as the main driver behind the increase in the use of different types of dental ceramics which were developed in the past few years. Options such as leucite or lithium disilicate glass ceramics and oxide ceramics such as alumina and zirconia appeared to be very promising for different indications. The development of these recently introduced ceramics broke the limit of using all-ceramic restorations in the anterior region only and they became available to be used in the posterior region and in multiple-units rather than just single units (Raigrodski et al., 2006).

The advantageous mechanical properties of zirconia make its introduction to the dental world of great importance. It particularly increases the treatment choices in restorative dentistry by increasing the variety of applications of ceramics in prosthodontics, due to its distinctive properties such as its biological inertness and acceptable opacity, providing highly aesthetic restorations (Denry and Holloway, 2010).

Zirconia has become increasingly used in frameworks of fixed partial dentures and particularly for long span replacement. This is mainly due to its high fracture toughness. In addition, with the aid of computer-aided design/computer-aided manufacturing technology (Guess et al., 2010), the production of excellent, long-life zirconia prostheses has become easily achievable (Denry and Kelly, 2008). It is also widely used as an integrated part of dental implants (Raigrodski, 2004, Aboushelib et al., 2005).

Its good chemical and dimensional stability, high mechanical properties, toughness and a Young's modulus similar to that of stainless steel, make zirconia widely used as a 'core' material for all-ceramic prosthesis (Aboushelib et al., 2005).

However, since its introduction as a core ceramic and its adoption as one of the more preferable available dental materials (Schmitter et al., 2012), the material has been faced with problems related to the adhesive delamination of the veneering porcelain material. This is most evident when this failure affects function (e.g. failure in approximal regions) or the aesthetic appearance of the restoration. The reconstruction of the restoration is then highly recommended (Guess et al., 2010b; Silva et al., 2010; Guess et al., 2010a). Delamination is related to the presence of localised tensile stresses

at the interface, which weakens the porcelain–zirconia bond strength (Queiroz et al., 2012). The delamination phenomenon of veneers has been found to be multifactorial in nature, and it is widely accepted that mechanical and adhesive deficiencies at the interface are regarded as the main causes of this problem (Guess et al., 2010b).

One of the solutions to overcome aforementioned problem is the use of a so-called monolithic or full-contour zirconia restoration, in which the zirconia will be directly exposed to the oral cavity and there is no need for veneering. In the last five years, there is a clear increase in the use of monolithic zirconia and there is a considerable amount of research on different aspects of this material.

Improving the translucency of monolithic zirconia and the resistance of this material to aging by playing with its constituent content, and the consequent effect of these changes on its mechanical properties, are of great interest, as zirconia still has a considerable possibility to be a ‘gold standard’ material in restorative dentistry.

Chapter 2 Literature Review

2.1 Ceramic

'Ceramic' derives from the Greek term *keramos*, which means "a potter" or "pottery" with roots in an older Sanskrit root meaning "to burn". Ceramics are regarded as one of the oldest materials developed by humans and were found as one of the components of early utensils (Volpato et al., 2010).

Ceramics have traditionally been defined by the American Society of Ceramics (ACerS) as inorganic, non-metallic materials, which are typically crystalline in nature, and are compounds formed between metallic and non-metallic elements. (Sukumaran and Bharadwaj, 2006, Raghavan, 2012). The definition of 'ceramic' is evolving and now includes glass, glass-ceramics and inorganic cement-type materials.

2.2 Ceramics in Dentistry

Dental ceramics have been defined as "*materials that are part of systems designed with the goal of producing dental prostheses which might be used to replace either missing or damaged dental structures*" (Arango Santander et al., 2010).

In 1774, the dissatisfaction of the French pharmacist, Alexis Duchâteau, with his ivory dentures led him to suggest that porcelain might be considered as a possible replacement for missing teeth, due to his observation that ceramic utensils had good abrasion resistance when used in managing chemical formulations. Later in 1788, with the assistance of a dentist, Nicholas Dubois De Chemant, Duchateau managed to fabricate the first dental porcelain composition based on "green" traditional porcelain (50% kaolin clay or Chinese clay ($\text{Al}_2\text{O}_3\text{-SiO}_2\text{-2H}_2\text{O}$), 25 % feldspar ($\text{K}_2\text{O- Al}_2\text{O}_3\text{-6SiO}_2$) and 25% silica or quartz (SiO_2) (Tandon et al., 2010); however, these materials are no longer used due to their high opacity. In 1838, Elias Wildman formulated a more translucent ceramic with shades much more related to natural tooth appearance (Al-Wahadni, 1999).

In 1889, Charles H. Land patented the first all-porcelain crown termed the “jacket” crown. A porcelain covering or “jacket” was used to restore a tooth and the material were enhanced progressively and it was widely used up to the 1950s (Taylor, 1922, Helvey, 2014)

Ceramic materials have been developed over the years to satisfy dental requirements. Today’s dental world comprises a large and diverse group of ceramic materials that offer patients a number of options when dealing with prosthetic treatments. These ceramic systems have been developed seeking high quality materials, both aesthetically and functionally (Arango Santander et al., 2010), and the main types of these ceramics which have been available for dental use are the feldspathic, the aluminous and finally the zirconia type (Volpato et al., 2010).

In terms of mechanical properties, the development of ceramic materials has shown a significant improvement (Raghavan, 2012) leading to an increase in metal free restorations and the rise of so-called ‘all ceramic’ restorations (Mehta and Shetty, 2010). In addition to the commonly used alumina, glass infiltrated alumina, glass–ceramics and tetragonal zirconia (ZrO_2) polycrystalline ceramics (Y-TZP), have been widely used as high-strength core materials (Liu et al., 2010c).

2.3 Classification of dental ceramics

Different classifications of dental ceramics have been proposed by different authors. They can be classified according to their clinical use, mechanical properties, composition, processing techniques, sintering temperatures and according their optical properties (O'Brien, 2008, Giordano and McLaren, 2010, Guess et al., 2011, Sakaguchi and Powers, 2012, Anusavice et al., 2013, Shen, 2013, Helvey, 2014). In 2015, a new more precise classification was proposed by (Gracis et al., 2015) which allowed easy inclusion of newly developed restorative materials.

Depending on their compositions, ceramics have historically been divided into three families as follows:

1. Glass Matrix Ceramics

2. Resin-Matrix Ceramics
3. Polycrystalline Ceramics

This classification has considered the new definition of porcelain/ceramic published by ADA, which defines ceramics as “*pressed, fired, polished or milled materials containing predominantly inorganic refractory compounds including porcelains, glasses, ceramics and glass-ceramics*” (American Dental Association, 2013). This effectively replaces the more traditional definition of ceramics as “*non-metallic inorganic materials usually processed by firing at a high temperature to achieve desirable properties.*” (Ahlberg et al., 2003).

2.3.1 Glass Matrix Ceramics

The family has three subdivisions including naturally occurring feldspathic ceramics, synthetic ceramics and glass infiltrated ceramics.

2.3.1.1 Feldspathic

This group of ceramics composed mainly of silicon dioxide (quartz or silica) and various amounts of alumina or aluminium oxide and a naturally occurring mixture of sodium aluminosilicate with potassium known as feldspar. Potassium feldspar ($K_2Al_2Si_6O_{16}$) forms leucite crystals (crystalline phase). This crystallisation makes this type of ceramic suitable for veneering metal substructure by decreasing the difference in the coefficient of thermal expansion between the substructure and the veneer to 10% or less. It also increases the strength of porcelain restoration (O'Brien, 2008, Sakaguchi and Powers, 2012, Anusavice et al., 2013). Examples include IPS Empress Esthetic, IPS Empress CAD, IPS Classic (all Ivoclar Vivadent); Vitadur, Vita VMK 68, Vitablocs, (all Vident).

2.3.1.2 Synthetic

These are either lithium disilicate based (and derivatives), e.g. Celtra Duo (Dentsply) ; 3G HS (Pentron Ceramics); Suprinity (Vita); IPS e.max CAD, IPS e.max Press (Ivoclar Vivadent); Obsidian (Glidewell Laboratories) or fluorapatite-based, e.g. IPS e.max Ceram, ZirPress (Ivoclar Vivadent) or leucite based, such as Noritake EX-3, Cerabien, Cerabien ZR (Noritake); Vita VM7, VM9, VM13 (Vident); IPS d.Sign (Ivoclar Vivadent) .

The lithium disilicate materials in particular have gained a lot of clinical use as they offer superb aesthetics and high translucency. The use of lithium disilicate as a monolithic restoration of a single crown showed a high success rate; in a retrospective study by (Fabbri et al., 2014), the success rate of 199 (114 upper-85 lower arch) monolithic single crowns out of 860 lithium disilicate restoration evaluated in this study was 95.4% in maxilla and 96.2 % in mandible after 3-6 years. A recent retrospective study by (Sulaiman et al., 2015c) evaluating at 4 years a total of 21340 lithium disilicate restorations, including 15802 monolithic restorations and 5538 layered crowns, showed layered single crowns fractured at approximately twice the rate of monolithic crowns.

2.3.1.3 Glass infiltrated

The In-Ceram family of materials was initially alumina based (In-Ceram Alumina, Vita) with subsequent materials being developed additionally incorporating magnesium (In-Ceram Spinel, Vita) or zirconia (In-Ceram Zirconia, Vita).

In-Ceram Alumina was the first glass infiltrated dental ceramic; it was launched in 1989 and was prepared by the slip-casting technique. A densely packed slurry of Al_2O_3 was sintered to a refractory die, and after formation of a porous skeleton of alumina particles, lanthanum glass used to infiltrate the porosity and increase strength, in a second firing. The composition according to the manufacturer was Al_2O_3 (82%), La_2O_3 (12%), SiO_2 (4.5%), CaO (0.8%), and other oxides (0.7%).

In 1994, In-Ceram Spinel was introduced. It was prepared in a similar way to In-Ceram Alumina but the glass was infiltrated into a synthetically produced porous magnesium aluminate (MgAl_2O_4) core.

In-Ceram Zirconia was the most recent modification of In-Ceram Alumina; partially stabilised zirconia oxide was added to increase the strength of the ceramic.

The composition according to the manufacturer was Al_2O_3 (62%), ZnO (20%), La_2O_3 (12%), SiO_2 (4.5%), CaO (0.8%), and other oxides (0.7%). Because of its opacity and the increased availability of lithium disilicate and zirconia

ceramics, especially for CAD/CAM fabrication, the use of this class of materials has greatly diminished.

2.3.2 Resin-Matrix Ceramics

This family is specifically formulated for CAD/CAM. It includes materials with a highly ceramic-filled organic matrix. With the presence of an organic matrix, it would not be possible to include this type within ceramic classification according to the traditional definition. This family of ceramics has been added according to the new ADA definitions of ceramic mentioned earlier. The materials classified under this family have a predominant inorganic refractory compound such as porcelain, glass, ceramic and glass-ceramic. These compounds form more than 50% by weight regardless of the existence of a less predominant organic phase (polymer) (Gracis et al., 2015). This type can be subdivided into three groups depending on the inorganic composition.

2.3.2.1 Resin nanoceramic

This type consists of 80% by weight nanoceramic particles to reinforce a highly cured resin matrix. Examples include Lava Ultimate (3M ESPE).

2.3.2.2 Glass ceramic in a resin interpenetrating matrix

This typically consists of a (86% by weight / 75% by volume) feldspathic ceramic and a (14% by weight / 25% by volume) polymer, e.g. Enamic (Vita).

2.3.2.3 Zirconia-silica ceramic in a resin interpenetrating matrix

This material has an inorganic content > 60% by weight. It has different organic matrices and is tailored with different ceramic weight percentages and types (e.g. silica powder, zirconium silicate, micro-fumed silica). Commercially produced by 3M ESPE, examples include MZ100 and Paradigm MZ-100.

2.3.3 Polycrystalline ceramics

The main feature of this type of ceramic is the fine-grain crystalline structure which is responsible for its strength and fracture toughness. The absence of a glass phase in the structure of this type of ceramic adversely affects its etching ability (Sriamporn et al., 2014).

2.3.3.1 Alumina

Alumina was first introduced in mid 1990s as a core material by Nobel Biocare to be used with CAD/CAM. This material consists of high-purity Al_2O_3 (up to 99.5%). It has a good mechanical properties including high hardness (17-20 GPa) and relatively high strength and high elastic modulus (300 GPa) (Guess et al., 2011). However, it was still liable to bulk fractures (Kim et al., 2007, Scherrer et al., 2008), which together with the introduction of more stable materials such as stabilised zirconia has led to a decrease in use of this material.

2.3.3.2 Zirconia-toughened alumina and alumina-toughened zirconia

This type of ceramic includes alumina-zirconia (zirconia toughened alumina [ZTA]) and zirconia-alumina (alumina-toughened zirconia [ATZ]) composites. In 1976, Claussen described that the addition of unstabilised zirconia to alumina can increase the fracture toughness of alumina. This was attributed to the dual interactions of the crack front with the second phase and with the pre-existing microcracks formed during transformation of zirconia from tetragonal to monoclinic phase (Claussen, 1976, Abi et al., 2013, Gracis et al., 2015).

2.3.3.3 Stabilised zirconia

Examples include Lava/Lava Plus (3M ESPE); In-Ceram YZ (Vita); Zirkon (DCS); Katana Zirconia ML and UTML (Noritake); Cercon HT (Dentsply); Prettau Zirconia (Zirkonzahn); IPS e.max ZirCAD (Ivoclar Vivadent); Zenostar (Wieland).

These types of zirconia are either partially or fully stabilised. Un-alloyed zirconia is unstable and a phase transformation from a tetragonal to monoclinic phase can occur at room temperature. Different types and percentages of oxides such as yttrium, magnesium calcium, and cerium can be used to stabilise tetragonal zirconia at room temperature (Piconi and Maccauro, 1999). Zirconia is discussed in more detail below.

2.4 Zirconia

The name “Zirconium” comes from the Arabic word “Zargon” which means “*golden in colour*” (Pilathadka et al., 2007, Vagkopoulou et al., 2009) which in turn comes from the two Persian words Zar (Gold) and Gun (Colour) (Piconi and Maccauro, 1999).

Zirconium (Zr) is a transition metal element, with an atomic number of 40. It is a considerably strong, ductile, malleable lustrous silver-grey metal. Its chemical and physical properties are similar to those of titanium (Ti) (Matinlinna, 2014). In nature, zirconium oxide, ZrO_2 is relatively abundant (about 0.02% of the earth's crust) (Lughi and Sergo, 2010). Interestingly, both Ti and ZrO_2 have been used in dentistry as implant materials as both have no inhibitory effect on bone forming cells (osteoblasts) which are crucial for the osseointegration process (Kobayashi et al., 1995).

2.5 Crystallographic structure of zirconia

Zirconia is polymorphous material. It's distinct crystallographic structures are mainly determined by the spatial arrangements of its constituent atoms. Each crystallographic structure has its specific geometry and dimensional parameters (Volpato et al., 2011).

At ambient pressure, pure zirconia can be found in three temperature dependant crystallographic phases. Monoclinic (M) crystallographic phase can be found between room temperature and 1170°C; the tetragonal (T) phase from 1170 to 2370°C; and the cubic (C) phase is from 2370°C until it reaches its melting point of 2680°C (Garvie et al., 1975, Green et al., 1989, Kisi and Howard, 1998, Denry and Kelly, 2008, Khamverdi and Moshiri, 2012, Shen, 2013).

Pure monoclinic zirconia assumes a base-centred monoclinic Bravais lattice arrangement with unit cell parameters ($a \neq b \neq c$) of 5.15 Å, 5.21 Å and 5.32 Å, respectively and an atomic inter-planar distance (d) of 3.16 Å, and interplanar angles ($\alpha = \gamma \neq \beta$) of 90° and 99.17° (Varez et al., 2007, Lughi and Sergo, 2010, Jum'ah, 2015). Pure tetragonal zirconia is present as a body-centred tetragonal Bravais lattice crystalline arrangement, with a unit cell parameter

($a=b\neq c$) of 3.598 Å and 5.185 Å, an atomic inter-planar distance (d) of 2.96 Å, and inter-planar angles ($\alpha=\beta=\gamma$) of 90° (Yashima et al., 1994). Pure cubic zirconia is a face-centred cubic Bravais lattice arrangement with a unit cell parameter ($a=b=c$) of 5.14 Å, inter-planar angles ($\alpha=\beta=\gamma$) of 90° and atomic inter-planar distance (d) of 2.94 Å (Katz, 1971, Jum'ah, 2015).

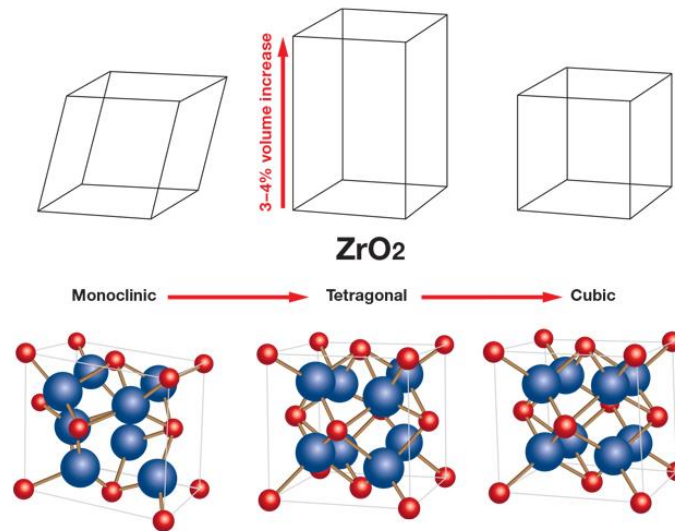


Figure 2-1 Polymorphic transformation of ZrO₂. KEY: Red balls =Zr,

Blue balls =Oxygen. Copyright © 2004, John Wiley and Sons.

Zirconia systems that are currently available for dental application involve ceramics with 90% or higher content zirconium dioxide (Y-TZP) and glass infiltrated ceramics with 35% partially stabilised zirconia (Mehta and Shetty, 2010).

2.6 Zirconia for Medical purposes

Zirconia was used as a biomaterial for the first time in 1969 by (Helmer and Driskell, 1969), as a new material in orthopaedics for hip-head replacement instead of titanium or alumina prostheses. They studied the biological reaction to zirconia by placing it in a monkey femur and concluded that no adverse responses arose (Manicone et al., 2007). The concerted use of zirconia as a biomaterial started in the mid 1980's to manufacture ball-heads able to overcome the mechanical limitations of the first developed alumina ceramic (Christel et al., 1988).

According to their bioactivity, ceramics can be classified into: bioresorbable, bioreactive or bioinert (Hench and Ethridge, 1975, Piconi and Maccauro, 1999, Piconi et al., 2003). Zirconia as a bioinert and non resorbable ceramic (Depprich et al., 2008) is used in many orthopaedic devices such as humeral epiphysis and hip endoprostheses. This is mainly due to its favourable mechanical properties including low wear and high stability (Boehler et al., 2000).

For medical purposes, zirconia is available in two types; either partially stabilised zirconia (PSZ) or fully stabilised zirconia (FSZ) depending on the amount and type (commonly either magnesia (Hannink and Garvie, 1982, Garvie et al., 1984) or yttria) of the stabiliser. The amount of stabiliser plays a key role in defining the type of zirconia and has a range of 3-9 wt% (Christel et al., 1988).

2.7 Zirconia in dentistry

The introduction of zirconia to the dental world was of great importance. In particular, zirconia increased the treatment choices in restorative dentistry by extending the variety of applications of ceramics in prosthodontics, taking advantage of its distinctive properties such as enhanced physical properties, its biological inertness and acceptable opacity, providing highly aesthetic restorations (Denry and Holloway, 2010).

Its good chemical and dimensional stability, high strength, high toughness and a Young's modulus similar to that of stainless steel, make zirconia widely used as a core material for all-ceramic prosthesis (Aboushelib et al., 2005). Based on those material properties, high occlusal stresses occurring during function were expected to be withstood by a zirconia core (Guazzato et al., 2004). In addition to that and by the aid of computer-aided design/ computer-aided manufacturing (CAD/ CAM) technology, the production of excellent, long-life zirconia prostheses has become easily achievable (Denry and Kelly, 2008). However, by way of extending ceramic use, its excellent mechanical properties have also led to zirconia being increasingly used as the framework of fixed partial dentures and especially for long span replacement. This is

mainly due to its high fracture toughness. It is also widely used as an integrated part of dental implants (Raigrodski, 2004, Aboushelib et al., 2005).

2.8 Challenges facing dental zirconia

Since its introduction as a core ceramic and its adoption as one of the more preferable dental materials (Schmitter et al., 2009), the resistance by the profession towards this material has been mainly related to the adhesive delamination of the veneering porcelain (Komine et al., 2010, Raigrodski et al., 2012) placed on the zirconia core, rather than failure of the core itself. The incidence rate of delamination has been reported in the wide range between 3-36% after 1-5 years for FPDs and for single crown restorations as about 2-9% after 2-3 years (Guess et al., 2011, Andreiuolo et al., 2013, Malkondu et al., 2016).

This is most evident when this failure affects function (e.g. failure in approximal regions) or the aesthetic appearance of the restoration. The reconstruction of the restoration is then highly recommended (Guess et al., 2010, Silva et al., 2010). Delamination or chipping of the veneer layer is related to the presence of localised tensile stresses at the interface, which weakens the porcelain–zirconia bond strength (Queiroz et al., 2012). The delamination phenomenon of veneers has been found to be multifactorial in nature, and it is widely accepted that mechanical and adhesive deficiencies are regarded as the main causes of this problem (Guess et al., 2010). In general, the zirconia core and veneer material bond strength might be affected by many factors such as a chemical mismatch due to the different structure of both materials and a physical mismatch of zirconia core and veneer porcelain, e.g. the difference in the coefficient of thermal expansion (Liu et al., 2010c). In addition to those factors other factors might be considered such as: poor ability to withstand fracture, poor framework design, low cohesion and shear tension between the zirconia core and veneering material (Rizkalla, 2004). (Baldassarri et al., 2012) revealed that clinical defects in the veneer material could be seen in the prosthesis due to the presence of a radial tensile stress between the core and the veneer. Amongst researchers in the dental field

there is a clear consensus that these problems should be solved in order to maximise the application of this material.

Traditionally, preparation of crowns and bridges involves a series of thermal sintering and cooling cycles which are carried out layer by layer until the restoration has been built up. It is essential that the thermal expansion between the porcelain and underlying framework, be it metal or ceramic, is matched in order to avoid cracking after firing (Swain, 2009) and also it has been found that the residual stress that might develop within the interface zone between the core and the veneer is a significant cause of the veneer fracture in zirconia prostheses (Queiroz et al., 2012). Zirconia frameworks that have been produced by CAD/CAM might be easily affected by any defects that might occur at the surface through the milling procedure (Wang et al., 2008). The Y-TZP metastability behaviour, also might lead to low temperature degradation (LTD) caused by the dual effect of time and water diffusion. LTD has a clear effect on the mechanical properties by inducing surface changes which, lead to the formation of micro-cracks and residual stress formation (Lughi and Sergo, 2010).

2.9 Proposed Solutions for Delamination

In order to find suitable solutions to overcome the problem that affects the durability and the function of zirconia veneered with porcelain, many studies have been performed. A study by (Queiroz et al., 2012) showed that a significant increase in the bonding between the veneer and zirconia substructure could be obtained by additional firing of the porcelain, while a study by (Kawai et al., 2010) suggested that the crystal phase around the zirconia/porcelain interface would not be affected by the extension of the firing period and a slight improvement might occur in the core-veneer bonding. Others stated that slow cooling regimes should be used concurrently with slow heating rates when firing porcelain fused to zirconia prostheses. Cooling regimes have been found to have more influence on the failure loads of porcelain to zirconia than heating rates and the choice of heating and cooling regimens during porcelain firing has the potential to increase or reduce internal stresses in layered porcelain and zirconia prostheses (Tan et al.,

2012). Indeed, the study by (Tan et al., 2012) demonstrated that the strength of porcelain fused to a zirconia could be doubled by the use of slow heating and slow cooling regimens. The porcelain adjacent to the interface has been found to be the affected part rather than the interface itself and this led to the conclusion that the residual stresses of thermal origin within the porcelain are the main cause of this damage.

Another proposed way of improving the bond is by considering the design of the framework and provide a minimum safe thickness that should be used (Aboushelib et al., 2009). There is a chance for avoiding delamination in zirconia-veneer bilayer composites by increasing the flexural strength of veneer porcelain to 300MPa (Liu et al., 2010c) and according to (Tholey et al., 2009) the use of 'wet' porcelain veneer appears to be a good way for enhancing the bonding between the core and the veneer. However, it has been observed that grain faceting at the surface of the zirconia grains beneath the veneering porcelain might originate due to the presence of moisture in the veneering powder. The extension of the surface faceting has been found to be affected by the degree of the moisture of the porcelain powder and the firing temperature.

(Thompson et al., 2011) suggested that the application of a liner for veneers might inhibit direct surface contact between the veneer and the zirconia which might normally result in an improvement in bond strength. The liner will result in an increase in surface contact by filling in any gaps at the interface. Another effective way of achieving strong and durable bonding between the veneer and the zirconia suggested by (Thompson et al., 2011) is by the use of air-abrasion at lower pressures in combination with appropriate adhesive primers. The liner that has been used as a colour modifier for the underlying white colour of zirconia has also been found to affect the bond strength in a positive way. (Aboushelib et al., 2009) stated that the use of a liner might increase the bond strength in certain types of zirconia and these findings agree with (Thompson et al., 2011) who stated that a significant increase in the bonding strength could be obtained by using a liner with layered veneers.

Surface treatment of the zirconia before addition of the veneering porcelain is regarded as the method of choice to avoid further surface defects (Wang et

al., 2008). (Kanat et al., 2014) concluded that the use of CAD-on technique for veneering could decrease ceramic chipping due to higher strength of ceramic and the interfacial bonding.

It is clear that every single step of the fabrication process has either a direct or indirect effect on the strength of the bonding of veneering porcelain (Choi et al., 2009).

Nowadays, with advances in CAD/CAM technology and to overcome the aforementioned problem of chipping/delamination associated with zirconia core and veneer system (Miyazaki et al., 2013, Stober et al., 2014, Malkondu et al., 2016, Özkurt-Kayahan, 2016), there is a clear increase in the trend of using monolithic zirconia restorations to eliminate the veneering step all together and to minimise tooth preparation taking the advantage of high strength of dental zirconia.

2.10 Full Contour Zirconia (monolithic zirconia)

Ceramic oxides used in dentistry such as zirconia have a higher strength than other types of dental ceramic. Their aesthetic properties are inferior to porcelain but still much higher than metal (Nakamura, 2015). Depending on its opacity, two types of monolithic zirconia are available, opaque and translucent zirconia. Opaque zirconia possesses significantly greater flexural strength than translucent zirconia; conversely, translucent zirconia has more natural aesthetic properties but lower flexural strength compared to the opaque material (Özkurt-Kayahan, 2016).

The opaque white colour of zirconia and its insufficient translucency (Özkurt-Kayahan, 2016) has made its use as monolithic restoration limited mainly to posterior regions (Guess et al., 2011, Preis et al., 2011, Rosentritt et al., 2012, Miyazaki et al., 2013).

Several approaches have been tried by different researchers to improve the translucency of dental zirconia to be used as a monolithic restoration with an attempt to protect its high mechanical properties including its flexural strength. These methods include modification of sintering temperature (Jiang et al., 2011b) and sintering time (Kim et al., 2013), type and amount of additives

(Casolco et al., 2008, Zhang et al., 2015, Zhang et al., 2016), fabrication processes and addition of colouring materials (Malkondu et al., 2016), and eliminating or reducing the amount of alumina Al_2O_3 content as a light scattering source (Zhang et al., 2012, Zhang et al., 2016). Reduction of oxygen vacancies, pores and defects (residual porosity is regarded as a primary source of light scattering in ceramic materials) can also improve the translucency (Peelen and Metselaar, 1974, Apetz and Bruggen, 2003, Anselmi-Tamburini et al., 2007, Yamashita et al., 2008, Tsukuma et al., 2008, Yamashita and Tsukuma, 2011, Klimke et al., 2011, Zhang, 2014, Denry and Kelly, 2014).

Increasing the amount of stabiliser was found to increase the translucency. Using more than 9 % by weight of Y_2O_3 (corresponding to 5.5 mol%) results in the formation of cubic zirconia and the material is in effect fully stabilised zirconia (FSZ) (Anselmi-Tamburini et al., 2007, Carrabba et al., 2017). This increase in translucency can be explained by the cubic phase of zirconia, unlike tetragonal, being isotropic in different crystallographic directions (see Figure 2-1), and due to this isotropic refractive index, the light scattering occurring at grain boundaries is decreased resulting in more light transmittance (Peuchert et al., 2009, Zhang, 2014, Harada et al., 2016). However, the fully stabilised cubic zirconia is more susceptible to mechanical damage and is more resistant to *LTD* as this material does not undergo transformation toughening (McLaren et al., 2017, Munoz et al., 2017).

Modifying the grain size of tetragonal zirconia has also been suggested by (Zhang, 2014) to improve translucency as it is known to be optically anisotropic and has a large birefringence and high reflective index compared to other dental ceramics.

The number of grain boundaries has a direct effect on the translucency; the fewer grain boundaries the more translucent and vice versa. Therefore the bigger the grain size the more translucent zirconia will be, due to less grain boundaries, however a bigger grain size makes the material more prone to *LTD* due to their weak metastability (Denry and Kelly, 2014).

The range of the grain size of Y-TZP is 0.2–0.8 μm . With this range some translucency can be explored up to 1.00 mm thickness. Producing a nano-

scale grain size (less than 100nm) which is significantly smaller than the wavelength of the visible light (400–700 nm) might result in transparent to translucent Y-TZP (Zhang, 2014). This small grain size may help in reducing the reflection or refraction of a ray of visible light and allow more transmittance (Klimke et al., 2011).

Zirconia has a high flexural strength which is ~ twice that of lithium disilicate (Succaria and Morgano, 2011) and due to its ability to resist high loads with only 0.5 mm occlusal thickness compared to existing ceramic restoration which require more tooth reduction, monolithic zirconia has been recommended to be used in patient with limited interocclusal space. Using CAD/CAM and eliminating the veneer layer by using full contour zirconia can reduce the error from lab steps and save both time and the tooth structure (Jang et al., 2011).

On the other hand using zirconia as a monolithic restoration will put the material at a direct contact with moisture, body temperature from the oral cavity and it will be directly subjected to mechanical loading from chewing, which can make it more susceptible to low temperature degradation (Munoz et al., 2017).

2.11 Low Temperature Degradation (*LTD*)

(*LTD*) can be defined as the phase transformation phenomena that can be triggered by water molecules after diffusion of water into the zirconia lattice over time at a wide temperature range (37–500 °C) (Yoshimura et al., 1987, Guo, 2004, Lughì and Sergo, 2010). It can be thought of as an unintentional *t-m* transformation that is not triggered by the local stress produced at the tip of an advancing crack (Lughì and Sergo, 2010) but rather by the humid environment of oral cavity (Borchers et al., 2010). (Figure 2-2).

The *t-m* transformation is an athermal and diffusionless transformation which is martensitic in nature. It is a common phenomenon in metallic system and can be applicable to non-metallic material such as zirconia (Subbarao et al., 1974, Schmauder and Schubert, 1986, Deville et al., 2004, Lughì and Sergo, 2010, Jum'ah, 2015). Martensitic transformation is characterised by a change in crystal structure in the solid state, which in turn results in a phase change by simultaneous, cooperative movement of atoms less than an atomic diameter. This phase transformation can result in a microscopically detectable changes in the shape of the affected area (Deville et al., 2004, Chevalier et al., 2009, Jum'ah, 2015).

The *t-m* transformation is accompanied by 3-5% volume expansion as a direct result of the difference in unit cell volume of monoclinic and tetragonal zirconia phase (140.96×10^6 vs. 67.12×10^6 pm³) (Subbarao et al., 1974, Badwal et al., 1993).

The consequence of *t-m* transformation at room temperature can result in excessive cracking and end up by catastrophic failure of zirconia as a result of the developing shear strain at unit cell level. This precluded zirconia from being used as a reliable ceramic material for many decades (Badwal et al., 1993, Lughì and Sergo, 2010).

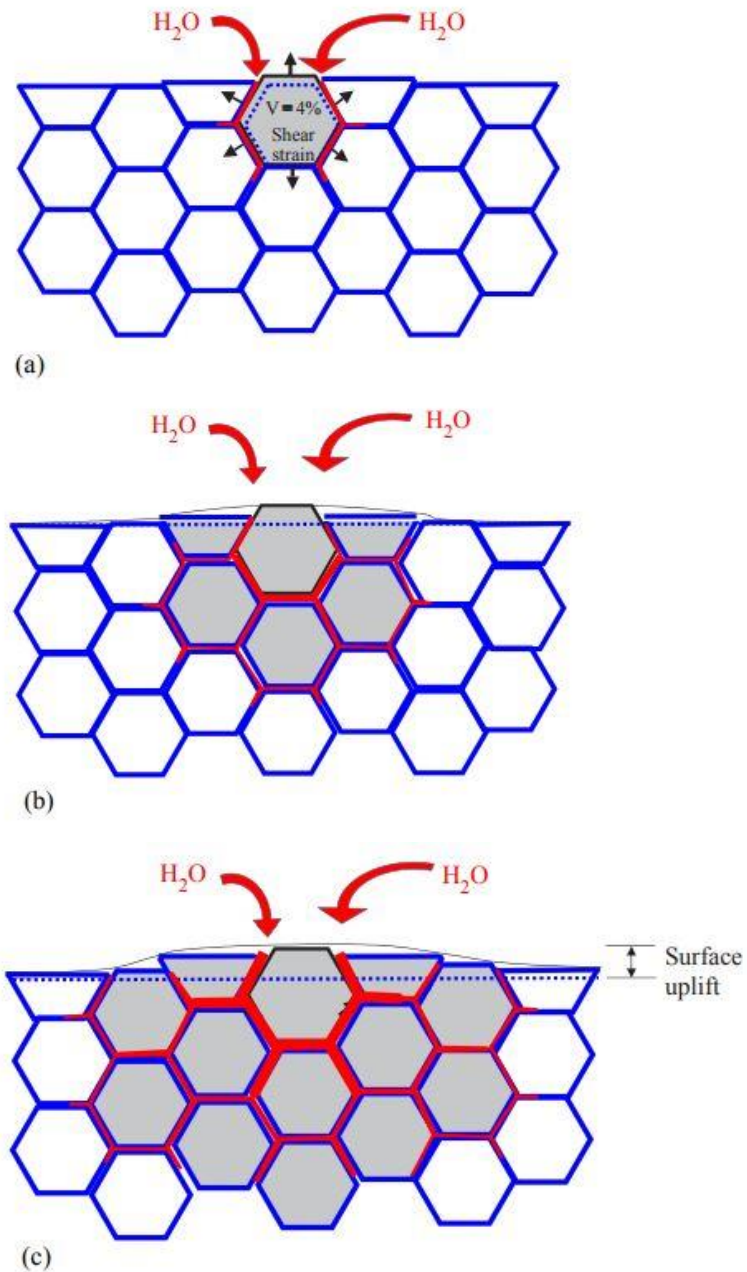


Figure 2-2 Schematic representation of aging process. (a) Nucleation on a particular grain (b) Growth of the transformed zone (c) Transformed grains are grey. Red path represents the penetration of water due to micro cracking around the transformed grains (Chevalier, 2006).

To make use of its high mechanical properties and to overcome the transformation problem, zirconia stabilization with different chemical oxides such as CaO, MgO, CeO₂ and Y₂O₃ was successfully achieved in the late 1920s. Fully stabilised and partially stabilised (metastable) zirconia became available at room temperature. This attracted a great attention from researchers (Ruff et al., 1929, Passerini, 1939, Duwez et al., 1951, Duwez et al., 1952, Gupta et al., 1977, Hellmann and Stubican, 1983, Garvie et al., 1984, Lin et al., 1988, Fassina et al., 1992, Lughì and Sergo, 2010, Jum'ah, 2015).

The *t-m* transformation within the metastable tetragonal zirconia can be a product of a mechanical origin through a propagating crack on the surface accompanied by the aforementioned 3-5% volumetric change. This volumetric expansion is responsible for the radial compressive stress that halts further crack propagation. This stress induced process of transformation is known as 'transformation toughening' which is responsible for the superior mechanical properties of zirconia compared to other available ceramics (Garvie et al., 1975, Gupta et al., 1978, Evans, 1983, Hannink et al., 2000, Guazzato et al., 2004).

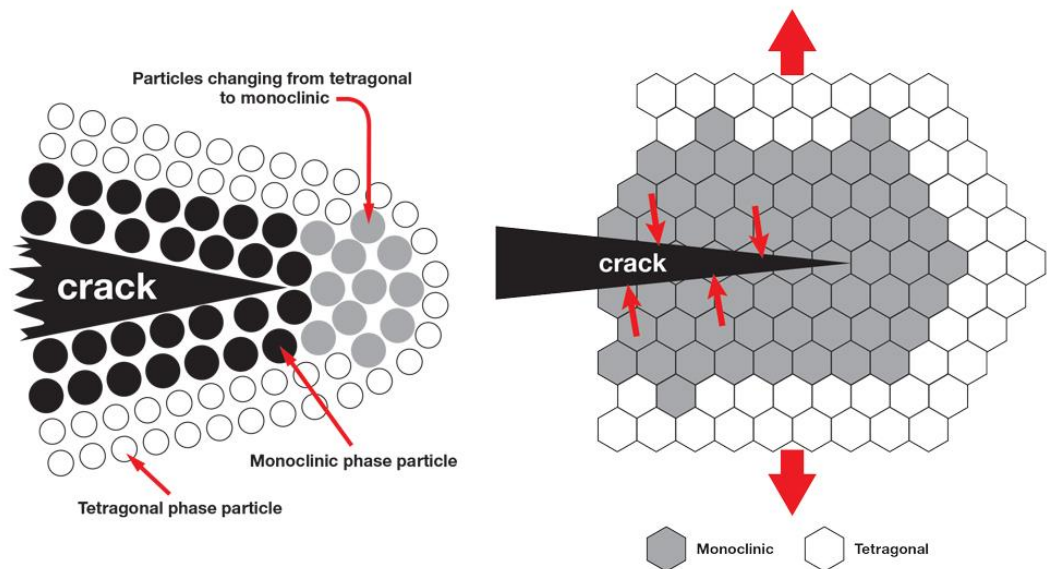


Figure 2-3 schematic representation of crack induced transformation.

© Glidewell Laboratories.

2.12 Transformation toughening of zirconia

The high fracture strength of Y-TZP and its optimal mechanical properties can be attributed to the phase transformation toughening mechanism (Lughi and Sergo, 2010). The trigger for surface toughening or transformation toughening mechanism is by superficial stress around microcracks. This stress is responsible for the phase transformation (tetragonal to monoclinic phase) of metastable Y-TZP grains adjacent to the crack (Garvie et al., 1975) which is accompanied by an increase in the volume of the involved grains. This 3-5% increase in the volume induces compressive stress on the advancing crack, preventing or slowing down crack propagation (Chevalier et al., 1999).

2.13 Mechanical Properties of Zirconia

There are many different factors that can affect the reported mechanical properties of zirconia as a dental material; intrinsic such as chemical composition and processing methods and extrinsic such as the experimental design used to measure the strength of zirconia (Ban and Anusavice, 1990, Pittayachawan, 2009, Janabi, 2014, Nakamura, 2015, Wongkamhaeng, 2016, Abdelaal, 2016).

2.13.1 Chemical composition

Chemical composition is regarded one of the key factors affecting the strength and behaviour of zirconia.

2.13.1.1 Colouring agents

Zirconia is an off white material and to get the most aesthetic result from it, different metal (e.g. Fe, Cu, Co, Mn) oxides are added to dental ceramic materials as a colouring agents (Milleding et al., 2003). A study by Shah et al. (2008) confirmed that adding some types of colouring oxides such as cerium chloride even with low concentration (1wt%) can result in a significant decrease in the strength of zirconia. On the other hand, some of the colouring oxides showed no effect on the strength of zirconia such as bismuth chloride (Shah et al., 2008). (Hjerppe et al., 2008) also reported that various colouring agents decreased the strength of zirconia. Using a liquid containing Er and Nd ions as colouring agents, they found a negative effect on both the flexural

strength and fracture toughness. This has been attributed to the formation of more cubic zirconia after adding the colouring ions (Ban, 2014). Shading or colouring time was also shown to have a negative effect on the strength of zirconia (Liu et al., 2010b).

2.13.1.2 Y₂O₃

The amount of dopants used to stabilise zirconia at room temperature is another composition related factor that has been found to have a direct effect on the strength of zirconia. Zhang et al 2017, in a study of the effect of different concentrations of Y₂O₃ on the mechanical properties of zirconia concluded that there was an inverse linear relationship between the Y₂O₃ concentration and the strength of zirconia, i.e. increasing the Y₂O₃ concentration resulted in strength reduction (Zhang and Asle Zaeem, 2017). This decrease in strength can be attributed to over stabilization of grains and reducing or eliminating the strengthening t-m transformation that can be induced by cracks (Bravo-Leon et al., 2002).

2.13.1.3 Al₂O₃

It has been reported by Samodurova et al. (2015) that the presence of Al₂O₃ in the composition of zirconia positively influences the nucleation of zirconia and promotes strong grain boundaries increasing zirconia strength (Samodurova et al., 2015) and It has a direct clear influence on the grain growth and the stability of tetragonal zirconia (Rao et al., 2004) by acting as a matrix for zirconia to be dispersed in it evenly (Kurtz et al., 2014) and tuning the amount of dopant inside zirconia lattice (Palmero et al., 2014). In literature the typical zirconia strength has been reported to be between 900-1200 MPa (Tinschert et al., 2000, Filser et al., 2001, Guess et al., 2008).

2.13.2 Processing Methods

In ceramic engineering, it is well known that the processing conditions can have a direct impact on the properties of any ceramic material including both mechanical and optical properties. These conditions including the heating regime (i.e. rate and duration of heating, interim and the final sintering temperature, sintering duration and cooling rate) can have a strong impact on the final mechanical and optical properties of the ceramics (Øilo et al., 2008).

These same conditions are equally applicable to ceramics when used as dental restorations (Sundh and Sjögren, 2006).

Processing methods of zirconia have been found to have a direct effect on its mechanical properties. This encompasses all steps, from methods of powder pressing to sintering and finishing.

Powder pressing can be done by three different methods, uniaxial pressing, isostatic pressing and hot isostatic pressing (Pittayachawan, 2009). The uniaxial press is good for shaping and is time and cost efficient as mentioned earlier, however, it produces less dense samples. Using isostatic pressing can produce more dense sample by applying pressure from all around the sample and results in samples with higher strength; however, this method is more costly in terms of time and expense (Pashchenko et al., 1995, Callister Jr, 2005). Both/either uniaxial and isostatic pressing techniques need to be followed by sintering of the samples. With hot isostatic techniques, there is no need for firing afterwards as the sample will be pressed and heat treated at the same time; it is useful in pressing samples of materials that do not form a liquid phase except at very high and impractical temperatures (Callister Jr, 2005).

Sintering also plays a pivotal role in determining the strength of zirconia as it increases the mechanical properties by increasing the density of the sintered block, and it is also responsible for transforming any monoclinic phase present in the pre-fired powders to tetragonal phase (Guazzato et al., 2004). Stawarczyk et al. (2013) studied the effect of different sintering temperatures on the strength of a single type of zirconia. The heating rate used was 8°C/min and a range of sintering temperatures from 1300°C to 1700°C at 50 °C increment were used with a dwell time of 120 mins. Their results showed the highest strength could be obtained between 1,400°C and 1,550°C and increasing the temperature to 1600°C resulted in significant decrease in the flexural strength. On the other hand the lowest mean flexural strength was recorded at 1,300°C and 1,350°C sintering temperature suggesting an optimum processing window (Stawarczyk et al., 2013). In a study by Ersoy et al. (2015) on the effect of different sintering temperatures on the mechanical properties of one brand of zirconia, samples were prepared in a partially

sintered state. The prepared specimens were divided into three different groups sintered at different final sintering temperatures and for various durations: 1510°C for 120 min, 1540°C for 25 min and 1580°C for 10 min. The results showed the highest flexural strength for the group sintered at 1580°C for 10 min (Ersoy et al., 2015). The duration of sintering also has been found of an effect on the flexural strength of zirconia. Chien (2015) studied the effects of sintering holding time on the flexural strength and hardness of translucent zirconia. They sintered three different commercial translucent zirconia's according to their manufacturers' instructions and compared this group with groups of the same materials sintered using different regimes with a final target temperature of 1600°C held for either three or six hours before furnace cooling. They concluded that the mechanical properties of full contour zirconia greatly depended on the grain size and that enlarging the grain size by both raising the sintering temperature and increasing the hold time can potentially produce an increase in flexural strength that was statistically significant. This study showed no effect on the microhardness of the tested materials (Chien, 2015).

2.13.3 Test Methods

The test methods used play an important role in determining the flexural strength of zirconia. In a comparative study of flexural strength test methods on CAD/CAM Y-TZP dental ceramics, Xu et al. (2015) used ISO 6872 guidance to prepare samples for biaxial flexural strength and uniaxial three and four points bending tests. Their results showed that biaxial flexural method produced the highest strength value and the more reliable one compared to the other two methods. This has been attributed mainly due to the edge flaws of beam shaped specimens for three and four points bend tests. These flaws result in undesirable edge failure instead of fracture originating from the intrinsic flaws of the material of the specimens (Xu et al., 2015b). Mijoska et al. (2015) also evaluated different testing methods on the mechanical properties of different types of dental ceramic used as veneers. They recommended not to use uniaxial test methods as they did not provide the real strength values of the ceramic materials and (conversely) gave high results which were less precise compared to biaxial (Mijoska and Popovska, 2015).

2.14 Colour and Translucency

It is well known that colour and translucency are highly connected properties. The natural tooth appearance is multifactorial; the result of its colour and translucency, which themselves are the product of the reflectance from dentin (the prime source of colour) modified by absorption, scattering and thickness of enamel (McLean, 1979, Seghi et al., 1986, Mohie el-Din Wahba et al., 2017).

The concept of colour in general is not easy to understand, difficult to define, and has historically been located more in artistic disciplines than to science (Vichi et al., 2011). Within dentistry, restoring the shape and function of the dentition is not enough without considering matching the colour between restorative materials and natural teeth, and it is often a difficult procedure. Many authors have tried in their studies to build a systematic way to address this issue. The first attempt to address colour selection in dentistry was by Clark in 1933 (Vichi et al., 2011), which was based on the Munsell colour system of 1905. This was the first colour system that systemically placed colour in three dimensional space (Figure 2-4 The Munsell colour system identifies colours into three colour dimensions, Hue, Value and Chroma (Kuehni, 2002). Hue (H) can be defined as the attribute of colour observation by means of which an object is determined to be red, yellow, green, blue, purple and so forth. Chroma (C) is defined as the aspect of colour perception that expresses the degree of departure from the grey of the same lightness. Value (L^*) is defined as the perception by which white objects are distinguished from grey objects and light from dark coloured objects (Hunter and Harold, 1987, Vichi et al., 2011).

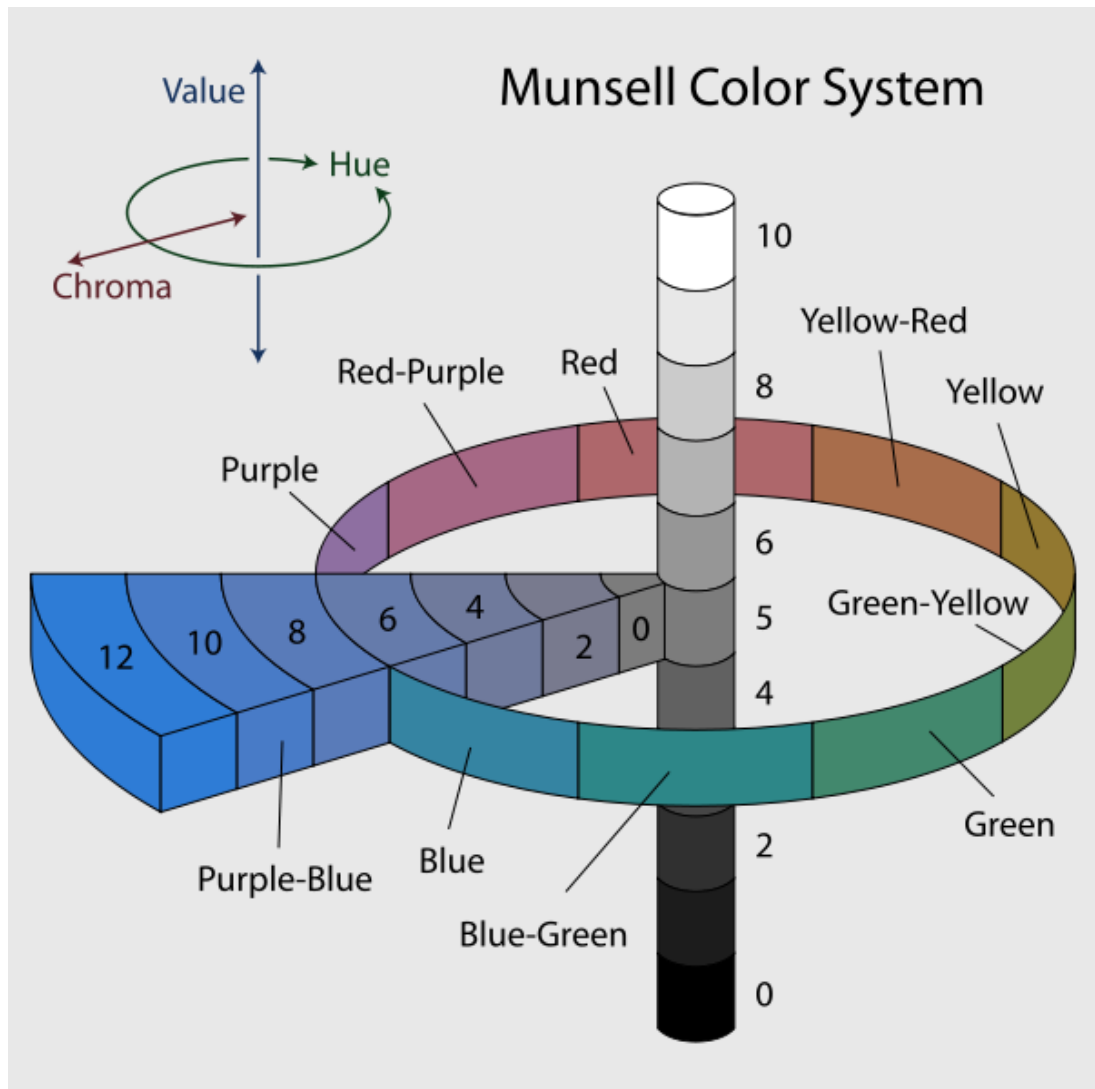


Figure 2-4 The Munsell colour system © Jacobolus

During the same period of Munsell system development, the Commission International de l'Eclairage published the first standards for colour matching and established some scientific parameters for colour assessment. Even after the development of these systems, colour measurement remained undeveloped and did not show any improvement until the 1950s due to the absence of a valid scientific tool to measure colour (Vichi et al., 2011). In 1970s, a series of studies were performed by Sproull in which the dental shades relation with the three dimensional nature of colour was studied in an attempt to improve colour matching in dentistry. A set of theoretical and practical suggestions were given to achieve the improvement in colour matching in dentistry. In addition to these suggestions the factors that can negatively affect shade taking were highlighted including the shade guide itself

at that time and its poorness in reflecting the complexity of appearance of the teeth (Sproull, 1973a, Sproull, 1973b, Sproull, 1974).

Industry has led the development in colour science to fulfil its need in defining colour, and in measuring and calculating the difference in colour in order to provide a proper colour control in its processes (Vichi et al., 2011). In 1976 and 1978, CIE developed the new system called CIE Lab (Roufs, 1978, l'Eclairage, 1986, l'Eclairage, 2004), Figure 2-5. It is a nonlinear transformation of the tristimulus space to agree with Munsell spacing (Paravina, 2004) and is generally used for evaluation of optical properties (l'Eclairage, 2004). It has been heavily used to measure and compare translucency among materials. It was the first system to allow expressing colour in numbers and calculating the difference between two colours with a possibility of corresponding to visual perception. It is an evenly spaced system compared to Munsell in terms of visual perception, this helps in correlating the spectral reading with the subjective observations (Dozić et al., 2003, Lee et al., 2010).

The CIE L^* parameter ranges from 0 to 100 and represents the luminosity (degree of lightness, brightness) of an object, the a^* parameters ranges from -90 to 70 and denotes greenness (positive a^*) and redness (negative a^*), and the b^* parameter ranges from -80 to 100 and denotes yellowness (positive b^*) and blueness (negative b^*), and the CIE standard illuminates are generally used (l'Eclairage, 2004) Figure 2-5. Chroma (C^*_{ab}) can be calculated with Equation (2-1)(Lee, 2015).

$$C^*_{ab} = (a^2 + b^2)^{1/2}$$

Equation (2-2)

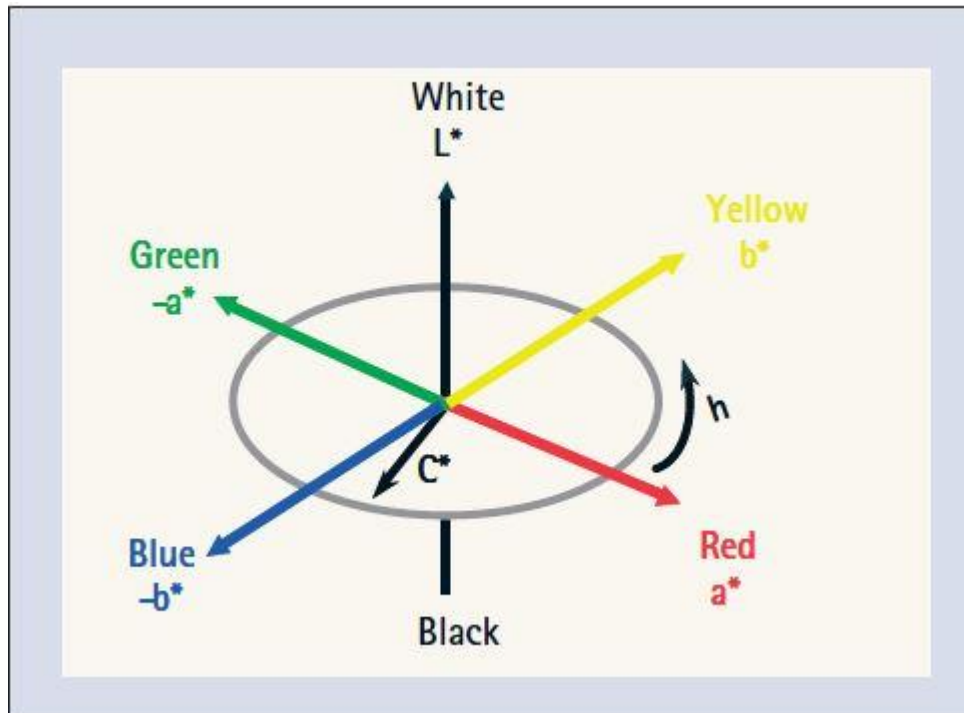


Figure 2-5 Representation of CIE L* a* b* space (Burkinshaw, 2004)

Even with the development of different instruments for measuring colours such as colorimeters and spectrophotometers, visual assessment in dental practice was still considered as one of the best approaches (Vichi et al., 2011). This is mainly due to the fact that the appearance of an object is not only controlled by the colour attribute of CIE Lab* but it can be heavily influenced by other geometric attributes of appearance which can include gloss, opacity, transparency, translucency, and optical phenomena such as metamerism, opalescence and fluorescence (Clark, 1933). All these appearance attributes made the optical characterisation of the tooth a complicated task and obtaining a high aesthetic result to be considered as an art form and not an easy systemised or instrumented procedure (Vichi et al., 2011).

Translucency is the ability of a material to allow light to pass through it. Accordingly, a material with low translucency is one with high opacity. As translucency is a measure of the relative amount of light transmitted through the material (Brodbeil et al., 1980) and one of the main parameters in matching the appearance of the natural tooth, it has been identified as a pivotal factor in controlling aesthetics and is a critical consideration for material selection (Miyagawa et al., 1981). Translucent materials allow light to pass

through only diffusely; they cannot be seen through clearly. (ISO-28642, 2016).

In addition to favourable mechanical properties, the translucency of dental ceramics is of crucial importance in aesthetic dentistry. (Brodbelt et al., 1980, O'Keefe et al., 1991). Several studies have used different methods in reporting the translucency and opacity of different restorative dental materials using a spectrophotometer (Powers et al., 1978, Brodbelt et al., 1980, Heffernan et al., 2002, Wang et al., 2013, Awad et al., 2015).

According to the (ISO-28642, 2016) guidance on colour measurement in dentistry and to the Commission Internationale de l'Eclairage (CIE, International Commission on Illumination) , calculating the colour difference (ΔE) is recommended to be based on (CIE) LAB colour parameters (l'Eclairage, 2004) .

Translucency of a material involves directly three parameters: the contrast ratio (CR), transmittance (T%) and translucency parameter (TP) (Carrabba et al., 2017).

Measuring the contrast ratio (CR) is one of the most commonly used methods to measure the translucency of dental ceramics. It can be defined as the ratio of the measurement of reflectance of a specific material against a black background to the reflectance of the same material against a white background of a known reflectance (Powers et al., 1978, Miyagawa et al., 1981, Heffernan et al., 2002, Yu et al., 2009, Liu et al., 2010a). It is an estimate of opacity. The CR value can be calculated using the Equation (2-3) or Equation (2-4).

$$CR = Y_b/Y_w \quad \text{Equation (2-3)}$$

Where; Y_b represents the spectral reflectance of light of the specimen over a black background and Y_w over a white background.

$$CR = L_b/L_w \quad \text{Equation (2-4)}$$

where; CR is the contrast ratio . L_b is the lightness measured over a black background. L_w is the lightness measured over a white background, The

subscripts *b* refers to the colour coordinates on the black background and *w* to those on the white background (Mohie el-Din Wahba et al., 2017).

CR ranges from 0 to 1, with 0 corresponding to transparency (totally translucent) and 1 corresponding to total opacity (absence of translucency) (Liu et al., 2010a, Carrabba et al., 2017).

The translucency parameter (TP) is the difference in the colour of a specimen measured over black and white backing and corresponds directly to a common visual assessment of translucency (Johnston et al., 1995, Johnston and Reisbick, 1997, Wang et al., 2013). It was originally introduced to assess the translucency of maxillofacial elastomer (Johnston et al., 1995). (Johnston and Reisbick, 1997) concluded that the major factors which can affect TP were the specimen thickness and the reflectance parameters of the black and white backings. It is one of the most widely used methods to compare relative translucency of dental materials.

The translucency parameter (TP) can be obtained using Equation (2-5),

$$TP = \sqrt{(L^*_b - L^*_w)^2 + (a^*_b - a^*_w)^2 + (b^*_b - b^*_w)^2} \quad \text{Equation (2-5)}$$

where L^* refers to the lightness, a^* to redness to greenness, and b^* to yellowness to blueness. The subscripts *b* refers to the colour coordinates on the black background and *w* to those on the white background (Wang et al., 2013). The higher the TP value the higher the translucency.

In addition to the aforementioned parameters, Transmittance percentage (T%) has also been used as a valid tool for evaluating translucency of dental ceramic. It is a measure of the fraction of incident light at a specified wavelength that passes through a sample (Harianawala et al., 2014). There are three types of transmission measurement which includes, direct transmission (when light goes through a tested object without a change in direction or quality), total transmission (measuring the diffuse light transmission in addition to the direct transmission) and spectral reflectance (measuring the fragment of the reflected light at an interface such as porosity)

(Harianawala et al., 2014, Harada et al., 2016). In dentistry, two types of T% can be used for measuring the translucency of dental ceramics: direct transmittance (Td%), and total transmittance (Tt%) (Brodbelt et al., 1980, O'Keefe et al., 1991, Kim et al., 2013, Harianawala et al., 2014, Awad et al., 2015, Harada et al., 2016). As Td% measures light that passes directly through the specimen without measuring the scattering or diffusing light, this is commonly used when the specimen to be measured is transparent or clear and therefore it might not be as relevant as Tt% in measuring translucency of dental materials. Tt% is most often used as a method for measuring translucency of dental ceramics. It measures all the light that passes through the specimen, which includes the direct transmitted and diffuse transmitted light (Brodbelt et al., 1980, Harianawala et al., 2014, Awad et al., 2015).

In a natural tooth, translucency is a product of a perceptible amount of light that passes through its enamel. This is mainly in the proximal and/or incisal aspect where enamel is of high proportion compared to underlying dentine. The light transmission is reduced with thicker dentine and thinner enamel as in the cervical region of the tooth (Barizon, 2011).

In addition to the thickness as a factor affecting the translucency of a material (Brodbelt et al., 1980, O'Keefe et al., 1991, Heffernan et al., 2002, Shokry et al., 2006, Ozturk et al., 2008, Yu et al., 2009), the translucency of enamel and dentine can be affected by the wavelength of the incident light. The smaller the wavelength, the lower the translucency value and vice versa (Cook and McAree, 1985, O'Brien, 1985, Watts and Addy, 2001, Paravina, 2004, Yu et al., 2009, Barizon, 2011).

(O'Keefe et al., 1991) studied the effect of different thickness and opacities of porcelain veneer on the light transmission. They stated that thickness was the primary factor affecting specular light transmission.

Surface gloss can affect the correct measurement of colour and translucency of tooth and porcelain due to specular reflection (O'Brien, 1985). Depending on the method of measurement, two types of transmittance can be identified. These two forms are specular and diffuse transmission or can be expressed as specular excluded and specular included. In the specular included method, all the light passing through the material plus all the light scattered in a forward

direction will be measured while for specular excluded, the proportion of light that does not reach the detector will be excluded from the measurement (O'Keefe et al., 1991). [NB in this study a specular excluded mode was used to avoid the error that can result from gloss reflection].

2.15 Retention of Ceramic Restorations

Achieving high retention and optimal marginal fit are of a considerable importance to the success of all ceramic restorations (Tinschert et al., 2001, Reich et al., 2005, Oyague et al., 2009). One of the main factors that determine the life of resin bonded restoration is adequate polymerization of resin cements. Insufficient polymerization of the resin cement can result in colour instability, toxicity from residual monomer, post-operative sensitivity and decreased bond strength leading to increased risk of caries as a result of increasing microleakage risk (Pilo and Cardash, 1992, Pires et al., 1993, Janda et al., 2004, Goldberg, 2008). The degree of polymerization of light-cured or dual-cured materials underlying the ceramic is highly affected by the translucency of dental ceramics. Light transmission through dental ceramic, such as veneers or even crowns and brackets, is crucial for adhesive luting materials. It is also of an importance to dual cured cementing materials that are sensitive to additional light curing (Ilie and Stawarczyk, 2014). The shade and the thickness of zirconia can have a direct effect on the degree of conversion of the luting cement, this means the thinner the restoration and the lighter its shade, the more irradiance energy passes through, resulting in optimal polymerization of the luting material (Myers et al., 1994, Rasetto et al., 2004, Passos et al., 2013, Ilie and Stawarczyk, 2014). The use of a dual cure luting cement was recommended for 1.5 mm thickness of light shaded zirconia or 0.5 mm thickness of dark shade zirconia. In addition to the thickness, shade, type of resin and composition of resin, the degree of cure can be affected by the output power, curing duration and the distance of light cure light-tip (Tanoue et al., 2003). An irradiance energy of $300\text{mW}/\text{cm}^2$ is recommended by International Organization for Standardization (ISO) and a standard depth of polymerization requirement is 1.5mm (ISO-10650, 2015). (Sulaiman et al., 2015a) in their study about the effect of monolithic zirconia with different thicknesses on light transmission stated that there was an

inverse relationship between translucency, irradiant energy and thickness of zirconia. Increasing the thickness resulted in reducing the translucency and irradiant energy. (Cho et al., 2015) studied the effect of different thickness of ceramic on the polymerization of different types of luting cement. They concluded that up to 0.9 mm thickness of ceramic has no effect on the degree of conversion and hardness of luting cement regardless whether it was light or dual cured. In addition, the dual cure resin cement showed a significantly lower degree of conversion with thickness of 1.2 mm of ceramic and an increase of curing time or light intensity was clinically recommended for dual cure resin cements for thickness more than this. It is clear that the performance of luting resin cements, light-cured or dual-cured, can be influenced by the amount of light transmission and the irradiant energy which both can be affected by the translucency and thickness of the ceramic restoration (Lee, 2015).

2.16 Aim of the study

This study aimed to comprehensively investigate the effect of accelerated aging on the mechanical and optical properties of disc samples made from four different types of zirconia powder expected to be used by up to 90% of dental zirconia manufacturers and to see how traditional and translucent zirconia behaved after aging in terms of their mechanical and optical properties.

2.17 Null hypothesis

1. There is no significant difference in the mechanical properties of all tested materials.
2. Aging has no significant effect on the mechanical properties.
3. There is no significant difference in the translucency of all tested materials
4. Aging has no significant effect on the translucency of all tested materials.

2.18 Objectives of the study

2.18.1 Mechanical properties

1. To measure the biaxial flexural strength according to ISO 6872.2015, together with characteristic strength and Weibull modulus of each material before and after hydrothermal aging. Aging was conducted using an autoclave at 134°C for 5 hours at 2.2 bar.
2. To measure the Vickers hardness of all materials before and after aging.

2.18.2 Structural analysis

1. To perform X-ray diffraction analysis on all materials; powder, sintered, before and after hydrothermal aging, followed by Rietveld analysis for quantification where possible of each phase; monoclinic, tetragonal or cubic zirconia.
2. To carry out SEM analysis to study the surface topography and measure the grain size of each tested material and to investigate fractured surfaces.
3. To use AFM to measure the surface roughness of all materials before and after aging.
4. To utilise FIB-SEM to see the effect of aging in depth for all tested materials.

2.18.3 Optical properties

1. To measure the translucency of all materials before and after aging with a spherical spectrophotometer. Translucency parameter TP, total transmission Tt% and contrast ratio CR were each measured to study the translucency.
2. To use the checkMARC® to measure direct transmission Td% of light through each sample.
3. To use a spherical spectrophotometer to measure the colour stability of the of all zirconia materials after aging.

Chapter 3 Materials and Methods

3.1 Materials

Five different types of zirconia powder were used in the current study;

- Three conventional zirconia core materials: TZ-3YS-E (3YE), TZ-3Y-E (3YE) and TZ-3YB-E (3YBE)
- Two full contour zirconia materials: Zpex (Zpex) and Zpex Smile (ZpexS)

All powders were supplied by TOSOH, Japan. Table 3-1 shows the content of all powder materials used in the study.

Table 3-1 Composition of powder materials

	TZ-3Y-SE	TZ-3Y-E	TZ-3Y-BE	Zpex	ZpexSmile
Actual Particle Size (μm)	0.09 (90nm)	0.04 (40nm)	0.04 (40nm)	0.04 (40nm)	0.090 (90nm)
Y ₂ O ₃ (wt%)	5.23	5.30	5.23	5.35	9.26
HfO ₂ (wt %)	< 5.0	< 5.0	< 5.0	< 5.0	
Al ₂ O ₃ (wt %)	0.25	0.25	0.25	0.052	0.048
SiO ₂ (wt %)	≤ 0.02	≤ 0.02	≤ 0.02	≤ 0.02	0.002
Fe ₂ O ₃ (wt %)	0.002	0.003	0.002	0.002	0.002
Na ₂ O (wt %)	0.007	0.028	0.022	≤ 0.04	
Specific Surface Area (m ² /g)	7 \pm 2	15.1	16 \pm 3	13 \pm 3	
Binder (wt%)			3	3	3

3.2 Sample Preparation

In this study, samples were prepared by different methods depending on the type of material used.

3.2.1 Uniaxial Press

This is a simple method using a die and press for the production of a wide range of engineering ceramics in different shapes and forms. It is cost effective, having a high production capacity in relation to time (Wang et al., 1992). It is mainly used to get the primary shape and to avoid wasting material (Arnaud, 2009), Figure 3-1.

In this study, this technique was used for producing samples by pressing each of the zirconia powders. A 20 mm die and a uniaxial press (Atlas Series Laboratory Hydraulic Press, Specac. USA) were used in the first step of sample production. In order to get discs of 1.2 ± 0.2 mm thickness and 14 ± 2 mm diameter (ISO-6872, 2015), 1.30, 1.30, 1.47, 1.50, 1.50 gm were used of each of the five materials 3YSE, 3YE, 3YBE, Zpex and ZpexS respectively. These specific weights for each material type were decided following pilot studies whereby discs of different thicknesses using different weights for each specific material were produced to get the right dimension after shrinkage of each zirconia powder following sintering. Powder was weighed using a balance with accuracy of 0.001gm (Ohaus Corporation, Switzerland). The press load was 70 MPa for 30 seconds according to the manufacturer's instructions. Despite the aforementioned advantages of this method, the uniaxial press still has limitations (i) to produce only simple not sophisticated shapes and (ii) to produce density heterogeneities in green state zirconia with different shrinkage, arising from the load being applied parallel to the long axis of samples rather than applying pressure uniformly (Wang et al., 1992, Arnaud, 2009). (Figure 3-1) illustrates how this press works.

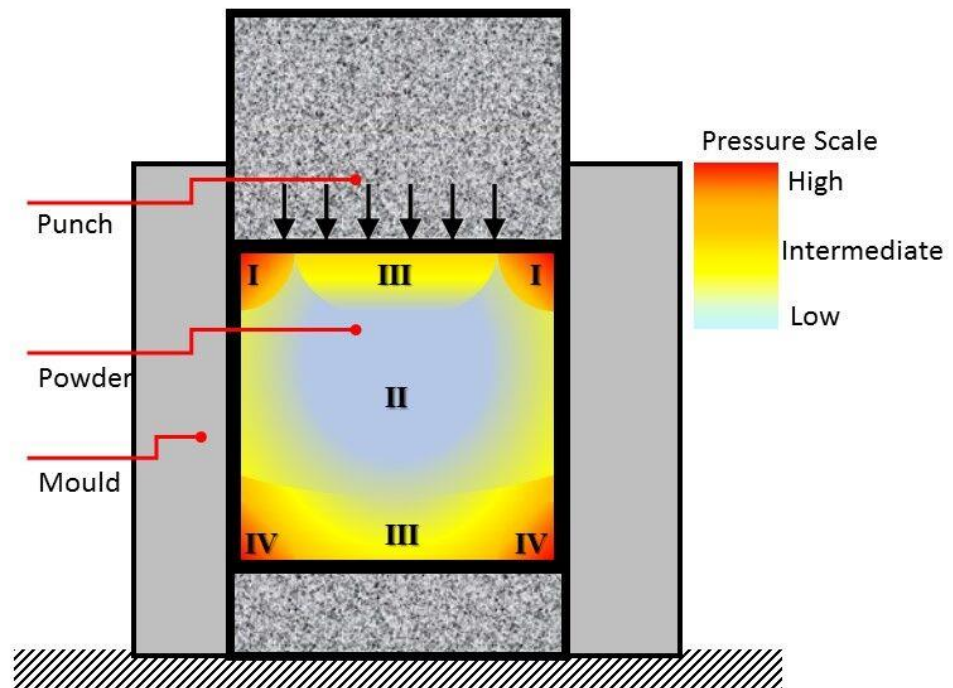


Figure 3-1 schematic illustration of Uniaxial press and pressure

distribution within the sample. KEY: numbers correspond to areas in the powder compact exhibiting high (I and IV), intermediate (III) and low (II) pressure during compaction

3.2.2 Cold Isostatic Press

Cold isostatic pressing is a powder-forming process where compaction takes place under isostatic or near-isostatic pressure conditions. In contrast to uniaxial pressing, this press allows the sample to receive a uniform pressure from all sides (Figure 3-2). The uniaxially pressed powder is first sealed in an elastomeric mould, which is then pressurised by a liquid, such that the powders become compacted under (hydrostatic) pressure. Typically, pressures up to 400 MPa are used on an industrial scale, although some laboratory equipment is designed to operate at pressures up to 1 GPa. The pressure medium must be compatible with the tool, the vessel, and the pumping system. In practice, special oils, glycerin or water with anticorrosive and lubricating additives are used. As these fluids are not incompressible at high pressures, they can store considerable elastic energy and, consequently,

safety aspects must be considered when designing and operating the pressing equipment (Riedel and Chen, 2011).

In this study, cold isostatic pressing was used to optimise sample properties (Arnaud, 2009) and to get uniformly pressed samples by applying uniform pressure. Samples initially prepared by uniaxial pressing were subsequently placed in a doubled latex gloves to protect them from contamination by fluid, and then immersed in the chamber of a cold isostatic press (Stansted Fluid Power, United Kingdom). These samples were pressed isostatically at 200 MPa for twenty minutes. Whereas it was possible to only produce single samples using the uniaxial press, multiple samples could be processed simultaneously in the cold isostatic press.

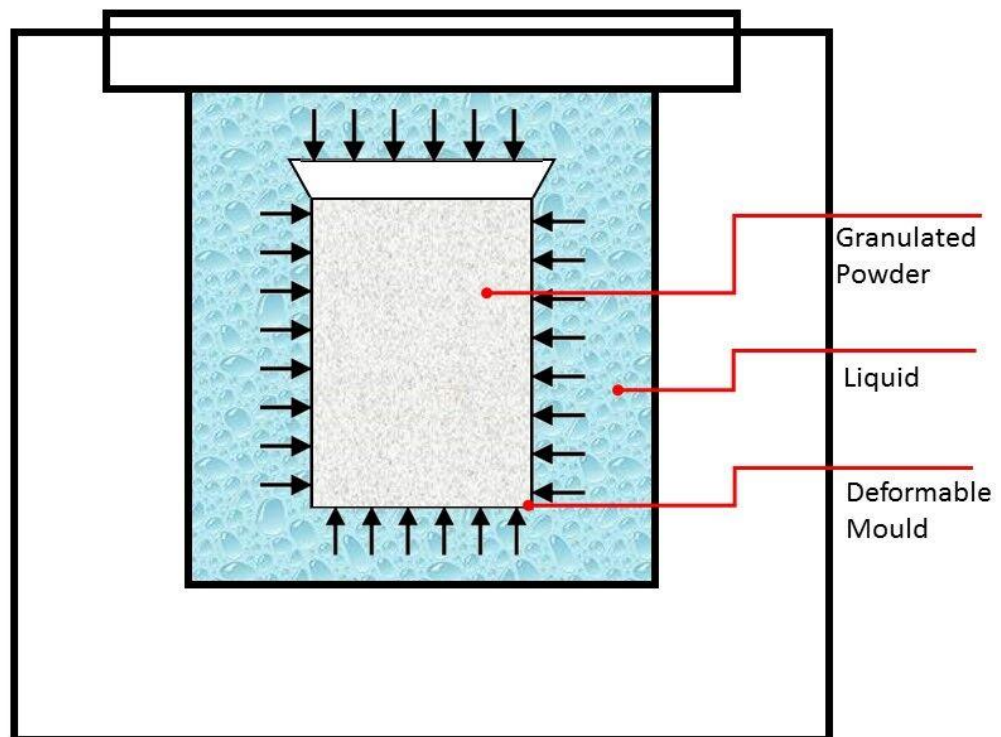


Figure 3-2 schematic illustration of Cold Isostatic press and pressure distribution.

3.2.3 Sintering

The green bodies produced following uniaxial and cold isostatic pressing of zirconia powders were sintered according to the manufacturer's instructions using a PyroTherm furnace (Elite, Leicestershire, UK). For 3YE, the target temperature was 1350 °C with a heating rate of 100 °C /hr and holding time of

2 hours followed by natural cooling to room temperature. For both 3YSE and 3YBE, the target temperature was 1450 °C with a heating rate of 100 °C /hr and holding time of 2 hours followed by natural cooling to room temperature. For Zpex and ZpexS the target temperature was 1450 °C with a heating rate of 50 °C until 300 °C and holding time for 5 hrs then further heating to 700 °C and holding for one hour then further heating to 1000 °C for one hour followed by natural cooling to room temperature then sintered at 1450 °C with heating rate of 600 /hr for two hours followed by natural cooling to room temperature. Zirconia beads (Yttria stabilised zirconia, YSZ, spherical, 0.5mm, Inframat, Advanced Material, USA) were used to allow uniform heating of all sample faces.

3.2.4 Hydrothermal Artificial Aging

Hydrothermal aging for samples was conducted by using an autoclave (Rodwell Ambassador, UK). The cycle was 5 hours at 134 C° and 2.2 bar which has been suggested to simulate 15-20 years of low temperature degradation (Chevalier et al., 2007). This is the most widely used zirconia aging process and forms part of ISO standard 13356:2015 which states that autoclave aging under these parameters should produce less than 25% phase transformation for the material to be biomedically accepted. The samples were placed in individual autoclavable small glass containers and immersed in distilled water then placed on a tray in the autoclave for aging. After finishing the cycle, samples were taken out and left to dry at room temperature to be used for further experiments.

3.3 Physical and Mechanical Properties

3.3.1 Shrinkage and Density

The shrinkage and density of all groups were measured. The variation in density can result in variation in shrinkage and can cause distortion and cracking during firing; such variation is a potential drawback of using uniaxial pressing alone as mentioned earlier (Richerson, 2005). This variation can result from either the friction between powder particles itself or between powder and the die wall or both of them. Areas with lower density during firing will either shrink more than the surrounded area or will not densify sufficiently

and both can result in an unacceptable restoration. Binders have been found to increase the strength of the “green” body and act as a lubricant by reducing particle-particle and particle – die friction during compaction (Richerson, Richerson, 2005, Callister Jr, 2005).

For density, 5 samples of each material were weighed, using a highly sensitive balance with accuracy of 0.001 gm (Ohaus Corporation, Switzerland), before and after sintering with measurement of the diameter and thickness using a high precision digital calliper (Mitutoyo, Japan). Density was measured before and after sintering according to Equation (3-1).

$$d = \frac{M}{V} \text{ (g/cm}^3\text{)} \quad \text{Equation (3-1)}$$

Where d is the density M is the mass in gram and V is the volume in cm^3 .

Sintering shrinkage (an average of 20-25% (McLean, 1965)) can result in significant discrepancies in the fit and adaptation of the restoration and in order to overcome this problem, the CAD/CAM process produces an enlarged pre-sintered restoration to compensate for the shrinkage after sintering of the restoration (Suttor et al., 2001, Piwowarczyk et al., 2005).

The linear shrinkage was determined by measuring the change in diameter of the specimen discs ($n=5$) before and after sintering using a high precision digital calliper (Mitutoyo, Japan) and Equation (3-5) for the calculation (Pittayachawan, 2009).

$$\text{shrinkage} = \frac{I_0 - I}{I_0} \times 100 \quad \text{Equation (3-2)}$$

Where I_0 is the initial diameter and the I is the diameter after sintering.

3.3.2 Flexural Strength

The mechanical properties of any dental material are regarded as the mirror for success of that material. Testing of mechanical properties can be done either *in vivo* or *in vitro*. *In vivo* methods can be subjective, take a long time and the results are difficult to analyse, while *in vitro* testing of materials can be more meaningful in terms of material properties (Mijoska and Popovska, 2015). In the mouth, forces generated from the clinical situation can result in

flexural forces, therefore for any dental material to be successful it needs to withstand repeated flexing, bending, and twisting. High flexural strength is desirable so the material can withstand the stress generated during chewing (Wang et al., 2003). For the reasons mentioned above, flexural strength is one of the most important parameters to be investigated and is generally considered a meaningful and reliable method correlating with clinical potential and also defines the limitation of use of different dental ceramics (Ban and Anusavice, 1990, Lawn et al., 2001, Guazzato et al., 2002, Isgrò et al., 2003, Mijoska and Popovska, 2015).

Strength is defined as the ultimate stress that is necessary to cause fracture and is strongly affected by the size of flaws and defects present on the surface of the tested material (Mecholsky, 1995, Guazzato et al., 2002). *“Flexural strength also known as modulus of rupture, or bend strength, or transverse rupture strength, is a material property, defined as the stress in a material just before it yields in a flexure test”* (Ashby and Cebon, 1993).

The flexural strength of ceramics can be measured by uniaxial or biaxial testing method. In uniaxial flexure tests, the principal stress on the lower surfaces of the specimens is tensile, which is usually responsible for crack initiation in brittle materials. However, these tests are usually used for engineering materials that are designed as large specimens (Ban and Anusavice, 1990). The uniaxial flexural test is either a three point (3PBT) or four point (4PBT) bending test. In the 3PBT, a bar-shaped specimen is subjected to bending by compressive loading through a central point equally distant from the two lower supports, producing tensile stresses in the lower surface that are likely to initiate fracture, Figure 3-3 (a). In this test, the stress will be confined to the area between the supporting rollers and the loading roller. The 4PBT uses the same bar-shaped specimens, but the bar is loaded by two load cylinders over the upper surface of the specimens, Figure 3-3 (b) which allow exposure of a bigger area of the material and a higher flaw containing area to the stress when compared to the 3PBT (Rodrigues et al., 2008).

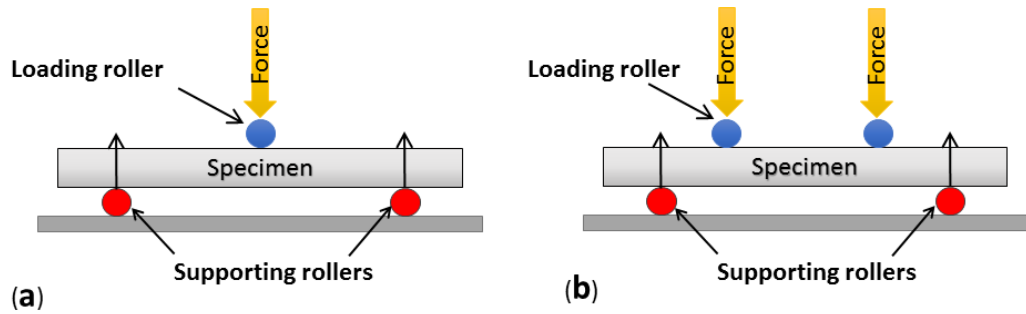


Figure 3-3 (a) Three Point Bending Test (b) Four Point Bending Test

In dentistry, brittle dental materials cannot be constructed as large specimens and often the materials are not available in large enough quantities to produce sufficient number of samples to get a statistically significant difference (Ban and Anusavice, 1990). The strength measurement of brittle materials by biaxial flexure is considered to be more reliable than the uniaxial conditions, because the maximum tensile stresses develop within the central loading area and spurious edge failures are eliminated (Kondo et al., 2010). It is simple to achieve with more precision compared to uniaxial method (Mijoska and Popovska, 2015) and provides a better simulation of clinically relevant sample size (Ban and Anusavice, 1990).

The biaxial flexural test can be determined, using three ball bearings supporting a disk-shaped ceramic specimen with specific dimensions, the balls are in equal distance from each other on a known radius and the load is applied centrally from the top (also known as piston-on-3 balls) (Kirstein and Woolley, 1967, Yilmaz et al., 2007),

Figure 3-4.

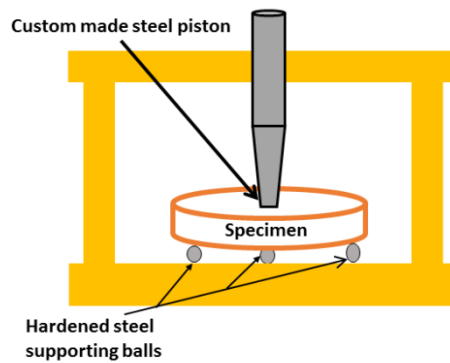


Figure 3-4 Biaxial Flexural Test

In this study, the strength of different types of pressed and sintered zirconia powders was measured with the biaxial flexural strength test (piston on 3 balls) and samples prepared according to ISO 6872:2015 as explained in Section 2.2.

[NB At this stage, 3YSE was dropped from the range of materials used in this study due to difficulty in processing it into disks at the uniaxial pressing stage emphasizing that care must be given when selecting zirconia powders with an emphasis placed on the processability of the green body during uniaxial pressing (Aziz et al., 2015)].

120 discs were prepared, 30 per each powder material; half were subsequently aged hydrothermally as in Section 2.3. This resulted in eight groups as follows, 3YE_BA, 3YBE_BA, Zpex_BA, ZpexS_BA, 3YE_AA, 3YBE_AA, Zpex_AA and ZpexS_AA (where BA represents Before Aging and AA, After Aging). The biaxial flexural strength (BFS) (n=15 discs) of the eight groups was measured according to ISO 6872:2015, samples were tested dry at room temperature. A universal testing machine (Model 3365, Instron UK) was used for this purpose. Prior to the test, the radius and thickness of each sample were measured three times using a high precision digital calliper (Mitutoyo, Japan) with an accuracy of 0.001mm and an average was obtained. Each disc specimen was placed centrally on three, industry-standard grade, hardened steel 5 mm diameter ball bearings. Ball bearings were placed 120° apart on a 10 mm diameter support circle.

Discs were loaded using a custom-made, steel, 1.5 mm diameter piston at a cross head speed of 1.00 mm/min until failure point. The UTM was equipped with a 5 kN load cell. The fracture loads were obtained from load-extension graphs generated by (Instron Bluehill software, version 3.65, USA). BFS values were calculated using following equations:

$$BFS(MPa) = -0.2387 \frac{\sigma(X - Y)}{d^2} \quad \text{Equation (3-3)}$$

$$X = (1 + \nu) \ln \left(\frac{r2}{r3} \right)^2 + \left[\frac{1 - \nu}{2} \right] \left(\frac{r2}{r3} \right)^2 \quad \text{Equation (3-4)}$$

$$Y = (1 + \nu) \left[1 + \ln \left(\frac{r1}{r3} \right) \right]^2 + (1 - \nu) \left(\frac{r1}{r3} \right)^2 \quad \text{Equation (3-5)}$$

Where;

σ : fracture load (N)

d: disc' thickness at loading point (mm)

ν : Poisson's ratio (assumed to be 0.25)

r1: radius of support circle (mm)

r2: radius of loaded area = radius of pushing rod (mm)

r3: radius of the disc (mm)

Following normality testing, SPSS statistics, version 21 (IBM, USA) was used to perform one-way analysis of variance (ANOVA) to assess statistical differences between the means of *BFS* of all groups and the effect of aging on each group.

3.3.2.1 Weibull Analysis

Under identical testing conditions, the maximum measured stress that a sample (for a given brittle material such as ceramic) can withstand before failure may vary from sample to sample. The size of physical flaws and their distribution within the surface or the body of each sample play an important role in determining the stress that can be withstood before failure in addition to defining the probability of failure of the given material. Depending on the distribution of these flaws, samples will be expected to behave more

consistently when flaws are clustered tightly and more inconsistently with a wider range of flaw sizes. Therefore to describe a strength of a brittle material such as a ceramic, it has been suggested that it should be presented as a distribution of values instead of one specific value (Davidge, 1979, Afferrante et al., 2006, Wachtman et al., 2009, Munz and Fett, 2013).

For more than 70 years, the statistical theory of brittle fracture proposed by Weibull (Weibull, 1939, Weibull, 1951) has been regarded as the basis of this statistical approach to property measurement (Evans, 1982).

The Weibull distribution is a shape parameter that maps the failure probability of a given component statistically at varying stress and can be used describe the variability in strength of the samples of a given material. The higher the Weibull modulus the more uniformly distributed flaws are throughout the material, whether that is inherent as a property of the material or as a result of its manufacturing process. On the contrary, a high variation in the flaws of the material and inconsistently clustered flaws can result in low Weibull distribution and a weak measured, variable strength of the material. The material with low Weibull modulus will be described as with low reliability (Klein, 2009).

The two parameter Weibull distribution function for a brittle sample with a volume (V) subjected to uniaxial fracture strength (σ) test is given by Equation (3-6).

$$f = 1 - \exp \left[-\frac{V}{V_0} \left[\frac{\sigma}{\sigma_0} \right]^m \right] \quad \text{Equation (3-6)}$$

Where;

f is the probability of failure,

m is the Weibull modulus,

σ , is the stress level below which the material will not fail (equals 0), and

σ_0 is the characteristic strength

V_0 is the chosen normalising volume.

There is an inverse relationship between the Weibull modulus, m , and the distribution of data. The smaller the distribution of fracture strength data the higher the modulus value which is representing the measure for the scatter of strength data (Herrero, 2007). The m value for dental ceramics typically has the range of 5-15. σ_0 is a characteristic strength value, "*the stress at which the probability of failure equals 63%*"(Herrero, 2007, Jum'ah, 2015).

The statistical distribution of *BFS* of all groups has been studied extensively. Two-parameter Weibull distribution analysis and 95% (2-sided) confidence intervals (95% *CI*) according to the maximum likelihood method were carried out on all groups before and after aging . Statistical software (Weibull ++, version 10; ReliaSoft Corp, Tucson, Arizona) was used for the determination of the two-parameter Weibull estimates and Origin Pro 93E, 2016 (OriginLab, USA) was used to plot the output data using Benard approximation.

3.3.3 Hardness

Hardness is considered as a crucial property to be investigated especially when comparing restorative materials (Albakry et al., 2003). It is one of the most frequently measured properties of ceramics. Its value helps to characterise resistance to deformation, densification, and fracture (Yilmaz et al., 2007) and most importantly delineates how abrasive the material could be to the natural dentition (Albakry et al., 2003). Vickers and Knoop are the most commonly used micro-hardness instruments. They make an impression in the material using diamond indenters. An attached optical microscope is used to measure the diagonal size (Quinn, 1998).

Hardness of ceramics could be affected by many elements including the process of manufacturing, chemical composition and starting particle size. (Maccauro et al., 2009, Abbas et al., 2015). The presence of porosity in any solid material can affect its mechanical properties including hardness.

3.3.3.1 Knoop Hardness

Knoop is mainly used for measuring the hardness of a very brittle materials or thin sheets by introducing a small indentation in the material for testing purposes (Knoop et al., 1939). It is highly sensitive to the material's surface characteristics in comparison to Vickers hardness test (Wang et al., 2003). In dentistry, it is most commonly used for measuring the hardness of resin

materials as an indicator for the degree of polymerization of resin composite and resin cement (Uhl et al., 2002, Hofmann et al., 2002, Caldas et al., 2003, Uhl et al., 2003, Fugolin et al., 2016, Ilie et al., 2017, Al Badr and Hassan, 2017). In addition to that, Knoop has been used heavily to indicate the degree of remineralization of enamel and dentin after different experimental treatment (Pereira et al., 1998, Shinkai et al., 2001, Wang et al., 2003).

3.3.3.2 Vickers Hardness

A square-based sharp pyramidal diamond indenter having specified face angles is forced into the test-piece surface under a defined force, held for a defined duration and removed. The indentation diagonal lengths are measured, the mean result calculated, and this value is then employed to calculate a hardness number which is equivalent to the mean force per actual unit area of indenter surface contacting the test surface (no units are given, but kgf/mm² are implied):

$$HVF = 1,8544 \frac{F}{d^2} \quad \text{Equation (3-7)}$$

Where:

HVF is the Vickers hardness number at applied force F (expressed as the mass in kg from which F is derived), and where d is the mean length of the diagonals of the indentation (expressed as mm) (ISO-843-4, 2015).

A Vickers indenter goes twice the depth of the Knoop indenter into the tested material. It is less sensitive to the conditions of material surface but more sensitive to measurement errors than Knoop test (Wang et al., 2003)

In this study, Vickers hardness was determined using a Duramin Microhardness Tester (Struers, Denmark) for all groups (n=5 discs) according to the ISO standard, (ISO-14705, 2016).

Measurements were conducted before and after aging to assess the effect of aging and how surface micro cracking resulting from transformation can affect the mechanical properties and also as an indication for the transformation (Chevalier, 2006). The instrument's camera was calibrated using an Olympus graticule at 100Nm. The hardness tester was calibrated using a Shimadzu test block with 300 gm load for 5 sec. Each disc was

subjected to four indentation tests performed on randomly selected areas. Average microhardness measurement was calculated for each sample. Vickers hardness was performed using 3 N loading for 5 sec. The indentation diagonal lengths were defined using an integral optical microscope under 40X magnification and Duramin 5 software was used for reading hardness value for each single test. Following normality testing, SPSS statistics, version 21 (IBM, USA) was used to perform one-way analysis of variance (ANOVA) to assess statistical differences between the means of hardness of all groups and the effect of aging on each group.

3.4 Structural Analysis

3.4.1 Scanning Electron Microscope (SEM)

A scanning electron microscope (SEM) is a microscope that depends in its scanning and image producing of a sample on a focused beam of electrons. The interaction between the atoms in the sample with the electrons from the microscope beam result in various signals which are responsible for producing a surface topography and information about the composition of the sample (Stokes, 2008).

SEM has been heavily used in dentistry. It has been used for evaluating and investigating different types of dental materials, such as ceramics (Luo et al., 2001), metallic dental materials (Cortizo et al., 2004) acrylic based materials (Lessa et al., 2007) and composite (Mitra et al., 2003). In addition to that , it has also been used in tooth structure investigation (Basdra et al., 1996). The SEM regarded as a versatile tool with the capacity of providing an observation of a large area of a specimen at low magnification (Shen, 2013) and it can also provide a high resolution images in a range of 1-10nm with the introduction of field emission scanning electron microscopes (FESEM) (Egerton, 2005, Shen, 2013). FESEM is very fruitful and powerful in studying ceramic surfaces and surface related phenomena (Ravishankar and Carter, 1999). SEM has been used for evaluating the effects of LTD on the surface of zirconia ceramic materials. It can show transformed zones, micro cracks and any uplifted grains as a result of aging (Chevalier et al., 2007, Jum'ah, 2015).

As a result of LTD , the scanned sample can be seen under SEM with areas of different contrast. Area with white bright colour can be referred to as a transformed area and this brightness is due to the increase in the contrast as a result of microcracking and loss of cohesion of the crystals as a product of LTD effect. On the other hand, the dark grey or black coloured area that can be shown on the scanned sample can be recorded as unaffected area by LTD (Chevalier et al., 2007). There are many other different signs that can be an indication of transformation due to LTD, such as intergranular cracks that can be seen using a high magnification during scanning. Twinning of the crystals is another sign that can be explored in the deeper layer of the tested samples during scanning of the cross section of the sample (Sanon et al., 2013, Keuper et al., 2013, Jum'ah, 2015). This twinning of the crystals can result from the mechanically-constrained transformed tetragonal grain within the crystalline lattice with the failure of formation of martensitic relief. This can be followed by loss of grain boundaries. All of these changes make the transformed layer to present as a distinctively heterogeneous compared to homogenous untransformed tetragonal crystals (Keuper et al., 2013, Jum'ah, 2015).

In addition to identifying the effect of LTD on zirconia ceramics, SEM is of high importance to be used to provide an information about the fracture initiation point during scanning the fractured surface. It is useful because it can detect the explicit marking on the fractured surface of the brittle material such as ceramic helping in fracture pattern recognition which is crucial for fracture analysis (Shen, 2013).

For the SEM imaging the Cold Field Emission Scanning Electron Microscope (CFE-SEM) (Hitachi SU8230) was used in Leeds Electron Microscopy and Spectroscopy Centre (LEMAS). A representative disc sample from each group in the study was mounted on aluminium stubs (Agar scientific, Cambridge, UK) using a conducting carbon sticker for examining the sample before and after aging. For fractography, a broken disc sample from each group studied in this study was mounted using a vertical sample holder to reduce the movement of the fractured disc during scanning. The SEM images were obtained with an accelerating voltage of 2 kv for analysing the possible changes in surface structure of zirconia groups after aging and to study the fracture pattern for the broken side of the sample. The samples were thermally

etched by heating them using a PyroTherm furnace (Elite, Leicestershire, UK) to 100°degree below their recommended sintering temperature at 250 degree/hour heating rate and 1.00 hour dwell time to reveal the grain boundary network as recommended by the manufacturer. All specimens were sputter coated with a 20nm of iridium using a high resolution sputter coater to reduce the charging of the zirconia discs (Agar scientific, UK) followed by cleaning using ZONE SEM sample cleaner and desiccator (Hitachi) before CFSEM examinations. The SEM images were collected in different magnifications for both the surface of the samples and to the broken side, in order to understand the fractography of each material.

3.4.2 Grain Size Measurement

The grain size measurement for the samples before and after aging was conducted by lineal intercept method which involved counting the number of interception made by known length test line (Wurst and Nelson, 1972) on a digitally calibrated SEM image of the sample surface using Fiji (Image j software), six lines in different orientation were used for each analysed image, then this **Equation (3-8)** used:

$$D = 1.56 \frac{C}{MN} \quad \text{Equation (3-8)}$$

Where D is the average grain size, C the total length of test line used, N the number of intercepts and M the magnification of the photomicrograph which has not been used in this study as the image already digitally calibrated. The 1.56 is the correction factor or the proportionality constant.

3.4.3 Focused Ion Beam/Scanning electron Microscope

With the continuous advances in nanotechnology, there is an increased demand for using high resolution microscopy. The scanning electron microscopy (SEM), transmission electron microscopy (TEM) or atomic force microscopy (AFM) can give nanoscale details but more likely in 2D rather than 3D (Holzer et al., 2004). Recently, focused ion beam nanotomography (FIB-nt) by using electron microscopy presents a powerful technique that allows 3D volume reconstruction of the material, on the sub-100-nm scale. The focused ion beam microscope is proposed to be as an innovative device for the high resolution measurement of residual stress at a sample surface (Korsunsky et

al., 2010). FIB/SEM analysis of metal-ceramic and zirconia-ceramic systems has been found very useful in the morphological and microstructural characterization of the interfaces, giving good knowledge about the interpretation of failures (Massimi et al., 2012). Preparing a cross section of the zirconia disc to study the effect of aging in depth can be a challenging procedure and lead to misleading result in terms of the amount of transformation resulting from LTD. This can be simply explained by the extra transformation that can result from grinding and polishing, which can cause stress induced transformation and subsequent micro cracking (Reed and Lejus, 1977; Jum'ah, 2015; Husain et al., 2016; Bartolo et al., 2017; Khayat et al., 2017; Park et al., 2017). According to (Keuper et al., 2013), FIB milling is an ideal tool for preparing cross sections of ZrO_2 without inducing a transformation process in the prepared area and its been used to study transformation in zirconia by several authors (Soldera et al., 2007, Gaillard et al., 2008, Sanon et al., 2013, Dehestani and Adolfsson, 2013). The integration of FIB with SEM and addition of an electron beam column results in the formation of the dual beam FIB-SEM. The advancement in this technology has made preparation and scanning of fine cross sections of sensitive material achievable and feasible and established an innovative way for advanced material analysis (Langford and Clinton, 2004).

To understand the effect of aging through a depth of the zirconia samples, 3D images of a representative samples were obtained before and after aging using a FEI Nova 200 FIB/SEM (Nanolab, USA). The system used was a combination of a high resolution field emission SEM with Schottky thermal field emitter and etch and deposition capabilities in addition to precise FIB. To operate the FIB at a voltage of 30 kV, a liquid gallium ion source was used.

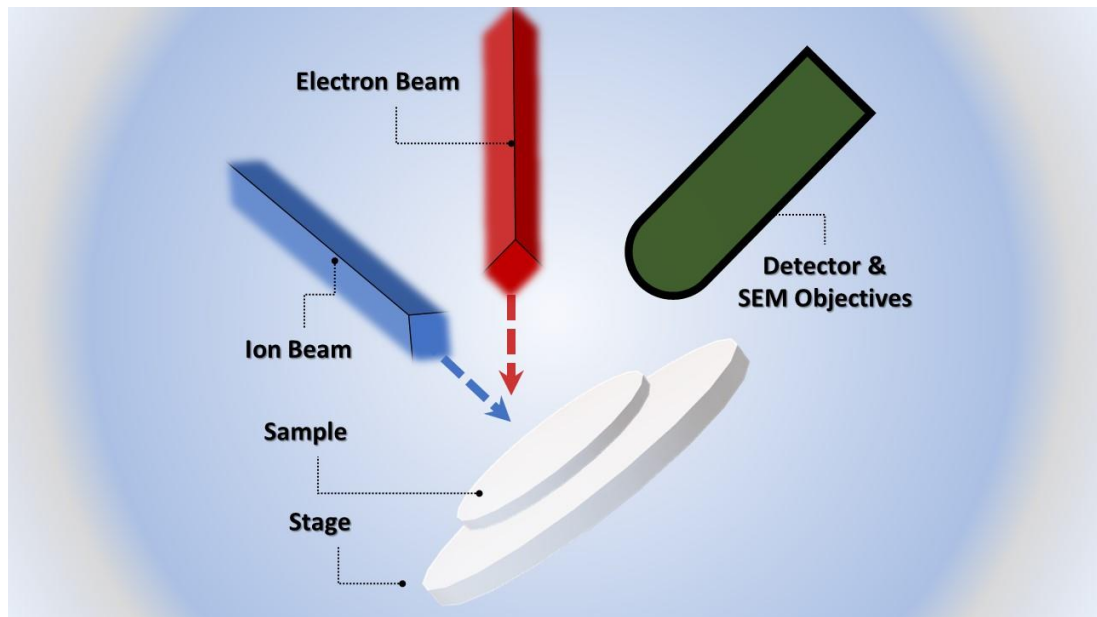


Figure 3-5 FIB-SEM setup used

A representative disc sample from each group in the study was mounted on an aluminium stub (Agar scientific, Cambridge, UK) using a conducting carbon sticker for examining the sample before and after aging. All specimens were sputter coated with a 20nm of iridium using a high resolution sputter coater to reduce the charging of the zirconia discs (Agar scientific, UK) followed by cleaning using ZONE SEM sample cleaner and desiccator (Hitachi). The samples were then transferred to the FIB-SEM at the Leeds Electron Microscopy and Spectroscopy Centre in the University of Leeds. A random area on the centre of each sample was chosen to be investigated and a 1 μ m thick platinum protection layer was deposited onto the sample using 3nA beam current to maintain the fine details of the top most surface of the studied disc by preventing ion induced damage and milling artefacts. A trench of 15 μ m wide, 30 μ m long and 30 μ m deep was cut 20nm in front of the protection layer. A cleaning cross-section 10 x 2 x 15 μ m was performed using 0.3nA which imparted less damage into the sample face and also to have a better beam profile. The final polishing cross section was performed at 50pA and 10 x 0.3 x 15 μ m. Figure 3-5 shows the setting of the FIB-SEM used in this study.

The sample was then returned to 0° tilt and rotated so that the ion beam can image the sample cross section. The imaging was performed using the ion beam at 30pA taking images while etching the sample to enhance contrast of the grain boundaries. The prepared area then examined thoroughly to see if

there was any effect of aging on homogeneity of crystals or any micro cracks, porosity and grain up-lift.

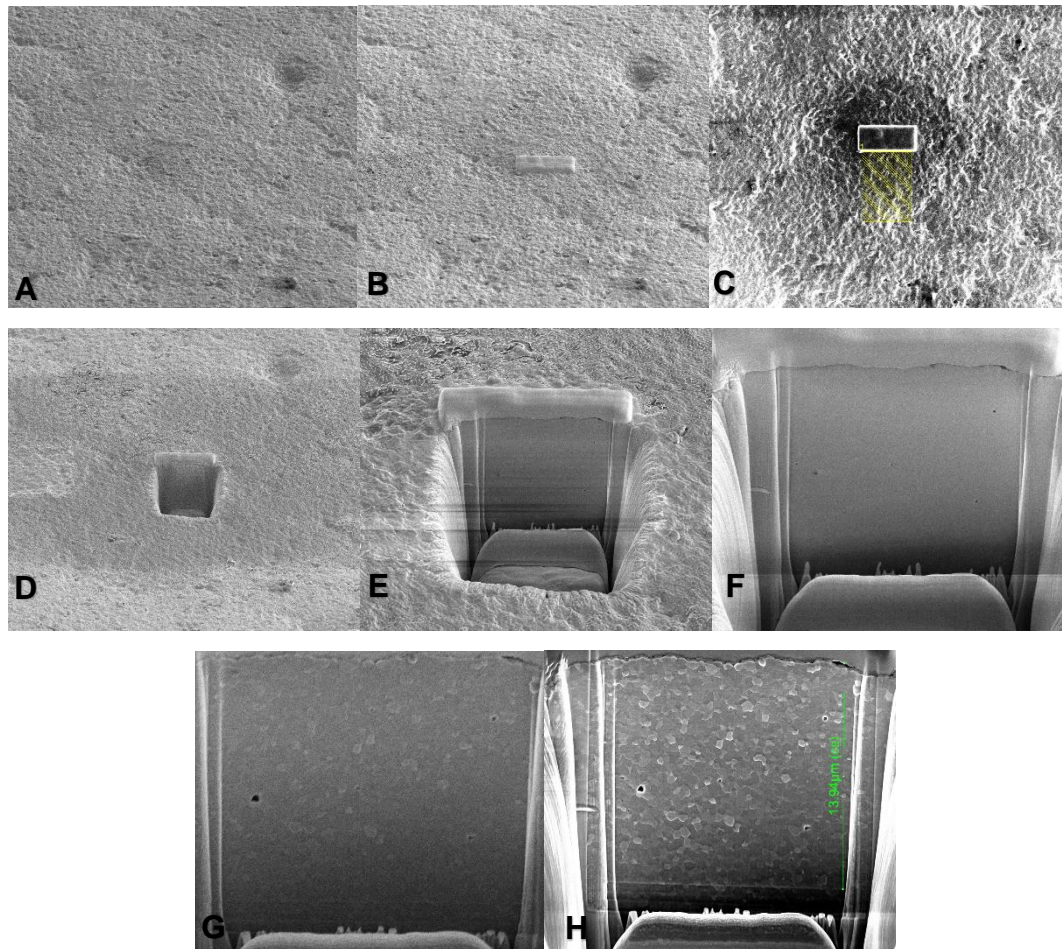


Figure 3-6 Stages of FIB-SEM sample preparation and Imaging (A)

Determination of area of interest (B) Platinum layer deposition (C) Area to be milled (D) Bulk removal (E) Bulk removal of depth (F) Cleaning cross section (G) first Ion Beam Image (H) Ion beam immersion image to improve resolution.

3.4.4 X-Ray diffraction

XRD is one of the most commonly used method for phase characterisation and quantification of zirconia ceramics (Deville et al., 2005), simply because it is non-destructive, rapid and resourceful technique being widely used for analysing the crystal phase of ceramic before and after different treatment (Egilmez et al., 2014, Siarampi et al., 2014, Vatali et al., 2014, Wang, 2014).

The X-ray diffraction pattern of a pure substance is like a fingerprint of the substance; the pattern is characteristic of the specific atomic arrangement within a given phase (Jenkins, 2000).

Bragg's law (Equation (3-9)) is considered as the basis for XRD, where the inter-atomic distance and electron density of the tested material can be indicated by the pattern and intensity of diffracted X-Ray beams. Furthermore, XRD can be used to conduct texture analysis with the ability of identification of preferred crystal orientation within the crystalline lattice. To understand the behaviour of a material mechanically, physically and chemically, it is crucial to study its texture as one of the important factors to be considered (Vanasupa et al., 1999, Almer et al., 2003, Jum'ah, 2015)

$$n\lambda = 2d \sin \theta$$

Equation (3-9)

Where:

n: integer,

λ : electromagnetic radiation wavelength,

d: the separation of the reflecting planes, and

θ : the angle of incidence of X-Rays

To check the phases and their percentage for the starting powder and sintered bodies and also the effect of aging and the amount of transformation of tetragonal to monoclinic, X-ray diffraction (XRD) (Phillips X'Pert diffractometer, Panalytical B.V, The Netherlands) with Ni filtered Cu K α 1 X-rays was used for phase characterization and tetragonal (t)- monoclinic (m) transformation. It was performed on powders and the sintered bodies of all groups before and after aging. Samples were mounted on a spinner sample holder using a small amount of plasticine that was completely imbedded under the sample (ISO-6872, 2015, Jum'ah, 2015). The beam length was adjusted to 2 mm and a 10 mm fixed incident beam mask was used for collimation of the width of exposed area.

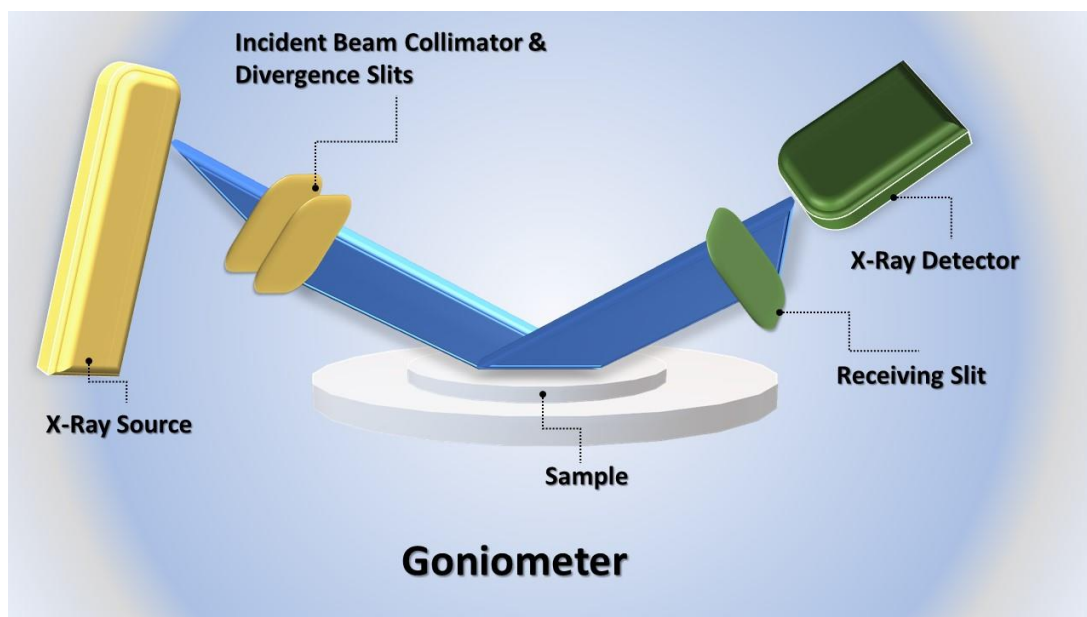


Figure 3-7 Classic Bragg-Brentano XRD setup

X'Pert Data Collector software (Panalytical B.V, The Netherlands) was used for collection of data in a classical Bragg-Brentano geometry from 27° to 33° 2θ with step size of 0.033 and counting time of 400 s/step and from 55 – 65° 2θ to determine the cubic and tetragonal peaks. To ensure that over the 2θ range, an equal area would be irradiated, automatic divergence slits (ADS) were used.

The phase quantification was conducted by High Score Plus software (Panalytical B.V, The Netherlands) with Rietveld refinement analysis to determine the amount of volume percentage of monoclinic, tetragonal and cubic phase in each sample. Figure 3-7 shows the XRD setup used.

This included opening the XRD pattern into High Score Plus and then determining the background followed by searching peaks. After auto fitting of peak profile, search and match was conducted with search-limiting for elements to those available from the manufacturers' data sheets. The best matching reference from the data base (the International Centre of Diffraction Data (ICDD) database) was selected and a refinement was conducted to measure the fraction of each phase. The selection of references was made depending on the best matching probability.

The reference diffraction pattern for monoclinic was based on Howard et al (1990) and Scott (1975) with a space group of P21/c and lattice parameters

of $a=5.1440 \text{ \AA}$, $b=5.1330 \text{ \AA}$ and $c=5.3470 \text{ \AA}$ (Howard et al., 1990) and $a=5.1590 \text{ \AA}$, $b=5.2110 \text{ \AA}$ and $c=5.3210 \text{ \AA}$ (Scott, 1975). The reference diffraction pattern for tetragonal was based on yttria stabilised tetragonal zirconia data by Bouvier et al (2000) and Ding et al (2012) with a space group of P42/nmc and lattice parameters of $a=3.5650 \text{ \AA}$ and $c=5.0370 \text{ \AA}$ (Bouvier et al., 2000) and $a=3.6170 \text{ \AA}$ and $c=5.0830 \text{ \AA}$ (Ding et al., 2012). The reference diffraction pattern for cubic was based on Buntushkin et al (1971) and Ding et al (2012) with a space parameter of $Fm-3m$ and lattice parameters of $a=5.9120 \text{ \AA}$ (Ding et al., 2012) and $a=10.4200 \text{ \AA}$ (Buntushkin et al., 1971). An agreement index that indicates the degree of convergence in the fit was used in the analysis and Weighted-profile R-factor (Rwp) was recorded. The refinement was accepted when Rwp was less than 10 (Jum'ah, 2015) however the maximum Rwp value recorded in this study was less than 6.

3.4.5 Surface Roughness Measurement

In clinical application, zirconia should be minimally polished following the manufacturer's instructions to obtain a lower value for surface roughness and to reduce the phase transformation (Preis et al., 2015). It has been reported that an increase in the surface roughness of ceramics can result in an increase in the wear of the opposing dentition in addition to compromising the restoration itself (Bollenl et al., 1997, Al-Hiyasat et al., 1998, Magne et al., 1999, Oh et al., 2002, Hmaidouch et al., 2014, Malkondu et al., 2016). Furthermore, an increase in the surface roughness of a ceramic restoration could result in favouring the restoration as a site for food debris accumulation (Alghazzawi et al., 2012) and subsequent plaque formation and periodontal problems. There is a controversy about the effect of LTD on the surface roughness of zirconia with some authors reporting that the surface roughness of zirconia can increase with aging (Roy et al., 2007, Kim et al., 2009b) and has a direct proportional relationship with the increase in monoclinic fragments as a result of aging induced tetragonal to monoclinic transformation (Haraguchi et al., 2001, Fernandez-Fairen et al., 2007, Alghazzawi et al., 2012, Kohorst et al., 2012). It has been proposed that the 3-5% volumetric expansion accompanying the transformation is responsible for the detachment of surface grains causing an increase in the roughness (Kim et

al., 2009a, Alghazzawi et al., 2012). On the other hand, (Cotes et al., 2014) reported that there was no relationship between aging and roughness.

Many methods are available for measuring surface roughness, such as laser reflectivity, stylus tracing, non-contact laser stylus metrology and SEM (Haywood et al., 1989, Whitehead et al., 1995). The most commonly used methods among these are probably laser reflectivity and the contact stylus tracing method (Whitehead et al., 1995). Taking into consideration the scale of the changes expected to occur after aging, AFM is regarded as extremely powerful for the detection of any changes at nanoscale that can result from aging (Deville et al., 2005).

The atomic force microscope (AFM) is a powerful microscope that can be beneficial for getting high resolution and achieving a sensitive examination to measure surface roughness at atomic level (Shen, 2013). This technique has many advantages, such as providing detailed surface information with high resolution. It is non-destructive and a versatile technique (Whitehead et al., 1995, Subasi and Inan, 2012).

The principle of how AFM works can be summarised in three stages which all work together; sensing of the surface, detection method and imaging. The sample surface will be scanned by a cantilever with a sharp tip and when this tip approaches the surface, there will be a generation of attraction force causing deflection of the cantilever toward the surface.

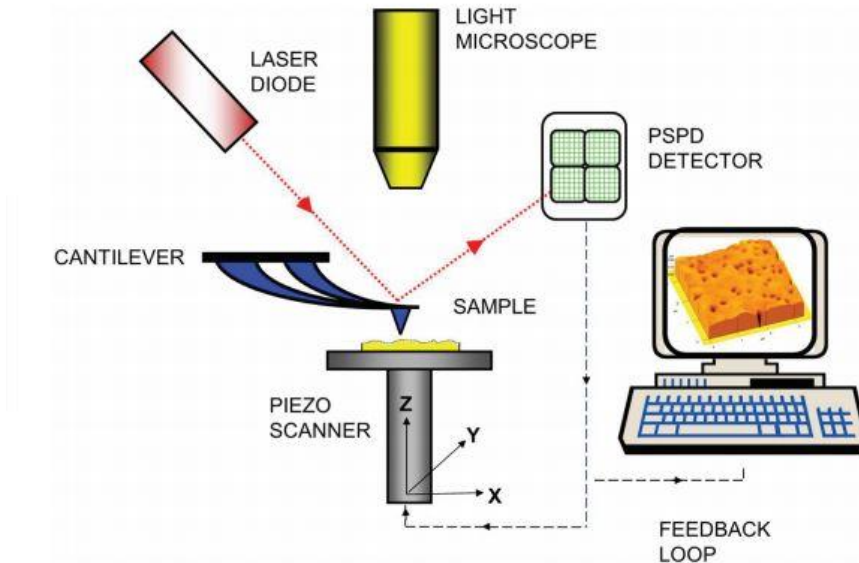


Figure 3-8 A schematic representation of the AFM instrument. (James et al., 2016)

Once the tip contacts the surface there will be the formation of a repulsive force causing a deflection of the cantilever away from the surface. This cantilever movement toward and away from the surface is detected by a laser beam. The flat top of the cantilever will cause a reflection of the incident beam and with the movement or deflection of the cantilever, the direction of the reflected beam will slightly change. AFM will generate an image of the surface of the sample by moving the cantilever over the area of interest of the sample. The deflection of the cantilever by the feature of the sample is controlled by a position-sensitive photo diode (PSPD). An accurate topographic surface image can be produced by the AFM with the help of feedback loop that is responsible for controlling the height of the tip above the surface (Binnig et al., 1986, Giessibl, 1995, Giessibl, 2003, ISO-6872, 2015, James et al., 2016).

In this study Atomic Force Microscopy (AFM) was used to measure the surface roughness of the zirconia samples before and after aging. A representative sample from each tested material were imaged on the Dimension Fastscan (Brüker, USA) at room temperature in air in tapping mode using Fastscan-A (Brüker, USA) probes.

Before imaging, the samples were mounted onto a metal disc using double sided adhesive tape. This was done to ensure that the sample did not move

when being imaged as small perturbations of the sample can distort the images. Using adhesive tape also allowed the sample to be recovered afterwards without causing damage, so that the same sample could be imaged pre- and post-aging. In some instances the samples were cleaned with MilliQ water to remove any surface debris or dust. Once washed, the samples were dried within a flux of N₂ gas.

Once prepared, samples were mounted onto the AFM stage ready to be imaged. Due to the nature of tapping mode, the cantilevers need to be tuned to their resonant frequency. This was done using the software's auto-tune feature, which sets the drive frequency at a 5% offset from the peak amplitude to account for interactions with the surface during imaging. The free-amplitude of the cantilever was set to 10 nm when tuning, but was changed during the process of scanning so as to improve image quality.

To gather suitable and reliable data on the surface roughness, images maintained the same resolution: 2 μ m x 2 μ m with 512 samples per line. For each sample images were captured from different areas on the same sample to give a better average of what the overall surface is like.

The average surface roughness (Ra) (the arithmetic average of the profile ordinates within the measured section) (Alghazzawi et al., 2012) and the maximum roughness depth (Rmax) which is the perpendicular distance between the highest peak and lowest valley of the roughness profile within the measurement line (Hmaidouch et al., 2014) were analysed by a single operator using height sensor images after flattening using NanoScope analysis software version 1.5 and Gwydion version 2.54. These two roughness parameters were measured and expressed in nanometres. Three different areas of 2 μ m x 2 μ m on each sample before and after aging were measured and the average was calculated.

3.5 Optical Properties

For a visual process to happen, three main elements should be available; object, light source and receptor ((Randall, 1997).

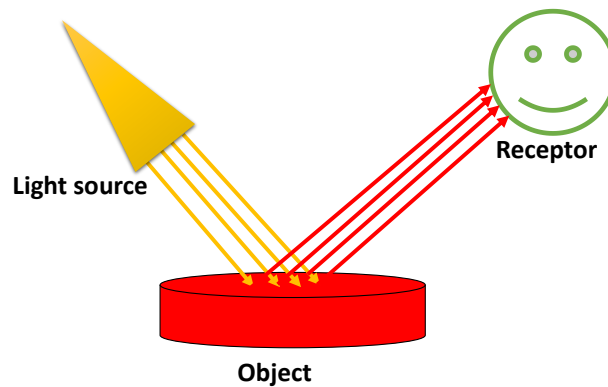


Figure 3-9 Elements of visual process

Colour perception is a subjective process that can be affected by several factors including physiological, environmental and experiential factors. Therefore the most reliable process of accurately communicating colours with others is to assign values to each colour (Harman, 1996, X-Rite, 2016) with use of an optical instrument for colour measurements. These values are called tristimulus data and can be either $L^* a^* b^*$ or $L^*c^*h^*$ (Chu, 2003). Different instruments can be used in measuring the translucency and colour of dental materials including colorimeters, spectroradiometers and spectrophotometers (Barizon, 2011).

3.5.1 Colorimeter

The colorimeter is the most common device used in quality control measurement comparing the colour of pairs of samples. It has the advantages of lowest cost and simplicity compared to other methods. They are also known as Tristimulus (three filtered) colorimeters which use red, green and blue filters with a fixed set of illuminant and observer conditions (Paravina, 2004, X-Rite, 2016). Its simplicity make the quantification of optical properties of dental materials more convenient (Johnston et al., 1996). However, a single type of light and the lack of ability to record spectral reflectance of media make colorimeters lacking the ability of a spectrophotometer which can compensate

for what is called metamerism (*a shift in the appearance of a sample due to the light used to illuminate the surface*) (Randall, 1997, X-Rite, 2016). Accordingly, the main difference between colorimeters and spectrophotometers is that colorimeters have the capacity to measure reflected light only in the area of three wavelengths (red, green, and blue) while spectrophotometers have the ability of measuring reflectance of light within the whole spectrum of visible light (Chu, 2003, Da Silva et al., 2008).

3.5.2 Spectrophotometers

Spectrophotometers are the amongst the most commonly used, highly precise and flexible devices for measuring surface colours. Their simplicity, ease of use and accuracy favour spectrophotometers for most colour matching measurements in dentistry (Paul et al., 2004). They measure the ratio of the reflected light from an object to the reflected light from a white reference along the visible spectrum (approximately at 10nm interval) (Chu, 2003, Paravina, 2004, Khurana et al., 2007, Kielbassa et al., 2009). In dentistry, spectrophotometers have been used widely to measure the translucency and colour of teeth and dental materials (Bolt et al., 1994, Paul et al., 2002, Ahn and Lee, 2008a, Chen et al., 2008, Ahn and Lee, 2008b). The use of a spectrophotometer was found to give an increase in the accuracy about 33% in more than 93% of cases compared to human visualization and conventional techniques (Paul et al., 2002). A spectrophotometer is composed of an optical radiation source, a detector, light dispersing means, and optical system for measuring and converting light obtained to understandable signal for further analysis. The produced data can be manipulated to be in a form that can be understood by dental professionals and researchers (Chu et al., 2010).

Nowadays, there are different primary types of spectrophotometer available for different purposes. These types can be categorised according the angle of illuminant to the object and it includes traditional 0°/45° (or 45°/0°) spectrophotometers, sphere (or diffuse/8°) and multi-angle (MA) spectrophotometers (X-Rite, 2016).

3.5.2.1 45°/0° -0°/45° spectrophotometers

These types are most commonly used for measuring colour of matte and smooth surfaces. Regardless of the geometry of the device, the first number always represents the angle of the illumination to the measured object while the second number represents the angle of viewing (Berns, 1981). These types of spectrophotometer measure the reflected light at a fixed angle to the measured object with the capacity to exclude gloss to closely replicate how a human eye views colour (X-Rite, 2016).

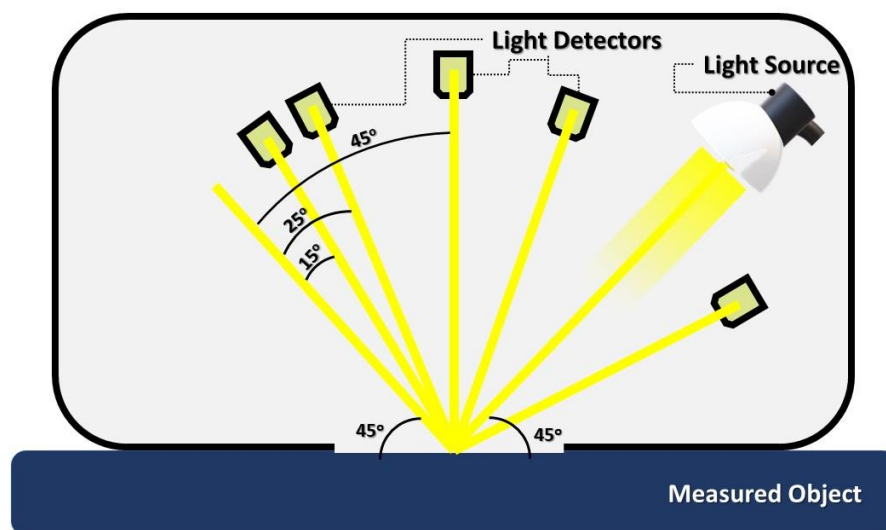


Figure 3-10 Geometry of 45°/0° spectrophotometer

3.5.2.2 Sphere Spectrophotometers

This type of spectrophotometer has a sphere geometry (d/8°). The sample will be illuminated diffusely (from all directions) with the help of the sphere and the reflected light is received by the detector at 8° angle from the surface of the measured sample; it can measure the whole reflected light at all angles. This gives it the ability to measure the colour in the way that closely replicate what a human eye would see. It is most commonly used for measuring colour of textiles, plastics, mirror and shiny surfaces (X-Rite, 2016). This type of spectrophotometer has been found to be more predictable and reliable in accurately measuring the shade of the teeth *in vitro*. It can produce up to 80% of agreement with itself over repeated measurements compared to 45% agreement in human intra-evaluators (Horn et al., 1998). It has been heavily

used in dentistry for measuring the colour and opacity of different types of dental materials such as composite (Vichi et al., 2004), porcelain (Seghi et al., 1986, Kim et al., 2003, Liu et al., 2010a, Spink et al., 2013) and zirconia (Jiang et al., 2011a, Kim and Kim, 2014, Harianawala et al., 2014).

The sphere is lined with low gloss, matte highly reflective white lining. This lining helps in projecting and diffusing the light acting as a nearly perfect white reflector. It reflects 99% of the light, and by the aid of its matte surface finishing, the reflected light will be scattered randomly in all directions. This process happens at every single point on the surface causing the sphere to look like the source of the light and the light coming from all directions at the same time Figure 3-11 (X-Rite, 2016).

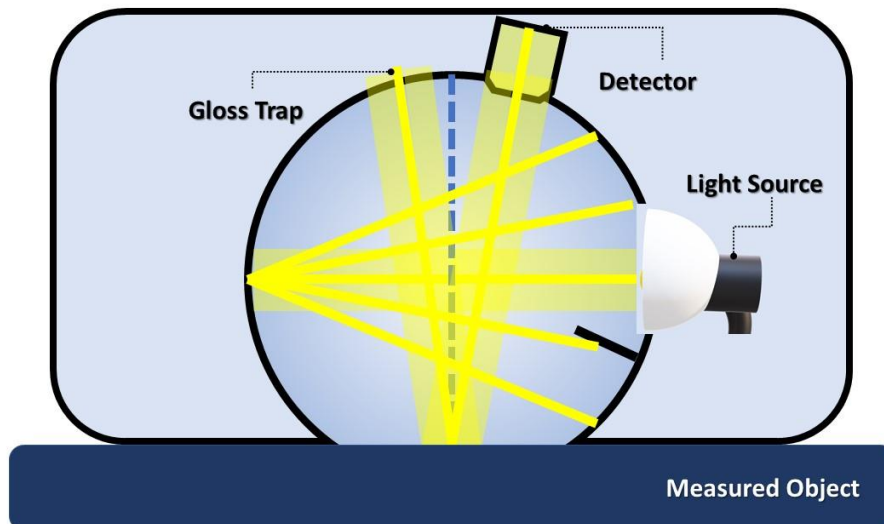


Figure 3-11 Geometry of sphere spectrophotometer Multi-Angle (MA) Spectrophotometers

MA spectrophotometers are most commonly used in industrial production applications such as measuring the colour of automotive coatings, metallic or pearlescent inks and cosmetics such as nail polish. The use of this type of spectrophotometer allows viewing the colour of the sample as if it is moved to be seen in different angles (X-Rite, 2016).

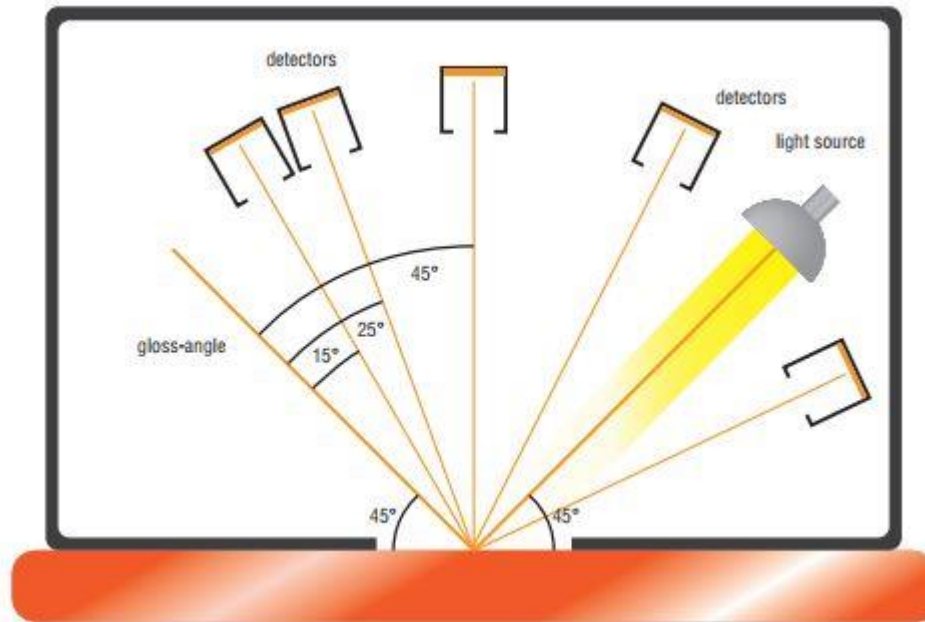


Figure 3-12 Geometry of Multi-Angle spectrophotometer (X-Rite, 2016).

3.5.3 Spectroradiometer

Spectroradiometers are an alternative to spectrophotometers that can be used in dentistry to measure colour and translucency. They can measure radiometric quantities including spectral irradiance (W/m^2) and spectral radiance (m^2Sr) (Paravina, 2004). From these data, the CIE tristimulus values can be measured using specific mathematical integrations. With chromaticity coordinates, luminosity can be measured giving the luminance (cd/m^2) and illuminance (lux) for spectral radiance and irradiance, respectively (Zalewski, 1995, Paravina, 2004). A study by Lim et al 2010, who compared the spectroradiometer to spectrophotometer in measuring the translucency parameters of ceramic materials, concluded that the measurements were significantly different but highly correlated (Lim et al., 2010) and they attributed that to the spectroradiometer using a large illuminating area compared to the spectrophotometer that could result in more reflected light over the white backing affecting resultant translucency values (Lim et al., 2010).

In this study the opacity (%), contrast ratio (CR), translucency parameters (TP), Chroma (C) in addition to difference in the colour (ΔE_{ab}) of the samples before and after artificial hydrothermal aging were calculated. These measurements were conducted on three different thicknesses 0.75, 1.00, 1.25 mm disc samples representing a wide average of different restoration

thicknesses used clinically including veneer and crown restorations. The measurements were performed on all groups in this study and samples were prepared and aged as mentioned earlier in sections 3.2 and 3.2.5 respectively. All the measurements were conducted in air at room temperature by the same operator.

3.5.4 Transmission, Contrast ratio, Translucency Parameters

For Total Transmission (Tt%), contrast ratio (CR), translucency parameters (TP) measurements, a spherical spectrophotometer (SP64, X-Rite, USA), Figure 3-13, was used with D65/10 illumination and specular excluded mode. Calibration of the spectrophotometer was done before the measurement at every day of measurements.



Figure 3-13 SP64 Spectrophotometer, X-Rite™

A calibration was conducted using the self-calibration function of the instrument by measuring white and black backing respectively according to manufacturer's instructions. An extra checking of the calibration was conducted by measuring 100% transparent and 100% opaque objects. Measurements were repeated at different times of the day and on different days to check the reproducibility of the measurement. The specular excluded mode was used in order to get more realistic results as this method will ignore the extra reflection that can result from measuring the gloss of the surface and it has been proven to be more useful in the detection of small colour differences of dental aesthetic restorative materials compared to specular included mode (Lee et al., 2001). As a pilot study, three measurements were

made for each sample used in both modes and the differences were negligible. The 8 mm aperture and a 14 mm target window were used.

For opacity (%) measurement every sample was measured against a black background, followed by a white background and after that the white background alone was recorded and the opacity percentage calculated automatically by the instrument.

For contrast ratio (CR) and translucency parameter (TP) measurements, the CIE $L^*a^*b^*$ coordinates were recorded from the screen of the instrument against black and white backing respectively and the CR measured according to the following equation:

$$CR = L_b/L_w$$

where; CR is the contrast ratio. L_b is the lightness measured over a black background. L_w is the lightness measured over a white background. The subscripts b refers to the colour coordinates on the black background and w to those on the white background (Mohie el-Din Wahba et al., 2017). Translucency parameter (TP) was measured according the following equation:

$$TP = \sqrt{(L_b^* - L_w^*)^2 + (a_b^* - a_w^*)^2 + (b_b^* - b_w^*)^2}$$

where L^* refers to the lightness, a^* to redness to greenness, and b^* to yellowness to blueness. The subscripts b refers to the colour coordinates on the black background and w to those on the white background (Wang et al., 2013). The higher the TP value the higher the translucency.

3.5.5 Colour Measurement

The difference in the overall colour (ΔE^*_{ab}) and Chroma C^*_{ab} of the samples (n=5) of each different group in this study before and after artificial hydrothermal aging, was conducted using an integrated sphere spectrophotometer (Color-Eye® 7000A Reference Spectrophotometer, GretagMacbeth, USA). The spectrophotometer was calibrated before measurements using a white reference tile provided by the manufacturer. The spectral reflectance was measured across the visible range excluding both UV and specular reflection (specular excluded) and collected using (Datacolor TOOLS™ software, USA); each sample was measured three times and the

average taken. Transmission was calculated by dividing the measured spectral reflectance of the specimen (placed between the white tile and the spectrophotometer aperture) by that of the reflectance of the white tile alone at each wavelength. From these values, CIE 1931 XYZ tristimulus values were calculated according to Table 5.17 of ASTM E308 (Illuminant D65, 2-degree observer). Finally, CIE 1976 L*a*b* were determined for each of the CIE XYZ values relative to the white tile and colour difference (ΔE^*_{ab}) between specimens calculated according to Equation (3-10):

$$\Delta E^*_{ab} = [(\Delta L^*)^2 + (\Delta a^*)^2 + (\Delta b^*)^2]^{1/2} \quad \text{Equation (3-10)}$$

where ΔL^* , Δa^* and Δb^* are the differences in lightness, green-red coordinate and blue-yellow coordinate, respectively (Lee et al., 2011, Pecho et al., 2012, ISO-6872, 2015, Ho et al., 2015). To check the colour stability of the material tested, ISO Standard (ISO-28642, 2016), Guidance on colour measurement in Dentistry, was used. According to the standard: “*If the colour difference measured before and after aging or staining is at or below $\Delta E^*_{ab} = 1.2$, it represents an excellent match; if this difference is between $\Delta E^*_{ab} = 1.2$ and $\Delta E^*_{ab} = 2.7$, it represents an acceptable match; if this difference is above $\Delta E^*_{ab} = 2.7$, it represents an unacceptable match.*”

For Chroma (C^*_{ab}) measurements, the following equation was used:

$$C^*_{ab} = (a^2 + b^2)^{1/2}$$

where a^* , b^* represent green-red coordinate and blue-yellow coordinates, respectively (Lee, 2015).

3.5.6 Irradiance measurements

The amount of irradiance passing through the zirconia discs was measured using a laboratory-grade NIST-referenced USB4000 spectrometer (MARC® [Managing Accurate Resin Curing] System; BlueLight Analytics Inc., Halifax, Canada). The amount of light irradiance for all samples was evaluated (i.e. amount of light received by the specimen) (wavelength range, 360–540 nm) and the total energy passing through the zirconia discs of three different thicknesses (0.75, 1.00, 1.25 mm) per each tested material in this study, (n=6) was performed using the spectrometer mentioned above. Irradiance was

measured at three different thicknesses with air as a reference followed by measuring the samples. A LED light-curing unit (Elipar S10, 3 M ESPE, St. Paul, MN, USA) with light irradiance of 1700mW/cm², curing time 10 s was used (Ilie and Stawarczyk, 2014, Sulaiman et al., 2015a). Each sample was tested on the bottom surface sensor of the MARC® resin calibrator. The light cure unit was stabilised using a specially made jig to ensure the stability and reducing the error in distance between the sample to be measured and the light cure unit . Measurements of irradiance was performed on all samples before and after aging.

Chapter 4

Mechanical Properties and Structural Analysis: Results and Discussion

4.1.1 Shrinkage and Density

Green and sintered densities for each material are presented in (Table 4-1). Following a normality test and one way ANOVA , Zpex showed a statistically significant ($p < 0.05$) higher sintered density compared to all other materials. There was no statistical difference in the sintered density of all other groups . For green density, Zpex, also showed statistically the highest green density, followed by ZpexS which showed significant higher density compared to 3YE and 3YBE; there was no significant difference in the density of 3YE and 3YBE.

Table 4-1 Green and Sintered Density

Material	Green Density	Sintered Density
3YE	2.50 (0.03)	5.88 (0.01)
3YBE	2.51 (0.01)	5.87(0.02)
Zpex	2.91 (0.01)	5.98 (0.01)
ZpexS	2.87 (0.01)	5.85 (0.01)

All the tested materials showed a linear shrinkage in the range of 20-25.25%, presented in (Figure 4-1).

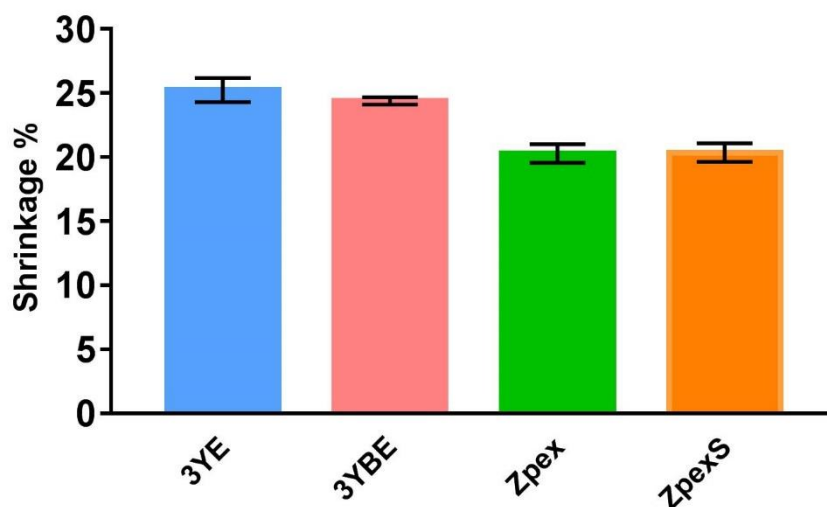


Figure 4-1 Percentage Shrinkage of all materials after sintering.

Following a normality test, one way ANOVA showed a statistically significant difference in the shrinkage between tested groups. Zpex and ZpexS showed statistically the least shrinkage compared to the rest of the groups and the highest shrinkage was recorded by 3YE.

4.1.2 Biaxial Flexural Strength Result

The mean values of biaxial flexural strength (BFS) of non-aged and aged groups are presented in (Table 4-2). BFS mean values for non-aged groups were (lowest to highest) from 604.13 MPa for ZpexS to 984.66 MPa for 3YBE while for aged group the range was 595.3 MPa for ZpexS to 1033.53 MPa for 3YBE. One-way ANOVA analysis followed by Tukey HSD test showed no statistically significant effect of aging on the strength of all tested groups ($p < 0.05$), however, the difference in the strength between all tested groups was statistically significant ($p < 0.05$) (Figure 4-2). Therefore, The first null hypothesis that the accelerated *in vitro* hydrothermal aging would not significantly affect the flexural strength was accepted for all tested groups. The second null hypothesis that there would be no difference in the flexural strength between all tested groups was rejected as significantly higher mean flexural strength ($P < 0.05$) was recorded for 3YBE, 3YE and Zpex compared to ZpexS.

In terms of ranking the mean BFS of the tested groups, from highest to the lowest, the order was 3YBE > 3YE > Zpex > ZpexS both before and after aging.

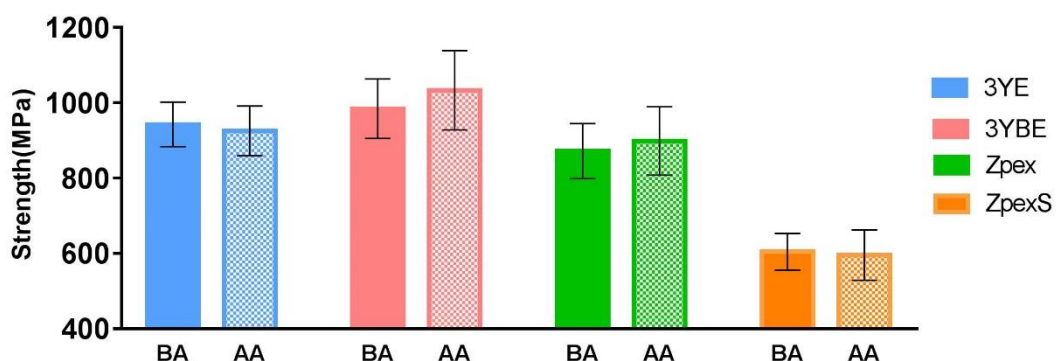


Figure 4-2 Bar Chart showing the BFS before (BA) and after aging(AA).

Before aging, 3YBE showed a statistically significantly higher strength compared to Zpex and ZpexS; 3YE showed significantly higher strength

compared to ZpexS; Zpex was significantly higher than ZpexS. There was no significant difference in the mean strength of 3YE and 3YBE.

The higher strength for 3YE and 3YBE can be explained by the fact that both of these materials contain higher amount of Al_2O_3 compared to Zpex and ZpexS. They contain 0.25 wt% compared to only 0.05 wt% for Zpex and ZpexS. This result agrees with Samodurova et al. (2015) who reported that the presence of Al_2O_3 positively influenced zirconia strength (Samodurova et al., 2015) through the nucleation of zirconia and promoted strong grain boundaries. (Rao et al., 2004) claimed that the presence of Al_2O_3 had a clear direct influence on the grain growth and the stability of tetragonal zirconia by acting as a matrix for zirconia to be dispersed in it evenly (Kurtz et al., 2014). It is also found to be responsible for tuning the amount of dopant inside the zirconia lattice (Palmero et al., 2014). The amount of tetragonal phase that can be retained at room temperature is mainly dependant on the concentration of yttria stabilizing oxide, grain size & distribution and the constraint applied by the matrix on these grains (Piconi et al., 2003). It was reported that reducing amount of Al_2O_3 in different scale in different types of zirconia can result in a weaker grain boundary (Zhang et al., 2016). Therefore, reducing the amount of Al_2O_3 in Zpex and ZpexS resulted in a lower strength compared to 3YBE and 3YE.

The significant difference in the strength between Zpex and ZpexS can mainly be attributed to the fact that ZpexS had more Y_2O_3 compared to Zpex. Increasing the amount of Y_2O_3 to more than 9 % by weight (corresponding to 5.5 mol%) means this material will have more cubic zirconia and has effectively changed from (PSZ) to (FSZ) (Anselmi-Tamburini et al., 2007, Carrabba et al., 2017). The loss in the strength of ZpexS as result of having more Y_2O_3 and therefore more cubic phase, can be explained by the high stability of the cubic phase and the corresponding loss of the advantage of stress induced *t-m* transformation which enhances the strength and fracture toughness of zirconia materials (Hannink et al., 2000).

It can be clearly seen that dropping the amount of Al_2O_3 and increasing the amount of Y_2O_3 showed a synergistic negative effect on the strength of ZpexS

and can clearly explain why this material showed significantly less strength compared to all other tested materials.

In the mouth, the exposed surface of zirconia is susceptible to a phase change from *t-m* which can be either stress induced transformation at a propagating crack on the surface due to cyclic loading during chewing, and/ or as a result of aging in the mouth. This is due to the fact of subjecting zirconia to humidity at low temperature for long time in a process called low temperature degradation (LTD), which may affect the mechanical properties of the material (Lughi and Sergo, 2010). A variation in strength may occur due to profound microcracking in the transformed region and this is mainly dependant on the balance between the amount of residual stress as a result of aging and microcracking within the transformed area (Chevalier et al., 2011).

The state of equilibrium and phase stabilization of zirconia can be changed under humidity, due to formation of zirconium or yttrium hydroxide at the grain boundaries. This in turn takes yttria out from grains resulting in phase transformation from tetragonal to monoclinic accompanied by 3-5% increase in volume (Figure 2-2) (Piconi and Maccauro, 1999). In terms of effect of hydrothermal aging on the strength, none of the tested material showed a statistically significant difference in the strength (Figure 4-2) after hydrothermal aging, however, Zpex and 3YBE groups showed a slight but clear tendency to an increase in the strength after hydrothermal aging.

Weibull statistical analysis of the flexural strength values and the characteristic strength for all tested groups before and after aging are presented in (Table 4-2), the range of the Weibull modulus, μ , for non-aged groups was 12.94 for Zpex to 19.07 for 3YE and for the aged groups was 7.75 for ZpexS to 16.80 for TZ-3Y-E. While there is no significant changes in the characteristic strength, σ^0 , before and after aging for all groups, the Weibull modulus μ showed a clear decrease after aging for all groups.

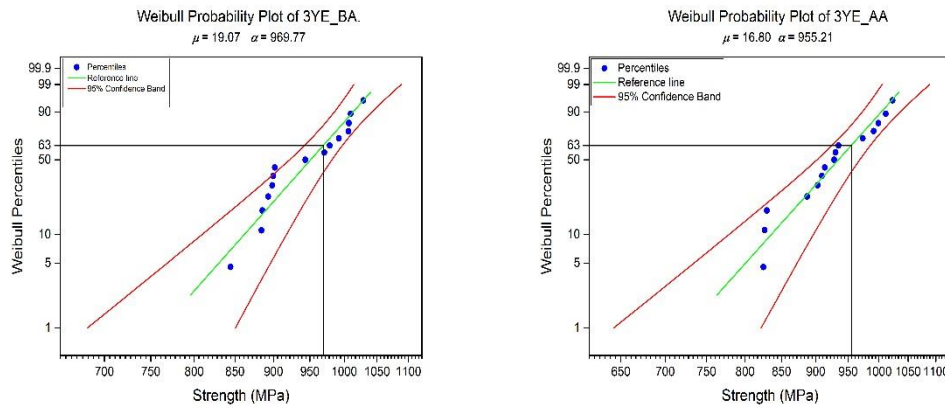


Figure 4-3 Weibull probability plot for BFS data of 3YE_BA and 3YE_AA.

BFS values represented by the blue circles plotted against Weibull percentiles. Characteristic strength (α) was calculated as the load where 63% of samples failed. Upper and lower **95% CI** bounds are represented by the red line.

For 3YE group, the aging showed no effect on the characteristic strength of the material, however the Weibull modulus (Figure 4-3) dropped from 19.07 to 16.80 which is still within the expected average for dental ceramic and the highest among all tested groups even after aging.

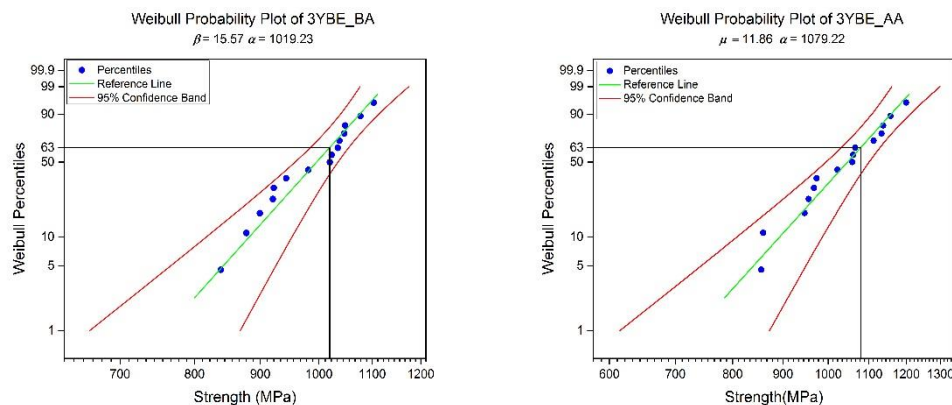


Figure 4-4 Weibull probability plot for BFS data of 3YBE_BA and

3YBE_AA. BFS values represented by the blue circles plotted against Weibull percentiles. Characteristic strength (α) was calculated as the load where 63% of samples failed. Upper and lower **95% CI** bounds are represented by the red line.

3YBE showed a drop in Weibull modulus μ (Figure 4-4) from 15.57 to 11.86 after aging with no clear effect of the characteristic strength.

Table 4-2 Mean Values of Biaxial Flexural Strength (BFS), Weibull modulus , characteristic strength and Hardness (HVF)

	Mean σ (MPa)	Std. deviation	Characteristic Strength σ^0 (MPa)	Weibull m	95% confidence interval for mean		Hardness Mean Values (HVF)+Std. Deviation
					Lower bound	Upper bound	
3YE_BA	942.86	59.16	969.77	19.07	910.10	975.62	1203.30 ±108.07
3YE_AA	925.80	65.89	955.21	16.80	889.30	962.29	1148.56 ±197.20
3YBE_BA	984.66	79.34	1019.23	15.57	940.72	1028.60	1271.40 ± 130.54
3YBE_AA	1033.53	105.49	1079.22	11.86	975.11	1091.95	1228.10 ± 127.83
Zpex_BA	871.89	72.80	904.76	12.94	831.58	912.21	1249.41 ± 110.59
Zpex_AA	898.9	90.62	914.58	7.75	782.02	935.57	1217.94 ± 85.43
ZpexS_BA	604.13	48.61	625.88	13.95	577.21	631.06	1211.24 ± 139.8
ZpexS_AA	595.3	66.7	619.3	9.44	543.14	630.96	1141.54 ± 82.99

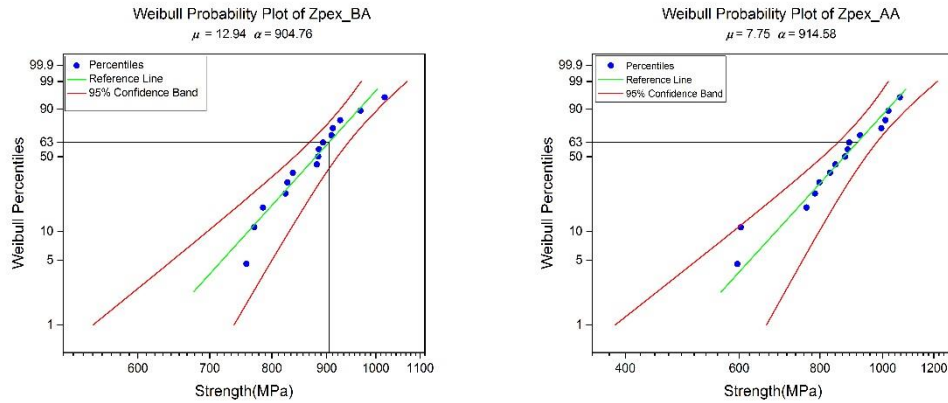


Figure 4-5 Weibull probability plot for *BFS* data of Zpex_BA and Zpex_AA.

BFS values represented by the blue circles plotted against Weibull percentiles.

Characteristic strength (α) was calculated as the load where 63% of samples failed.

Upper and lower **95% CI** bounds are represented by the red line.

For both translucent zirconia groups, before and after aging, the Weibull modulus μ also dropped as in the conventional zirconia groups. For Zpex (Figure 4-5), the Weibull modulus μ dropped from 12.94 to 7.75 after aging while for ZpexS (Figure 4-6), it dropped from 13.95 to 9.44.

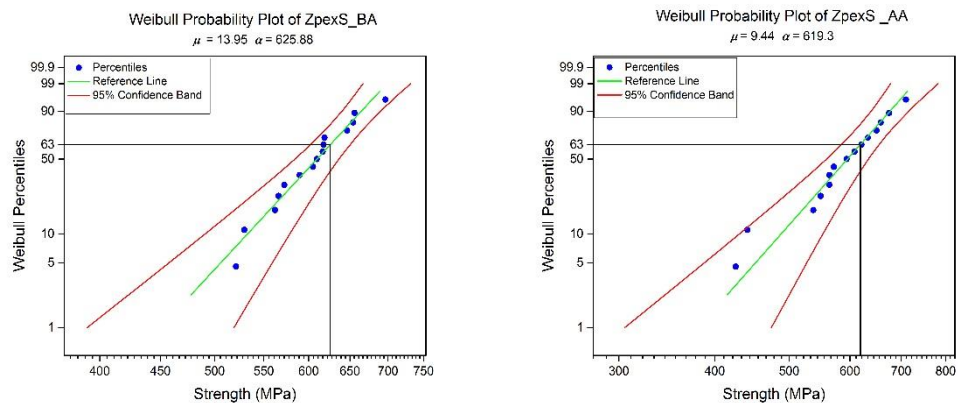


Figure 4-6 Weibull plot probability plot for *BFS* data of ZpexS_BA and ZpexS_AA.

BFS values represented by the blue circles plotted against Weibull percentiles.

Characteristic strength (α) was calculated as the load where 63% of samples failed.

Upper and lower **95% CI** bounds are represented by the red line.

The Weibull modulus for all tested groups from the highest to lowest for both before and after aging groups was in the order of 3YE>3YBE>ZpexS>Zpex.

Curves or stoops in a Weibull distribution function are often suggestive of fracture resulting from multiple flaw types. On the other hand, a good Weibull fit can be taken as an indication of a single, dominant flaw type and an endorsement of 'satisfactory care in testing procedures' (Quinn and Quinn, 2010). Despite aging showing no effect on the mean or characteristic values of strength of all tested groups, Weibull modulus for all of tested groups clearly dropped after aging (Figure 4-3 to Figure 4-6). Given that all the specimens were prepared and tested by the same operator and in the same way using the same equipment, these results indicate that aging had an effect, e.g. changes in residual stress in the materials after aging and/or an increase in the porosity of the material after aging that resulted in different flaws within the material affecting failure strength reliability. Even with this drop in Weibull modulus after hydrothermal aging, all tested materials had very reproducible flexural strengths in excess of the minimum recommended for clinical use, even after accelerated aging mimicking 15-20 years of clinical service (Table 4-2) (Aziz et al., 2016). Most ceramics used for medical purposes are reported to have Weibull modulus in the range of 5 to 20 (Guazzato et al., 2005) for untreated samples and up to 25 for samples treated by, for example, grinding (Inokoshi et al., 2017).

4.1.3 Hardness Results

The mean hardness values are presented in (Table 4-2). The range of hardness for the tested groups before aging was from 1203.30 ± 108.07 for 3YE_BA to 1271.40 ± 130.54 for 3YBE_BA while for the after aging groups was from 1141.54 ± 82.99 for ZpexS_AA to 1228.10 ± 127.83 for 3YBE_AA. Following normality testing, one-way ANOVA analysis followed by a Tukey HSD post hoc test, showed no statistically significant difference in hardness values between all tested groups and aging had no significant effect on any of the tested materials ($p > 0.05$).

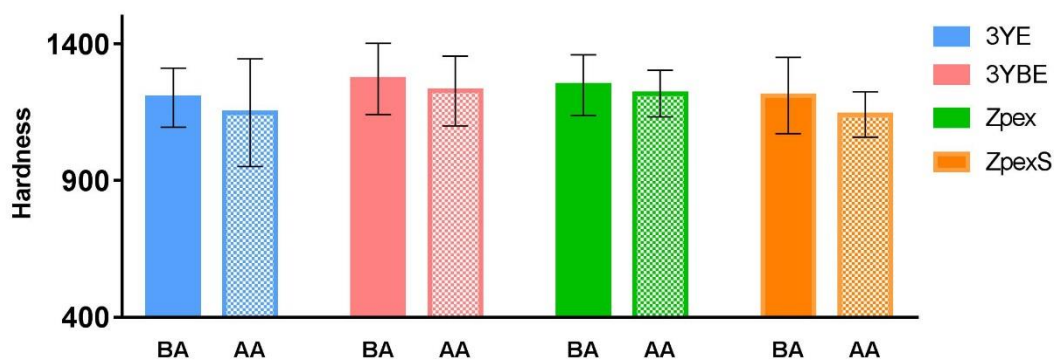


Table 4-3 Bar Chart showing Hardness before and after aging.

4.1.4 XRD

4.1.4.1 Starting Powders

Rietveld analysis for the XRD patterns of the starting powders of 3YE and 3YBE (Figure 4-7) showed 20 volume% of monoclinic phase and 80 volume% of (tetragonal and cubic) phases recorded with weighted R profile of 2.57 and 5.19 for 3YE and 3YBE respectively. [NB the weighted R profile is one of the most commonly used discrepancy factors in Rietveld analysis; a lower R value indicates a better fit of the analysis]. As mentioned earlier, it was very difficult to differentiate between tetragonal and cubic phases due to the peak overlap issue between these two phases (Kobayashi et al., 1981). For Zpex powder the analysis revealed 30 volume% of monoclinic and the rest was (tetragonal and cubic) while ZpexS showed only about 6 volume % monoclinic and the rest was (tetragonal and cubic) (Figure 4-7).

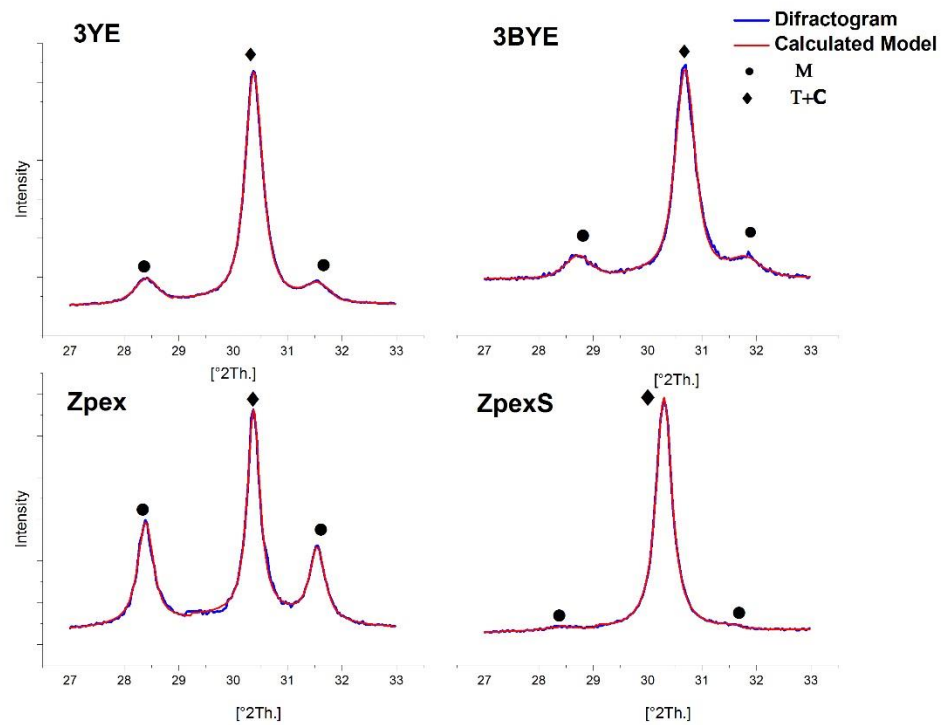


Figure 4-7 XRD pattern and Rietveld analysis for powders of all tested

groups. (Blue) representing diffraction pattern obtained by plotting intensity of diffracted signal against 2θ . (Red) representing the calculated model from reference diffraction patterns for monoclinic, tetragonal and cubic phases obtained from (ICDD database) fitted to raw XRD data.

4.1.4.2 Post-sintering

After sintering all tested material showed a single peak of (tetragonal and cubic) zirconia phases at $30.3\ 2\theta$. There was no detectable monoclinic phase in any of the tested groups (Figure 4-8).

4.1.4.3 Post-aging

XRD followed by Rietveld analysis conducted after hydrothermal aging showed that aging had an impact on the stability of tested materials (Figure 4-8). Rietveld analysis of the 3YE diffraction pattern obtained after aging, showed no detectable transformation while for 3YBE and ZpexS the analysis showed about 5 ± 1.2 volume% of monoclinic fraction phase and the rest was (tetragonal and cubic) phases. Zpex was the material that showed the highest amount of transformation, $\sim 22\pm 1.5$ volume% of monoclinic fraction phase after hydrothermal aging, the rest being (tetragonal and cubic)

phases. The weighted R profile for Rietveld analysis for all groups were between 2.5 to 7.2.(Figure 4-8).

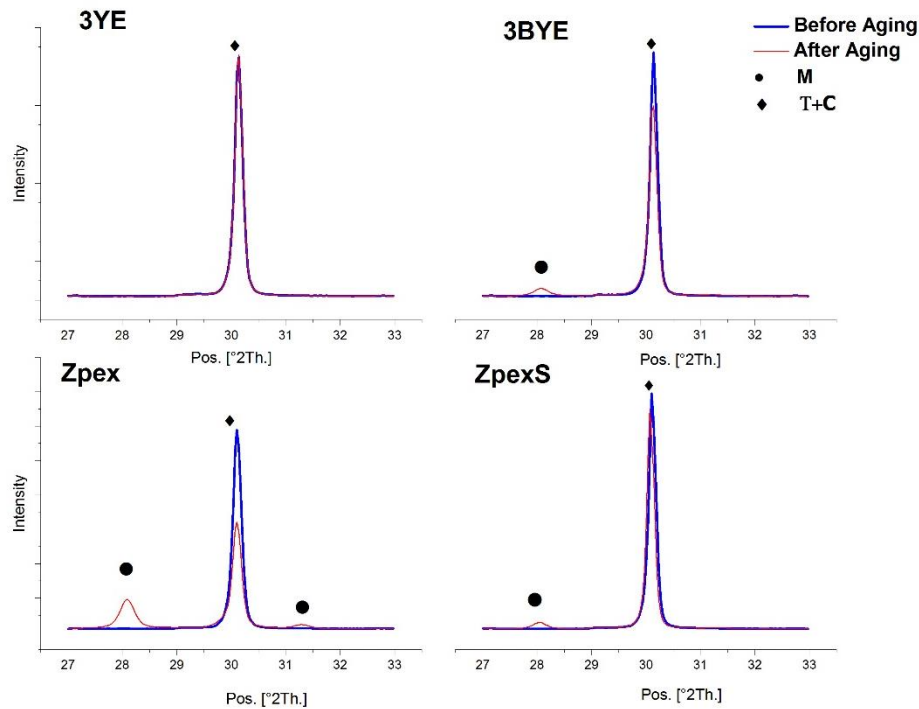


Figure 4-8 XRD pattern and Rietveld analysis for all tested groups showing the transformation after aging.

As it was very difficult to determine the exact volume of tetragonal and cubic phases due to the aforementioned overlapping peak dilemma of the two phases, the relative amounts of each phase were inferred from compositional and strength data, i.e. the presence of 0.25 Al₂O₃ in 3YBE and 3YE with less amount of Y₂O₃ compared to ZpexS, *and* their high flexural strength would suggest that these two materials had a higher amount of tetragonal phase to cubic phase compared to ZpexS, which showed a significantly lower flexural strength that was attributed to its being essentially cubic zirconia. For Zpex, the Y₂O₃ content was similar to the 3YE and 3YBE materials and yet it still had a statistically significant reduced flexural strength, however, the difference was not as a big as between 3YE, 3YBE and ZpexS.

Accordingly, the reduced strength for Zpex was attributed to a reduced amount of Al₂O₃ and as this material showed the highest monoclinic volume after hydrothermal aging, this would suggest that it had a higher tetragonal zirconia phase content than ZpexS. This result agrees with a recent study by (Zhang et al., 2016) who studied the effect of aging on mechanical properties

of high translucent zirconia. They stated that zirconia with 5 mol% of Y_2O_3 showed 54% of cubic and the rest was tetragonal while zirconia with 3mol% Y_2O_3 showed up to 90% of tetragonal zirconia.

The highest amount of transformation that Zpex showed after hydrothermal aging was attributed to a lower amount of Al_2O_3 compared to 3YE and 3YBE, as the addition of Al_2O_3 to zirconia clearly reduces aging, or at least reduces drastically its kinetics (Chevalier, 2006, Chevalier et al., 2009, Zhang, 2014).

Another possible reason can be related to a non-homogenous distribution of Y_2O_3 within the tetragonal phase of the starting powder of Zpex, that means the concentration of dissolved Y_2O_3 within some of the tetragonal phase particles was less than the critical amount (2.75 mol%) to keep the tetragonal phase stable, regardless any other factor (Ohmichi et al., 1999). The presence of alumina was reported to have a preventative role in zirconia LTD (Zhang et al., 2015). A lower amount of Al_2O_3 also means less tuning control to the dopant concentration inside zirconia (Palmero et al., 2014) which can affect the stability of tetragonal zirconia.

The fact that Zpex Smile, with the same amount of Al_2O_3 , showed less amount of transformation, is mainly attributed to its higher concentration of Y_2O_3 which resulted into higher percentage of the most stable cubic phase.

In general, transformation that resulted from hydrothermal aging was limited and had no significant impact on the mechanical properties of tested materials. Kim et al,2009 stated that flexural strength might begin to decrease between 12% and 54% of monoclinic concentration (Kim et al., 2009b), however, in this study even with the 22% of monoclinic after hydrothermal aging of Zpex, there was no significant changes in the strength. This would implicate that LTD can result in a structural changes of zirconia but doesn't necessarily affect its mechanical properties. This also agree with (Chevalier et al., 2011) who reported that LTD is not systematically associated with a loss in strength and strength might increase after aging.

4.1.5 SEM

The SEM images of the surfaces of thermally etched zirconia groups scanned before and after hydrothermal aging are presented in (Figure 4-9 to Figure 4-12). 3YE and 3YBE showed a dense homogenous microstructure in

terms of grain size with well-defined grain boundaries. Both showed some black dots marked as alumina on the surface of some grains. 3YE showed a few pores both before and after aging and after aging the grain boundaries were less defined while for 3YBE no pores can be identified. Zpex and ZpexS showed relatively less homogeneity in terms of grain size which can be attributed to its higher sintering temperature (Janney et al., 1992) compared to conventional groups. In addition to the sintering temperature, increasing the amount of yttria in ZpexS has clearly contributed to the formation of more cubic zirconia grains of bigger size which can be identified as the predominant grains in SEM images of ZpexS. All groups showed no evidence of grain growth after aging at least for the examined area. Zpex after aging showed some surface changes, white bright areas which can be an indirect indication of transformed area of tetragonal to monoclinic phases, however, it still could not be used for bulk quantification of phase transformation (Umeri, 2010). For ZpexS, even with a small amount of alumina content, it can be clearly seen on the surface of the grains in the SEM images.

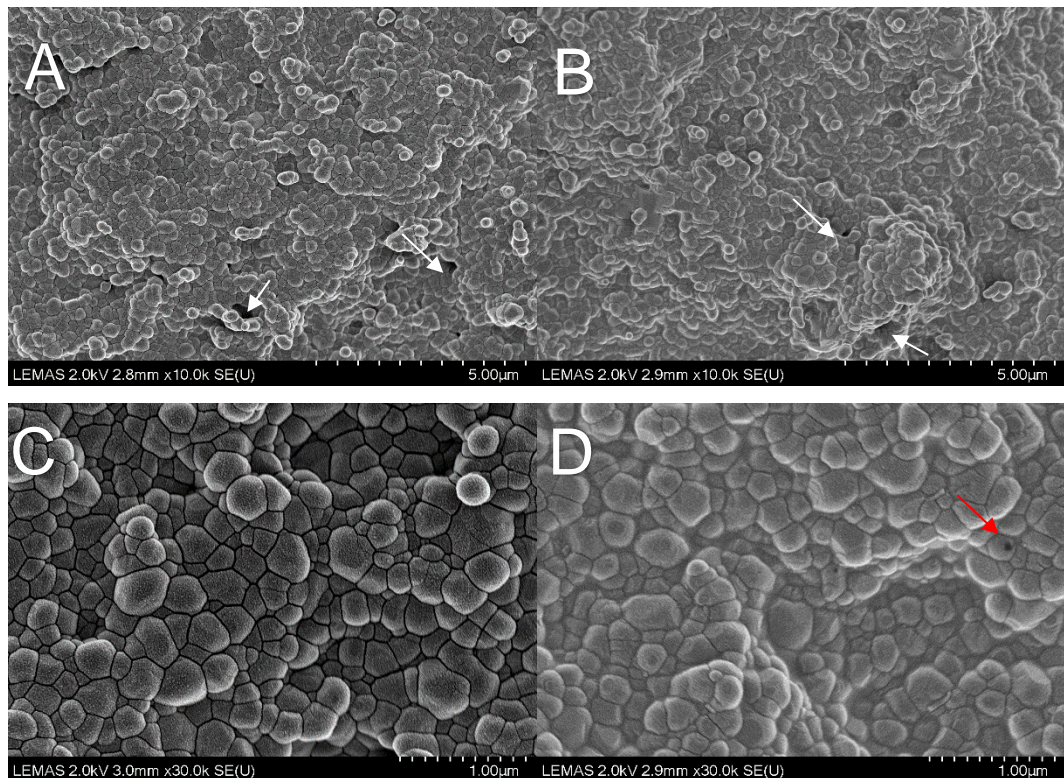


Figure 4-9 SEM images showing the surface topography of 3YE. (A) low magnification image, Before aging showing dense homogenous microstructure and well defined grains boundaries with few pores of different sizes indicated by small white arrows. (B) After aging, showing less defined grains boundaries and more fade in general compared to (A) and also showing some pores indicated by white arrows. (C) high magnification before aging, showing well defined grains boundaries and homogenous microstructure. (D) high magnification after aging image, showing homogenous, condensed and less defined grains boundaries and more fade compared to (C). Red arrow indicating alumina on the surface.

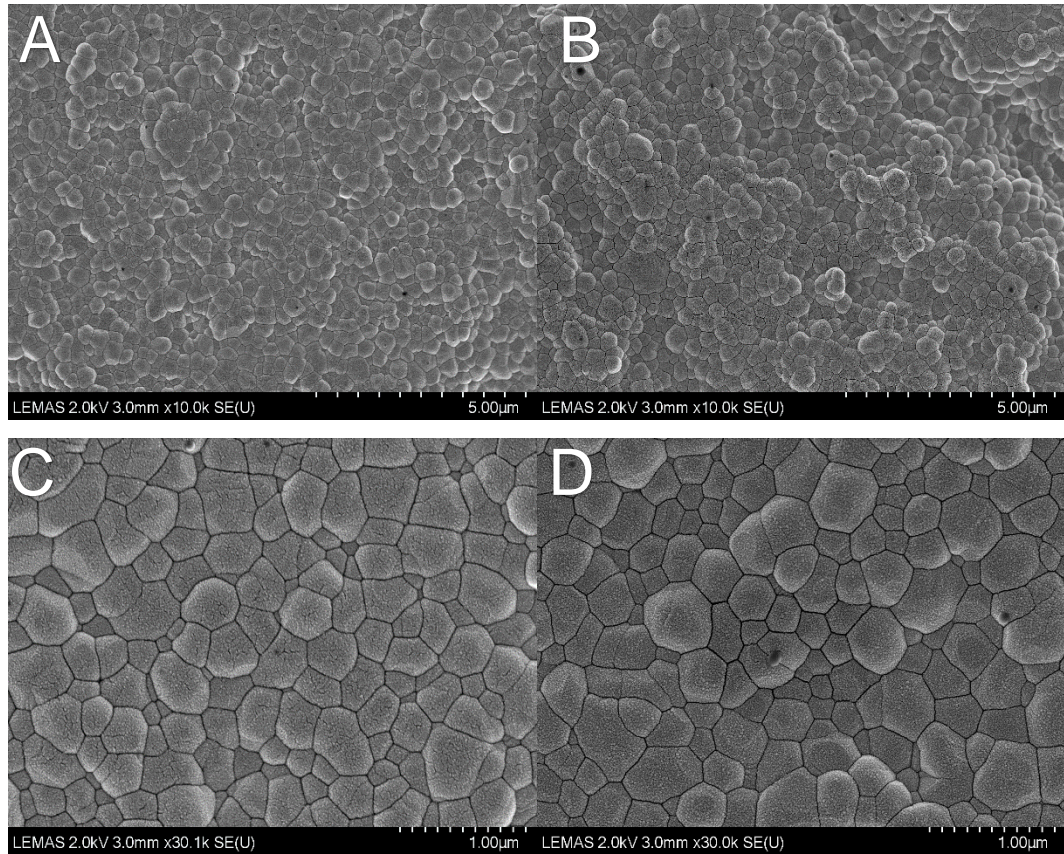


Figure 4-10 SEM images showing the surface topography of 3YBE.

(A) low magnification image, Before aging showing dense homogenous microstructure and well defined grains boundaries and no pores identified. (B) After aging image, showing well defined grains boundaries. (C) high magnification before aging, showing well defined grains boundaries and homogenous microstructure with no pores identified. (D) high magnification after aging image, showing homogenous , condensed microstructure .

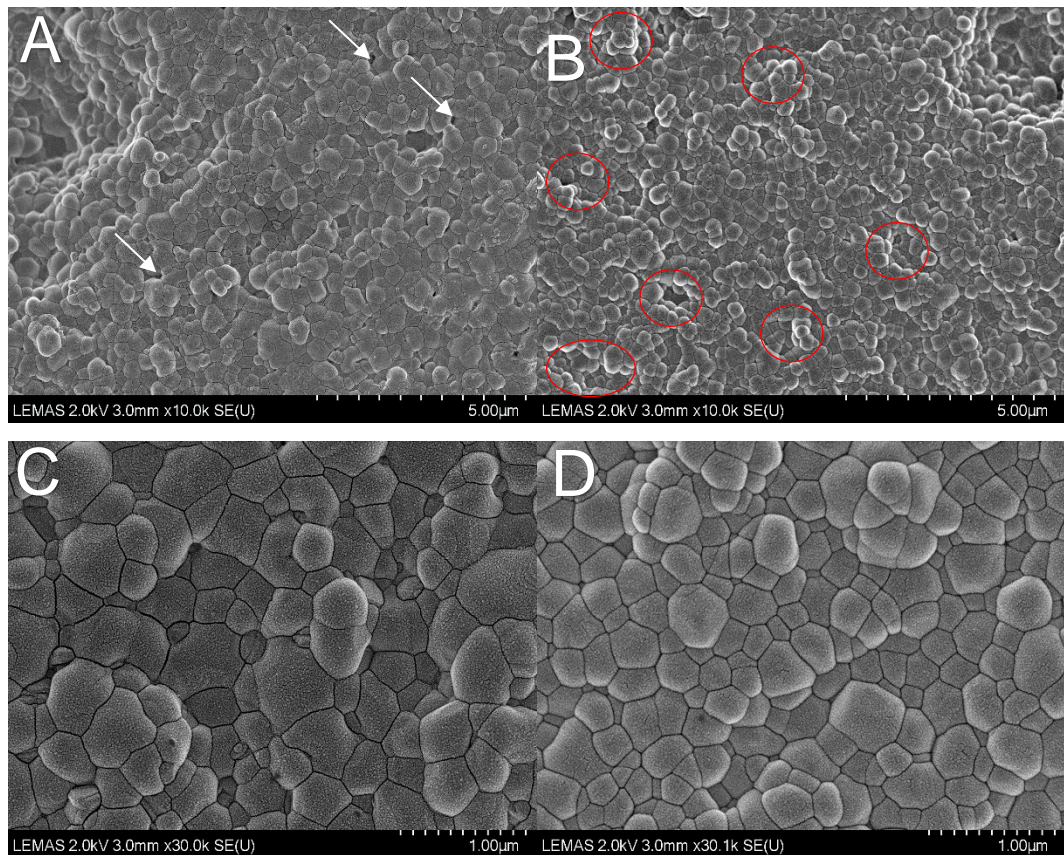


Figure 4-11 SEM images showing the surface topography of Zpex.

(A) low magnification image, Before aging showing dense less homogenous microstructure compared to 3YE and 3YBE, well defined grains boundaries with few pores indicated by small White arrows. (B) low magnification, after aging image, showing white bright transformed areas indicated by Red circle.(C) high magnification before aging, showing well defined grains boundaries and a mix of grain size with no pores can be identified.(D) high magnification after aging image, showing condensed microstructure with more than one area of different contrast indicating the transformation.

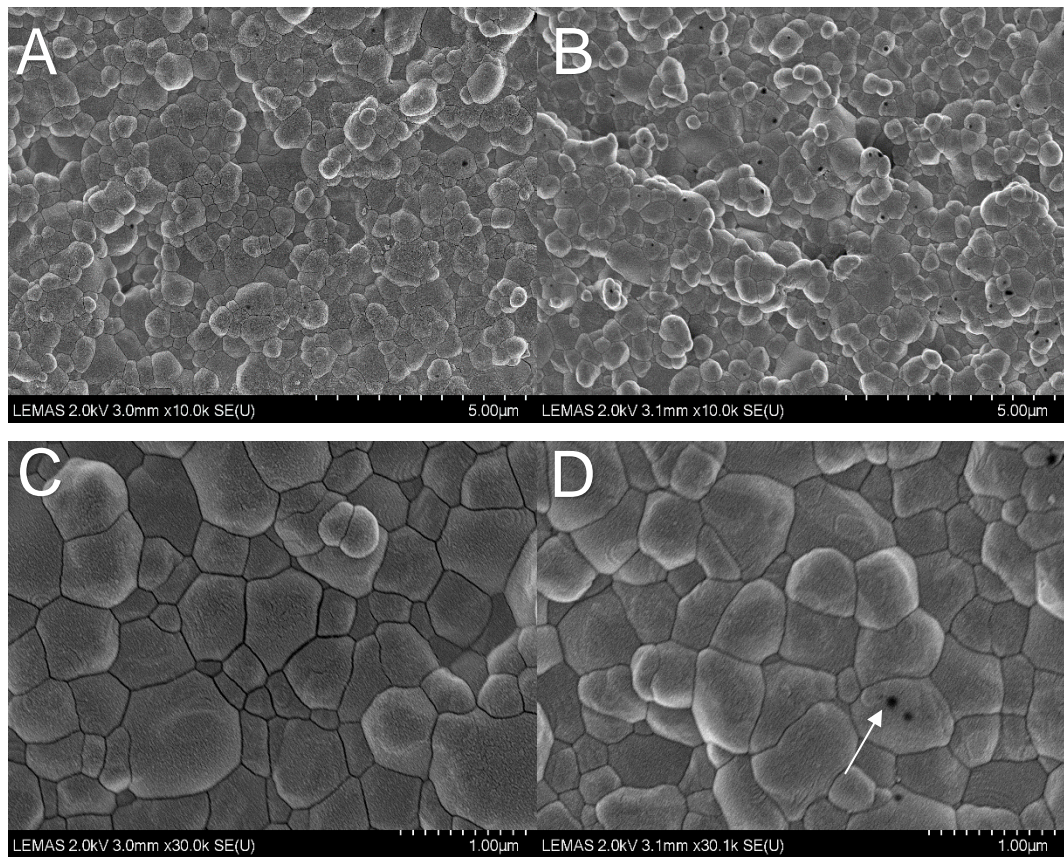


Figure 4-12 SEM images showing the surface topography of ZpexS.

(A) low magnification image, Before aging showing dense well defined less homogenous microstructure compared to 3YE and 3YBE. (B) low magnification, after aging image, showing some bright areas as an indication of t-m transformation. (C) high magnification before aging, showing well defined grains boundaries and a mix of grain size with no pores can be identified, big grain (cubic) can be clearly seen. (D) high magnification after aging image, showing dense, well defined grain boundaries with no detectable changes can be seen. White arrow indicate alumina on the grain surface.

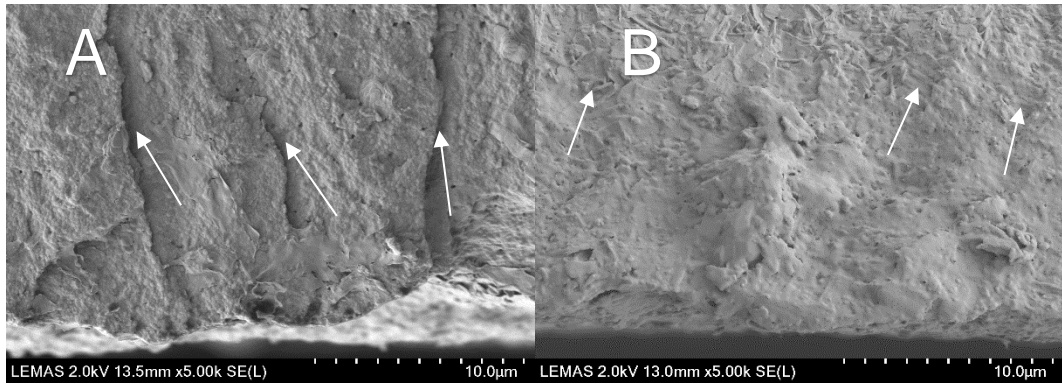


Figure 4-13 SEM images of the fractured surface of 3YE before (A) and after (B)Aging. Hackles indicated by white arrows.

SEM of the fractured surface for 3YE showed a very rough appearance compared to after aging. Before aging hackle can be seen clearly compared to after aging as it became more shallow and the surface in general looks smoother than before aging, indicating a possible different flaws that can be generated by residual stress after aging.

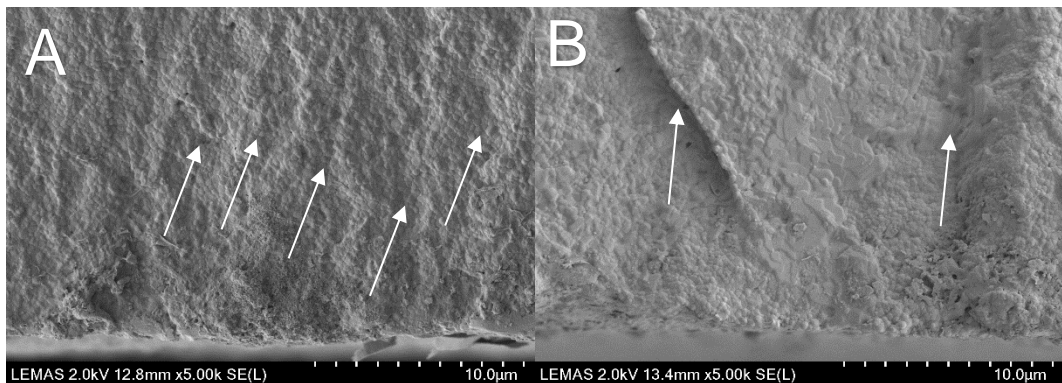


Figure 4-14 SEM images of the fractured surface of 3YBE before (A) and after (B)Aging. Hackles indicated by white arrows.

SEM of the fractures surface of 3YBE, showed a dense, homogenous structure with multiple shallow hackles, while after aging showed a smoother structure in general with more defined hackles compared to before aging. This can be considered as an indication of different flaws before and after aging

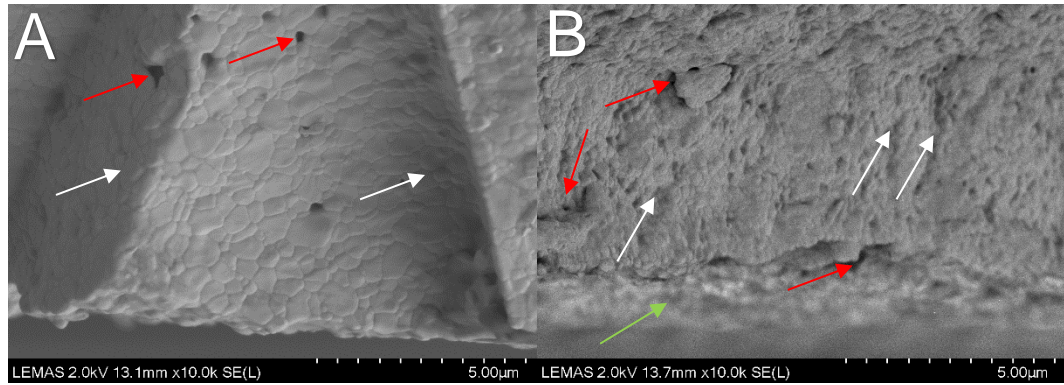


Figure 4-15 SEM images of the fractured surface of Zpex before (A) and after(B)Aging. Hackles indicated by white arrows, pores indicated by red arrows, green arrow indicates area of transformation.

SEM images of the fractured surface of Zpex , showed large broad hackles (coarse hackles) with very smooth surface and few pores before hydrothermal aging. After aging, SEM image showed a shallower less defined hackles and in addition to the pores, a very rough surface that appeared blurred during scanning. This can be attributed to the transformation of t-m after aging and uplifting of the grains.

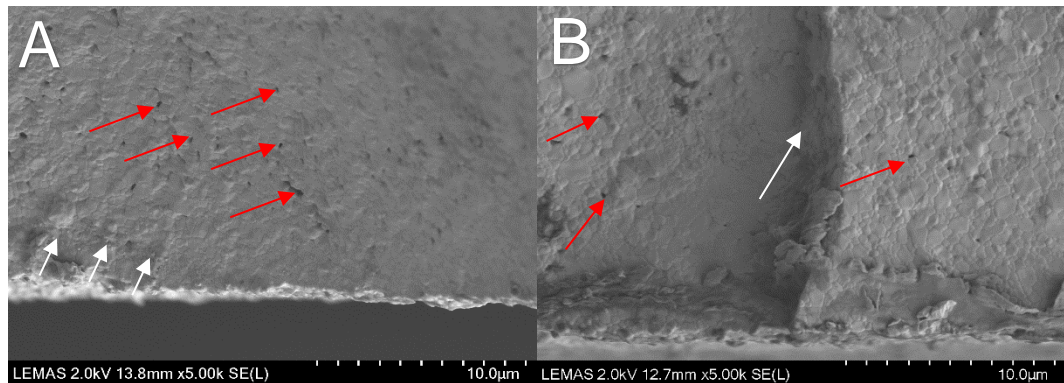


Figure 4-16 SEM images of the fractured surface of ZpexS before (A) and after(B)Aging. Hackles indicated by white arrows, pores indicated by red arrows.

SEM images of the fractured surface of ZpexS, before hydrothermal aging showed a considerable amount of pores and less defined hackles compared to after aging. After aging, in addition to pores, rougher surface and a coarse hackle can be identified.

These coarse hackles are most commonly seen in ceramics with a variation in the microstructure. In ZpexS, this can be explained by the mixture of cubic and tetragonal phases. It is most commonly seen in low strength zirconia

ceramic and especially in the presence of porous structure. It is the sole feature that indicates the direction of the crack propagation (Shen, 2013).

4.1.6 Grain size results

The grain size of all tested groups before and after hydrothermal aging are presented in Table 4-4. Following normality testing, one way ANOVA analysis followed by Tukey HSD post hoc test showed no significant statistical changes in the size of grains before and after hydrothermal aging, however there was a statistical significance in the difference of the mean of grain size between different groups. The order of the groups according to grain size measurements starting from the group with the bigger grain size to lower was in the order of ZPexS>Zpex,3YBE>3YE.

Table 4-4 Grain size result before and after aging.

Materials	Grain Size/nm	
	Before Aging	After aging
3YE	259 ± 8	262 ± 27
3YBE	362 ± 50	364 ± 31
Zpex	413 ± 26	416 ± 41
ZpexS	536 ± 40	534 ± 43

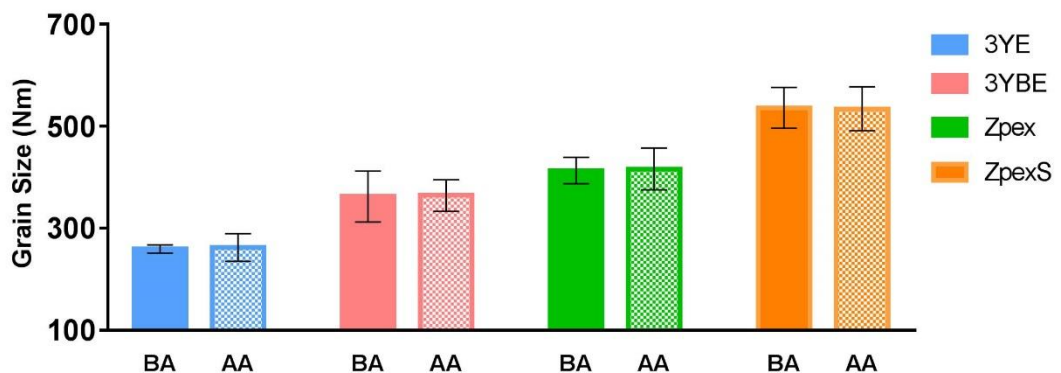


Figure 4-17 Bar chart showing the mean and standard deviation of the grain size before and after aging.

The LTD is a multi-factorial process in nature in which, crystal structure, grain size, residual stress, amount of dopant (Hallmann et al., 2012) and the

sintering temperature play important roles. Sintering temperature and time played a clear role in the final grain size. Comparing the grain size of three of the tested groups 3YE, 3YBE and Zpex as all of them have the same particle size in the starting powder, showed that increasing the sintering temperature and time resulted in a bigger grain size. (Ěastkova et al., 2004, Hallmann et al., 2012) reported that the LTD is strongly related to the grain size and the higher the sintering temperature the more phase transformation. (Cales et al., 1994) and (Gremillard et al., 2004) reported that decreasing the grain size plays an important role in aging resistance. The increase in sintering temperature might result in higher tensile stress leading to more transformation as Zpex showed however, this cannot be confirmed as a main reason behind transformation.

In terms of particle size effect of the starting powder, the material with the finer particle size showed a significantly more strength compared to a powder with a coarse particle size and this was clearly seen as 3YE, 3YBE and Zepx, all showed a higher strength compared to ZpexS. This would suggest, the smaller the grain size the higher the strength; however this excludes the nature of the phases to should be taken with that caveat; grain sizes of the same phases are not being compared. The smaller the grain size the less transformation as that can be clearly seen in 3YE with grain size of ~ 260 nm compared to ~ 415nm of Zpex; this agrees with (Lin et al., 1988) who reported that the increase in grain size could facilitate the transformation by lowering the nucleation barrier, however, ZpexS showed less transformation with a bigger grain size of ~535 nm and this bigger grain size resulted from the cubic grain as a product of the increase in the amount of Y_2O_3 . This would suggest, grain size can be of limited impact on the stability of material against LTD and the main factor that control the size of the grain in addition to sintering temperature, is the composition of the material. This means the effect of grain size on material behaviour after hydrothermal aging would be directly correlated to the main composition of the material as a primary factor in addition to the sintering temperature.

4.1.7 FIB-SEM

The ion beam and SEM images for FIB section of 3YE (Figure 4-18) revealed dense, homogenous, crystal structures. Both images showed pores both before and after hydrothermal aging with more pores can be seen clearly after aging. After aging FIB section was examined thoroughly for any signs of transformation, such as microcracking, crystal twinning, crystal pull-out or loss of material homogeneity. No signs of t-m transformation can be detected in the surface, subsurface or bulk layers of the material.

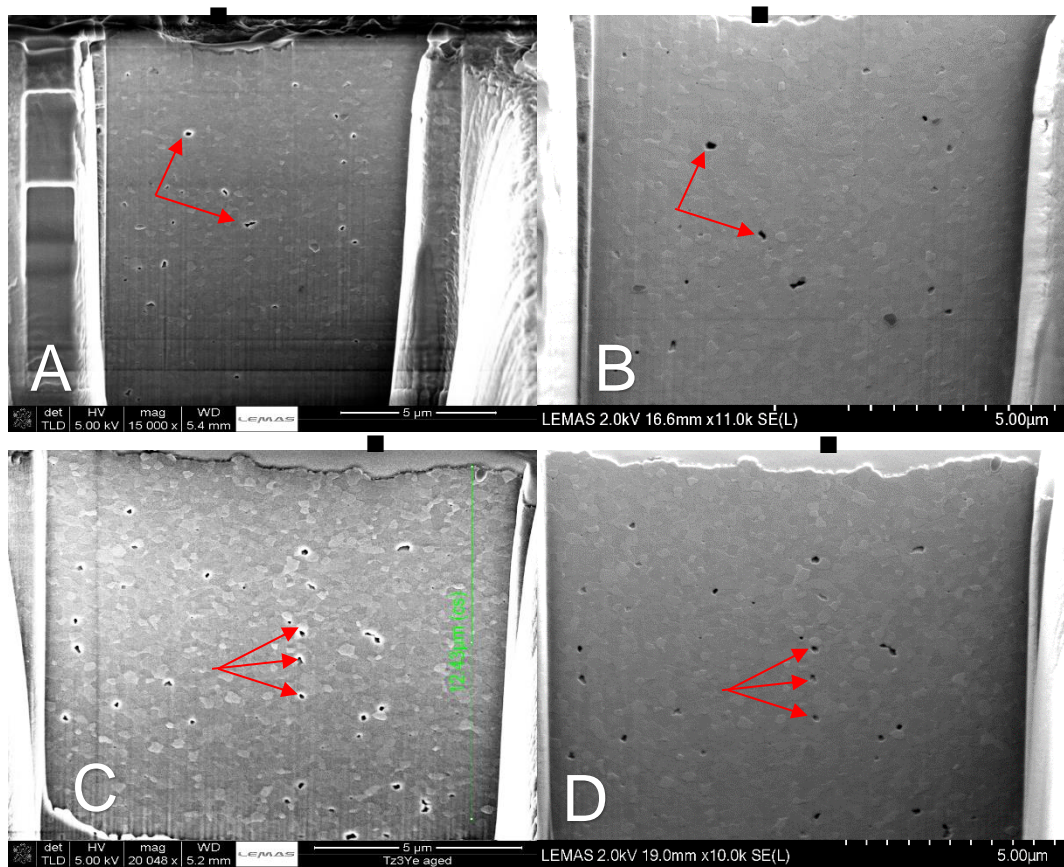


Figure 4-18 Ion beam images and SEM images for FIB prepared section

for 3YE. Platinum layer is annotated with (■) (A) Ion beam image before hydrothermal aging showing , densely packed homogenous crystals with few pores can be seen clearly indicated by red arrows.(B) SEM for the FIB section before aging.(C) Ion beam image after hydrothermal aging showing no signs of t-m that can be detected in the surface, subsurface or bulk layers of the material. There is a clear increase in the number of pores after aging can be clearly seen both in this image and in (D) SEM for the FIB section after aging.

For 3YBE, both ion beam and SEM images for FIB section (Figure 4-19) showed well-defined, densely packed homogenous crystals with few pores can be seen before aging. After aging, thorough examination of the images showed there was a clear increase in the pores, however signs of transformation could not be detected .

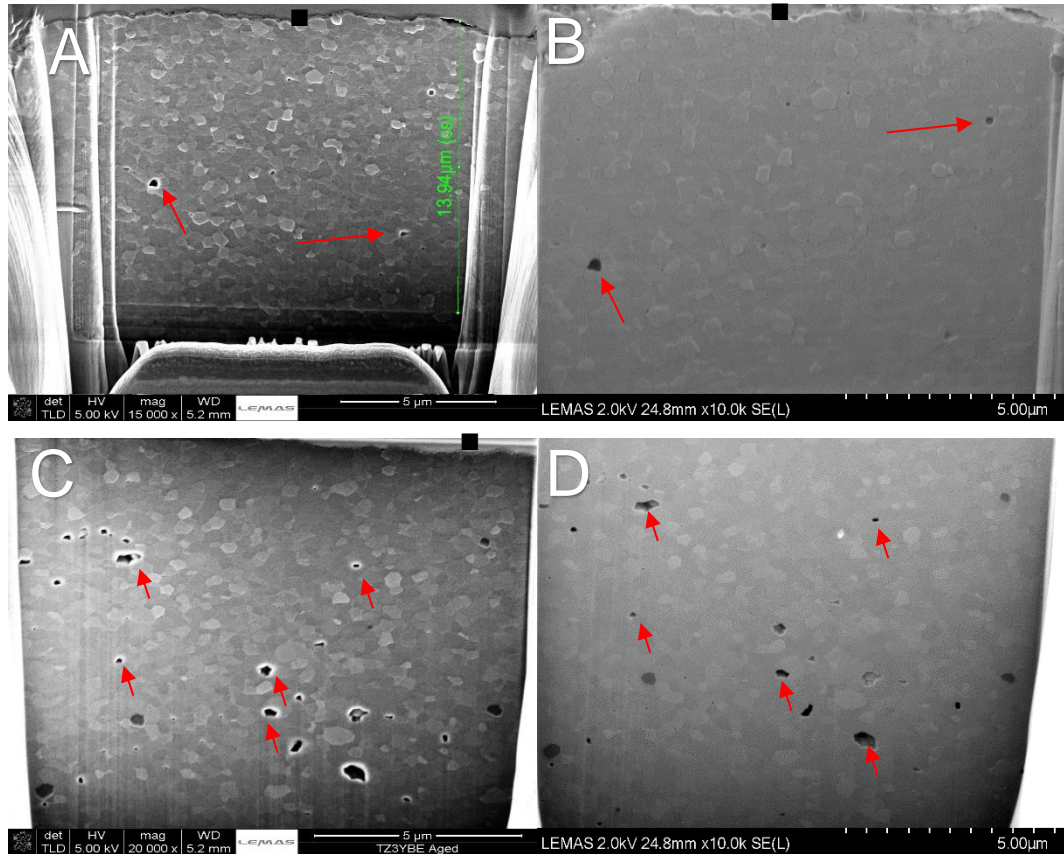


Figure 4-19 Ion beam images and SEM images for FIB prepared section

for 3YBE. Platinum layer is annotated with (■) (A) Ion beam image before hydrothermal aging showing well-defined, densely packed homogenous crystals with few pores can be seen clearly indicated by red arrows.(B) SEM for the FIB section before aging.(C) Ion beam image after hydrothermal aging showing no signs of t-m that can be detected in the surface, subsurface or bulk layers of the material. There is a clear increase in the number of pores after aging can be clearly seen both in this image and in (D) SEM for the FIB section after aging.

While for Zpex, the examination of both images (Figure 4-20), in addition to a clear increase in the porosity after hydrothermal aging, showed a loss of homogeneity in the top layers (~ 3μm) located above the dashed line on the image, the area is also mottled and more whitish in appearance. Furthermore, loss of clear grain boundaries can be seen compared to the rest of the image

underneath the dashed line. These signs which could not be seen in the main bulk, can be regarded as an indication to the transformation of *t-m* on the surface of the sample. The bulk of the sample down to the dashed line showed a characteristic features similar to before hydrothermal aging counterpart apart from the clear increase in the porosity.

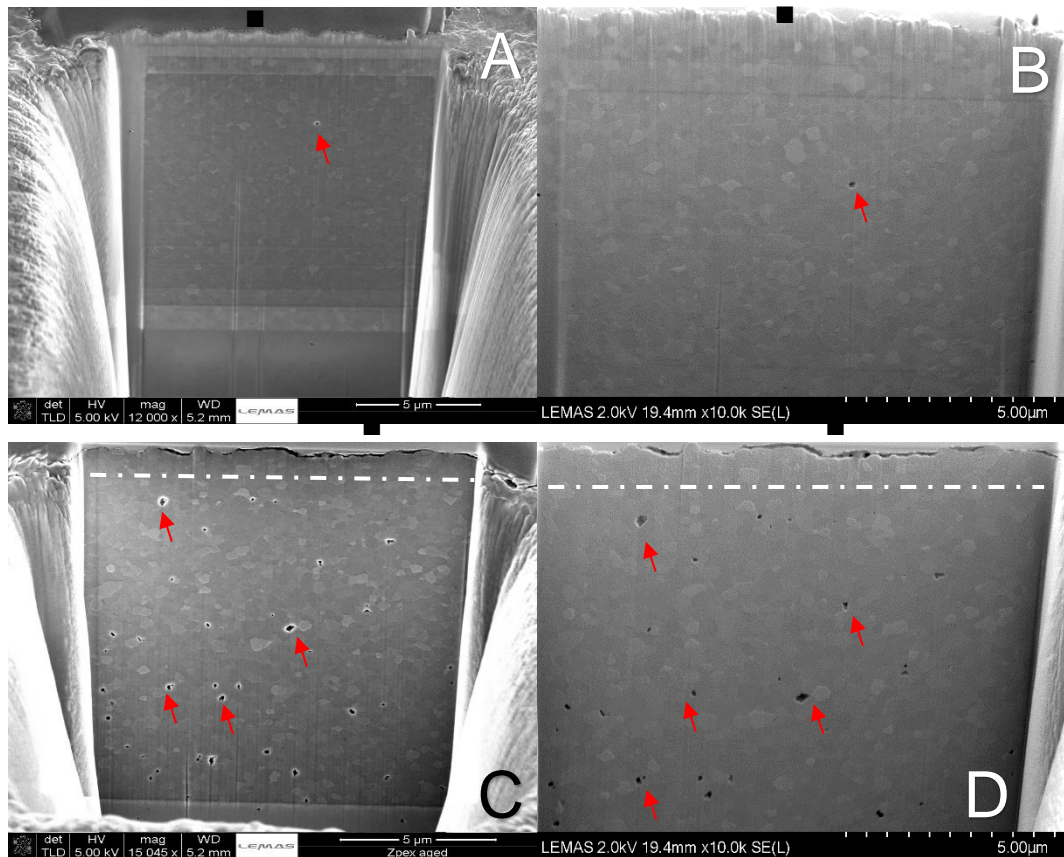


Figure 4-20 Ion beam images and SEM images for FIB prepared section

for Zpex. Platinum layer is annotated with (■) (A) Ion beam image before hydrothermal aging showing well-defined, densely packed homogenous crystals with very few pores can be seen clearly indicated by red arrows.(B) SEM for the FIB section before aging.(C) Ion beam image after hydrothermal aging showing less defined grain boundaries in the area above the dashed line and change in the contrast compared to the rest of grains under the line. There is a clear increase in the number of pores after aging can be clearly seen both in this image and in (D) SEM for the FIB section after aging, showing heterogeneous, mottled, whitish area above the dashed line which can be an indication for *t-m* transformation.

ZpexS showed well-defined, densely packed, different size of grains (Figure 4-21) with few pores both before and after hydrothermal aging.

Interestingly, no clear increase in the pores can be detected after hydrothermal aging however, the pores looked smaller in size.

FIB-SEM results, in addition to the signs of transformation detected for Zpex, showed in general an increase in the porosity after hydrothermal aging and this may be due to opening of already existing closed pores or micro cracks (Luo et al., 2016), by internal stress that can be developed during aging. The dissociation reaction of water under aging condition, is another reason that could be considered behind the increase in porosity. This is because hydrogen ions and hydroxide ions are strongly corrosive and with the small size and reactivity of hydrogen ions, they can penetrate the surface of ceramic and cause the observed pores (Bunker, 1994, Cesar et al., 2007). In addition to the aforementioned reasons, selective leaching of certain ions added as a modifier by ion exchange reactions may create pores or channels within the glassy matrix of ceramics (Bunker, 1994, Cesar et al., 2007, Geisler et al., 2010). However this might not be applicable to zirconia used in this study as no ions have been added to its main composition. Due to the difficulty of determining the depth of transformation and whether the increase in porosity is a result of transformation or not, the most reasonable scenario behind the increase in the porosity would be the opening of already existing pores due to increase in the internal stress as a result of aging.

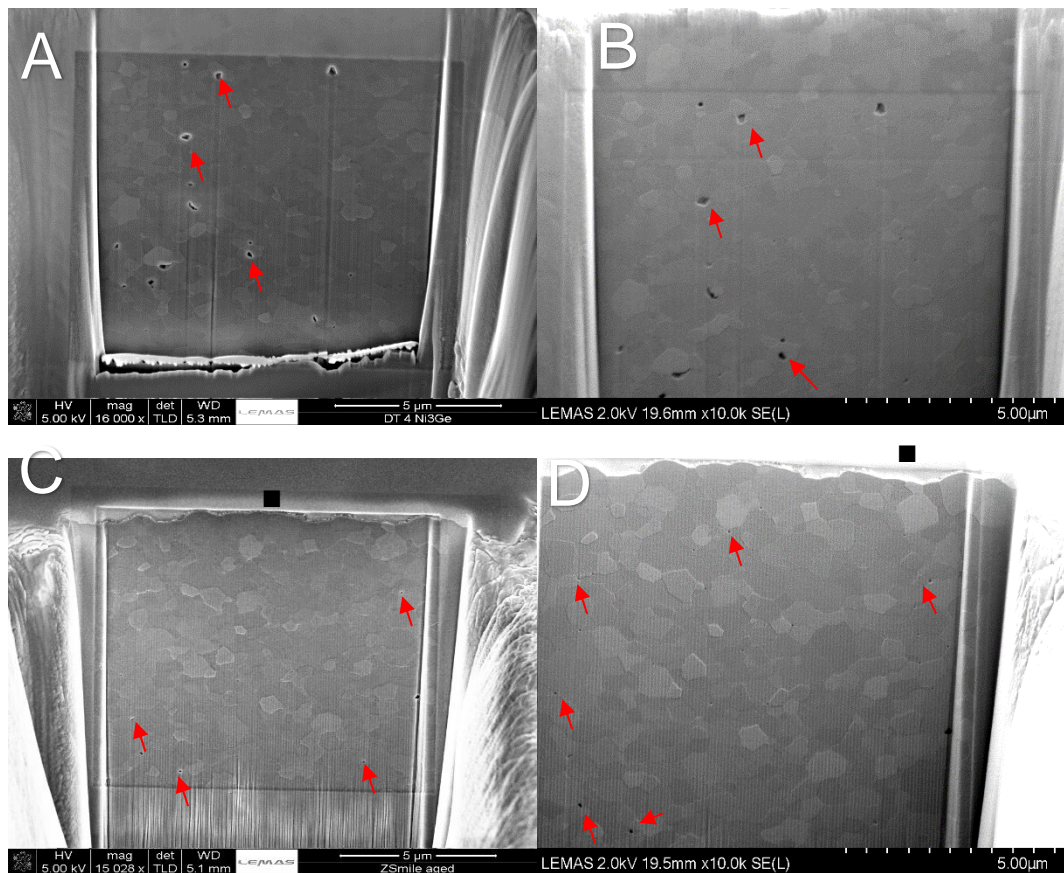


Figure 4-21 Ion beam images and SEM images for FIB prepared section

for ZpexS.

Platinum layer is annotated with (■) (A) Ion beam image before hydrothermal aging showing well-defined, densely packed, different size of crystals with few pores can be seen clearly indicated by red arrows. (B) SEM for the FIB section before aging. (C) Ion beam image after hydrothermal aging showing dense, different size grains with well-defined boundaries. There is no increase in the number of pores after aging however the pores appeared smaller (D) SEM for the FIB section after aging, with no signs of transformation can be detected.

Further investigations will be needed to determine the main cause behind the increase in pores and larger and different areas on each sample need to be prepared and examined to understand this phenomena more clearly to hopefully give a clearer understanding about transformation within the bulk. After thorough examination of all FIB-SEM sections for any signs of LTD including; microcracking, crystal twinning, crystal pull-out or loss of material homogeneity, none of the samples showed clear signs of aging other than Zpex which showed a 2-3 μm of the superficial layer of heterogeneous, ill-

defined grains boundaries which can be attributed to the tetragonal to monoclinic transformation.

4.1.8 Surface Roughness Results

Surface roughness (Ra) and (Rq) mean values of each material for before and after hydrothermal aging groups are presented in (Table 4-5). In a comparison between surface roughness values of the different groups, they were in the order from the roughest to the smoothest, 3YE>ZpexS>Zpex>3YBE, for before-aging groups while after aging they were in, 3YE>Zpex>ZpexS>3YBE. All the groups showed a clear increase in the roughness values after hydrothermal aging, However, there was no statistically significant difference ($p<0.05$) in the roughness between before and after hydrothermal aging, apart from Zpex which showed a significant increase in the roughness after aging.

Table 4-5 Mean and Standard deviation for surface roughness before and after hydrothermal aging.

Material	(Ra) mean±SD (Nm)	(Rq) mean±SD (Nm)
3YE_BA	31.20 (2.22)	40.47 (3.89)
3YE_AA	47.64 (16.78)	63.46 (21.29)
3YBE_BA	10.72 (2.28)	14.15 (3.14)
3YBE_AA	29.92 (17.20)	37.86 (21.96)
Zpex_BA	16.91 (1.86)	21.92 (3.34)
Zpex_AA	38.76 (8.36)	49.18 (10.29)
ZpexS_BA	29.56 (2.20)	39.05 (2.82)
ZpexS_AA	30.74 (12.92)	39.18 (15.47)

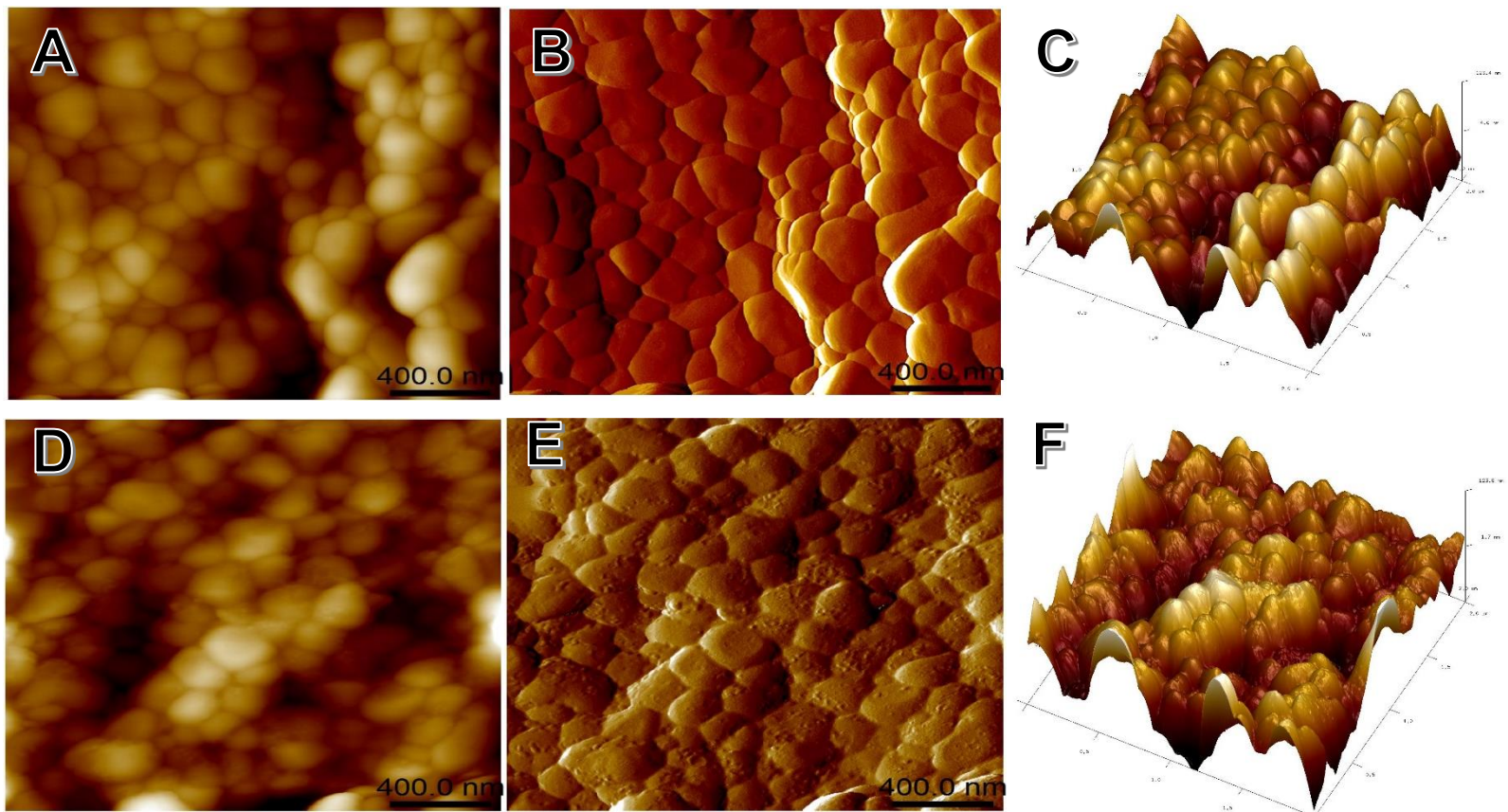


Figure 4-22 AFM for 3YE before and After aging. (a) height sensor BA (b) amplitude view BA (c) 3D view BA (d,e,f After aging).

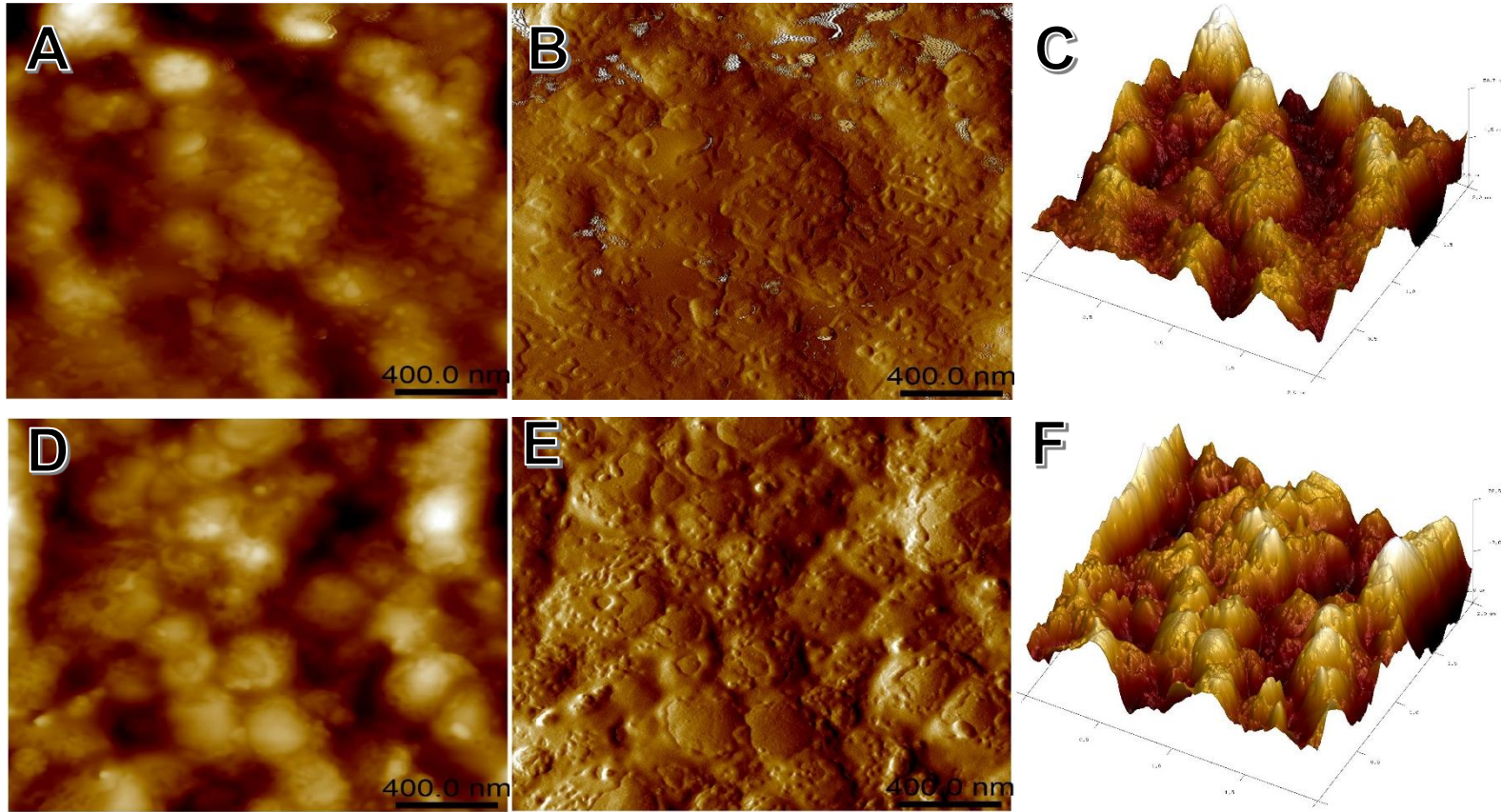


Figure 4-23 AFM for 3YBE before and After aging. (a) height sensor BA (b) amplitude view BA (c) 3D view BA (d,e,f After aging).

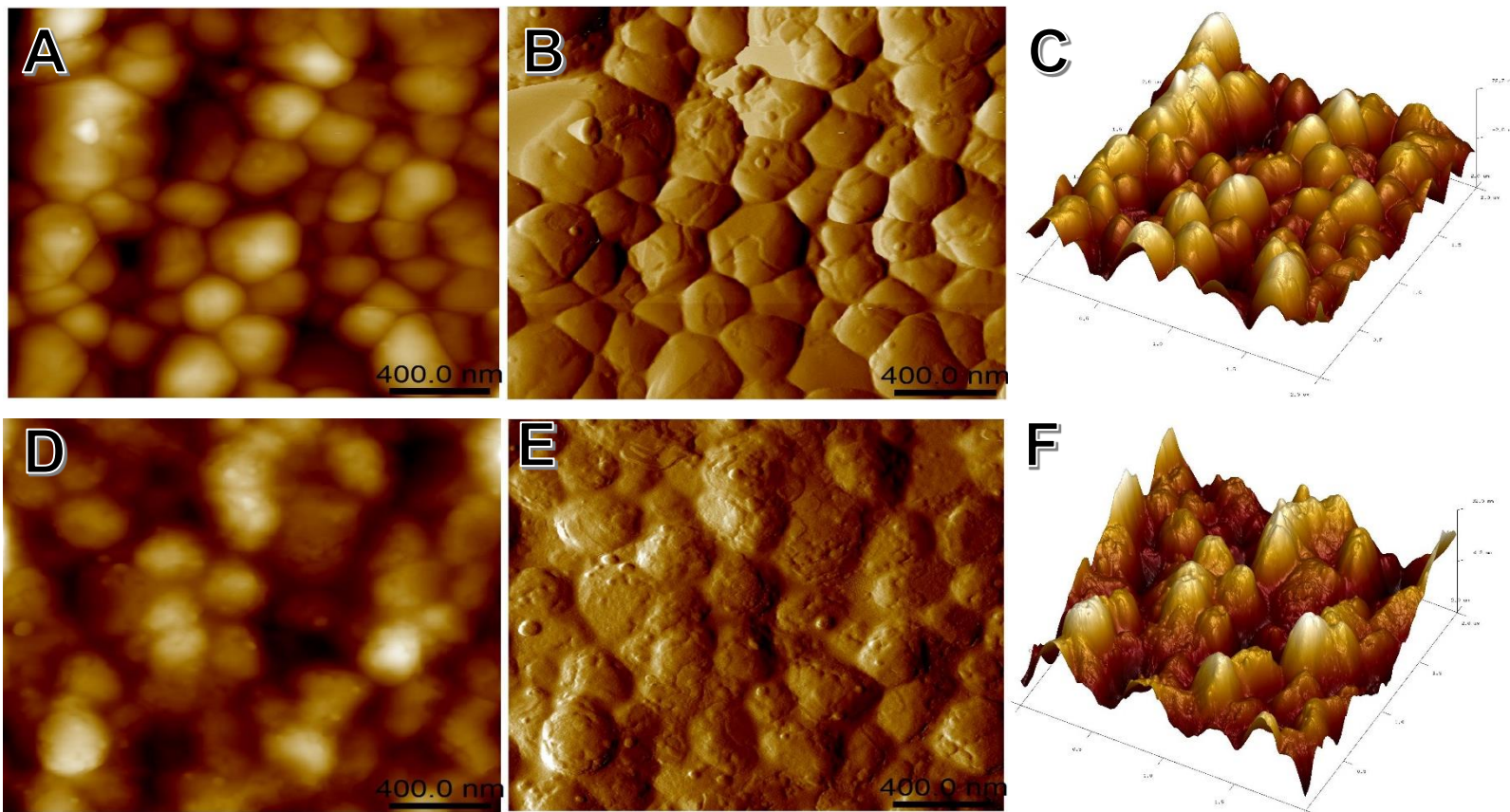


Figure 4-24 AFM for Zpex before and After aging. (a) height sensor BA (b) amplitude view BA (c) 3D view BA (d,e,f After aging).

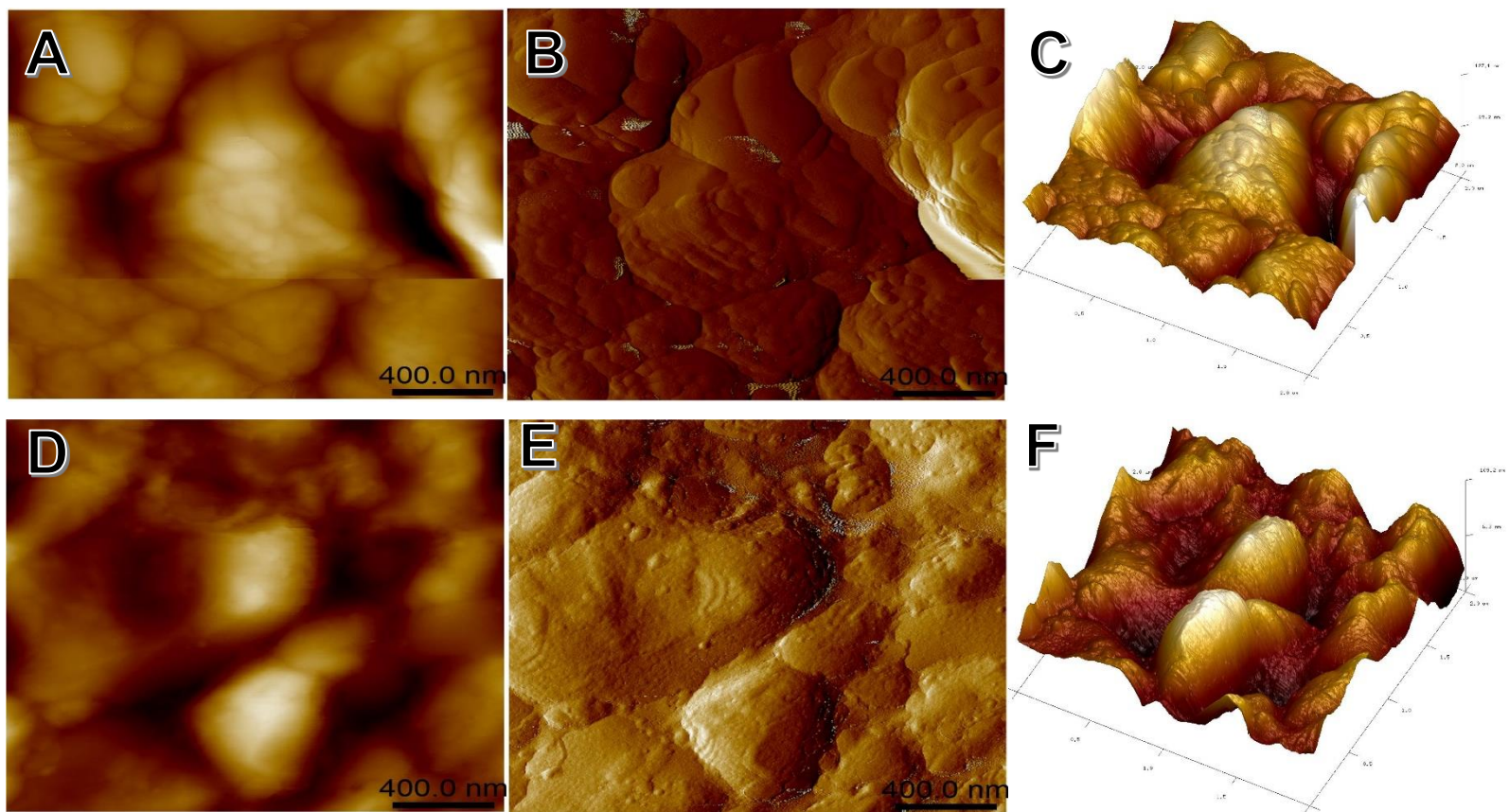


Figure 4-25 AFM for ZpexS before and After aging. (a) height sensor BA (b) amplitude view BA (c) 3D view BA (d,e,f After aging).

The materials in this study showed a higher surface roughness compared to other zirconia types studied by different authors. Casucci, et al,2010 reported Ra of 7.31,7.27 and 6.94 nm for Cercon® , Aadva Zr and Lava™ respectively, however these were obtained after polishing of the samples. In this study samples were not touched by any polishing machine to avoid any transformation that can result and the samples were almost mirror polished after complete sintering.

It can be clearly seen that all AFM images showed a different surface texture after hydrothermal aging but the most affected surface by aging was Zpex (Figure 4-24). This is mainly can be attributed to highest amount of transformation showed by Zpex after aging and might be caused by uplift of monoclinic grains resulting in this increase in the roughness. This result is consistent with (Roy et al., 2007, Kim et al., 2009b) who reported that the surface roughness of zirconia can increase with aging and has a direct proportional relationship with the increase in monoclinic fragments as a result of aging induced tetragonal to monoclinic transformation (Haraguchi et al., 2001, Fernandez-Fairen et al., 2007, Alghazzawi et al., 2012, Kohorst et al., 2012). The 3-5% volumetric expansion accompanying the transformation is responsible for the detachment of surface grains causing an increase in the roughness (Kim et al., 2009a, Alghazzawi et al., 2012), however, the result did not agree with (Cotes et al., 2014) who reported that there is no relationship between aging and roughness as measured using a digital optical profiler.

Chapter 5

Optical Properties: Results and Discussion

5.1 Effect of thickness

The effect of three thicknesses (0.75,1.00,1.25 mm) on the translucency parameter (TP), contrast ratio (CR) and total transmittance (Tt%) was assessed for each material group. The null hypothesis that the thickness has an effect on the translucency was accepted. Following normality testing, one way ANOVA showed that thickness has a significant effect on all measured parameters ($p < 0.05$). Increasing thickness led to decrease in the TP, Tt% and an increase in contrast ratio (CR).

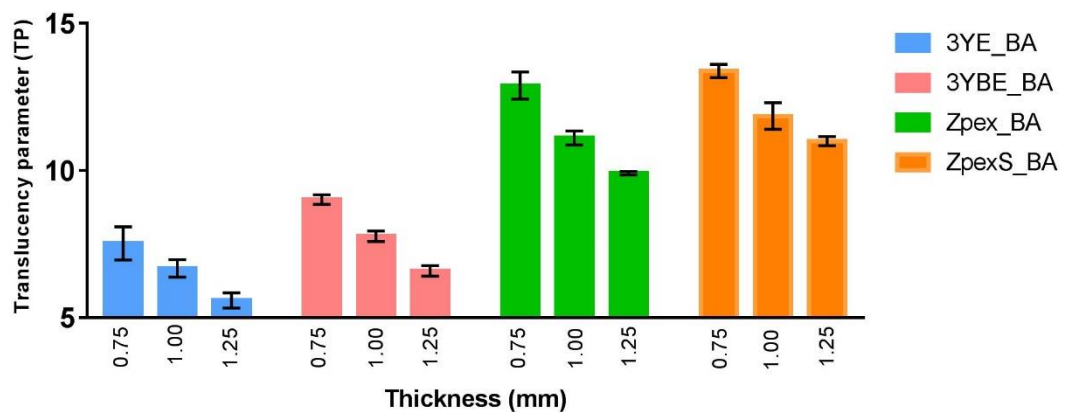


Figure 5-1 Effect of thickness on Translucency Parameter (TP). The bar chart showing clearly the significant difference in the TP for different thickness for each material.

5.1.1 Translucency parameter

Translucency parameter (TP) showed a significant decrease with an increase in thickness; 0.75mm thickness showed the highest (TP) while the 1.25 mm thickness disc showed the lowest (TP) and this was applicable to all of the materials involved in the study. However the amount of TP difference between thicknesses was different and material dependant (Table 5-1).

Table 5-1 Mean, SD and R² of Translucency parameter

Thickness (mm)	0.75	1.00	1.25	ΔTP			R ²
				0.75- 1.00mm	1.00- 1.25 mm	0.75- 1.25mm	
Material							
3YE_BA	7.52 (0.56)	6.67 (0.29)	5.58 (0.25)	0.85	1.09	1.94	0.94
3YBE_BA	9.01 (0.16)	7.76 (0.18)	6.59 (0.18)	1.25	1.17	2.42	0.99
Zpex_BA	12.89 (0.46)	11.11 (0.23)	9.91 (0.05)	1.78	1.2	2.98	0.97
ZpexS_BA	13.38 (0.22)	11.85 (0.45)	11.00 (0.15)	1.53	0.85	2.38	0.88

The general trend showed that the more translucent the material the more sensitive TP was to thickness changes. For all groups apart from 3YE group, the difference between the thinnest and the thickest sample was considered to be perceptible by 50% of the population at $\Delta TP=2$ or more (Paravina et al., 2015, Lee, 2015).

All of the groups involved in this study showed a significant linear relationship ($P < 0.0001$) between the thickness and the TP with R² ranging from (0.88-0.99) (Table 5-1). The same data can be plotted to investigate the exponential relationship between TP and thickness claimed by Wang et al. (2013) for different types of glass ceramics and zirconia (Wang et al., 2013). For 3YE, 3YBE, Zpex and ZpexS, R² values of 0.94, 0.99, 0.98 and 0.89 were recorded, similar to the R² values of the linear plots. It may be that over the range of TP measured in this study, it is impossible to determine if the relationship is linear or exponential. Many factors can have an effect on determining the relationship, this might include the material type and its coefficients of absorbance and reflectance, thicknesses of the samples and the method of measurements in addition to the type of instruments. In the current study, the more translucent zirconia, ZpexS, Zpex and 3YBE showed a greater change in the translucency as a function of thickness compared to less translucent one, 3YE. This result agrees with the findings of Antonson

and Anusavice, 2001 and with Wang et al,2013 (Antonson et al., 2001, Wang et al., 2013).

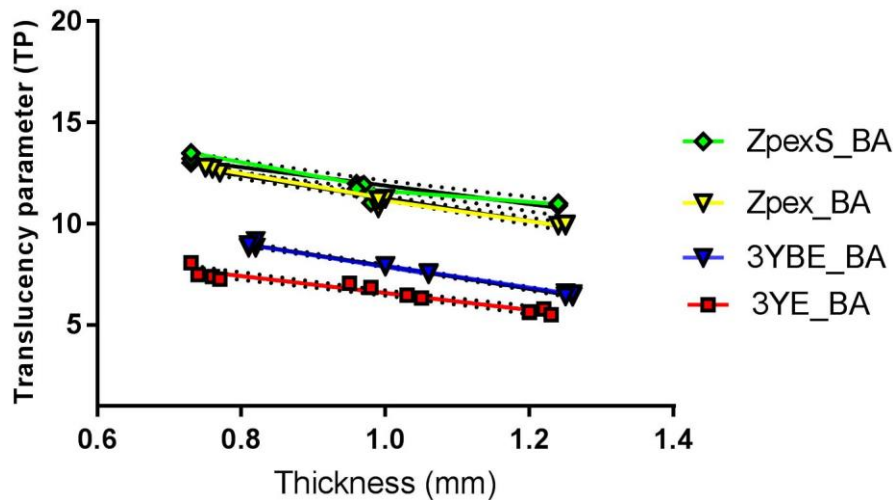


Figure 5-2 Plot of the thickness against transluency parameter (TP) of all groups before aging. All groups can be clearly seen showing a linear relationship, however there are some outliers which can affect the strength of the linearity of the relationship.

This means the aesthetics will be less affected by the increase of thickness of least translucent zirconia compared to the one with more translucency. The clinical importance of this finding suggests considerable attention should be given to thickness when using a material of high translucency, for example, a veneer to an anterior tooth (Wang et al., 2013).

TP can be affected by the method of measurements used. Lim et al. (2010) compared TP measured by spectrophotometer (SP) and spectroradiometer (SR), they found that even if the colour measuring mechanism looks similar, there was a clear difference in TP measurements between the two methods. TP measured by SR showed a higher value compared to the one measured using SP. This difference was attributed to the fact that SR measurement used an illuminating area that was bigger than that of SP which could result in more reflected light over the white backing (Lim et al., 2010). Yu et al. (2009) reported that the bigger the aperture used for measuring TP, the higher the measured TP value compared to a smaller aperture (Yu et al., 2009).

5.1.2 Transmittance

Results of measurement of transmittance (Tt%) (Figure 5-3) followed the same trend as translucency parameters. Following normality testing, one way ANOVA followed by Tukey tests ($p < 0.05$) showed that there was a significant decrease in the transmittance with increasing thickness for all tested groups. 0.75mm thickness groups showed significantly highest transmittance compared to 1.25 mm group which showed the lowest transmittance .

The difference between the thinnest and thickest sample of all groups is presented in (Table 5-2)..

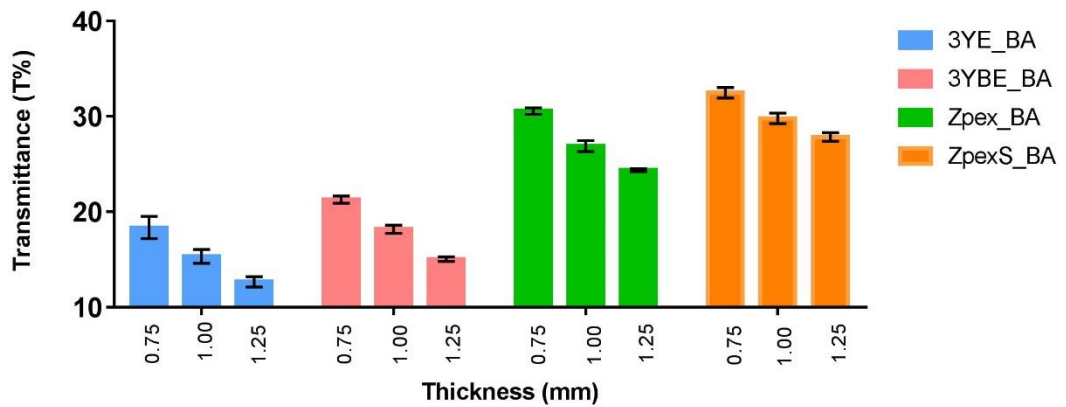


Figure 5-3 Effect of thickness on Transmittance (Tt%). The bar chart showing clearly the significant difference in the Tt% for different thickness for each material.

Table 5-2 Mean, SD and R² of Transmission %

Thickness (mm)	0.75	1.00	1.25	$\Delta Tt\%$			R ²
				0.75- 1.00mm	1.00-1.25 mm	0.75- 1.25mm	
Material							
3YE_BA	18.37 (1.17)	15.34 (0.72)	12.68 (0.53)	3.03	2.66	5.69	0.96
3YBE_BA	21.28 (0.38)	18.19 (0.42)	15.05 (0.18)	3.09	3.14	6.23	0.99
Zpex_BA	30.57 (0.33)	26.91 (0.58)	24.38 (0.15)	3.66	2.53	6.19	0.99
ZpexS_BA	32.48 (0.54)	29.81 (0.55)	27.86 (0.45)	2.67	1.95	4.62	0.94

Tt% appeared more consistent in terms of measurement for all groups. This can be attributed to the precision of the spectrophotometer as this reading was reported directly from the spectrophotometer (with no interference from a human being to do the calculation).

The transmittance value for all groups showed a significant linear relationship with thickness ($P < 0.0001$) and R² ranging from (0.94-0.99)(Figure 5-4). The result of Tt% is highly correlated with TP. Pearson rank test showed a significant strong positive correlation with a correlation factor 0.94 between Tt% and TP. This was applicable to all of the thicknesses.

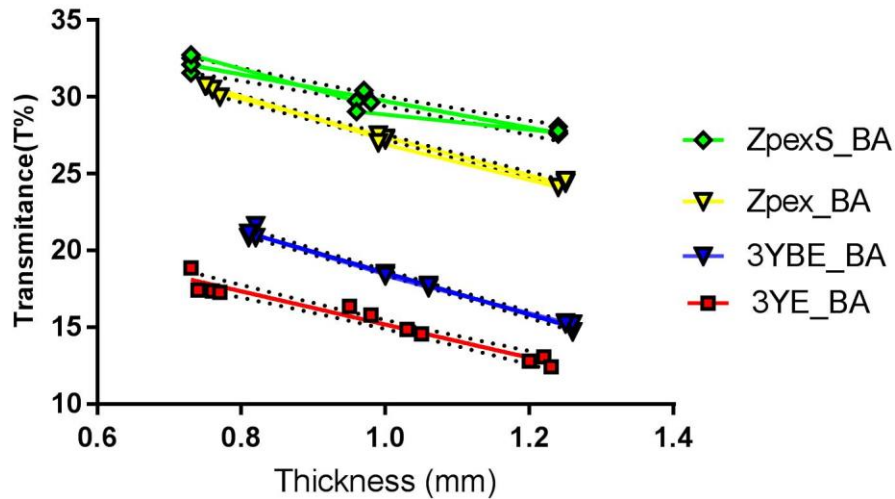


Figure 5-4 Plot of the thickness and Transmittance (Tt%) of all groups before aging.

5.1.3 Contrast Ratio

Contrast ratio (CR), as one of the most commonly used parameters for measuring relative translucency, showed a statistically significant increase with the increase in thickness. The thicker the sample, the statistically significantly higher the contrast ratio compared to thinner one. [NB, zero value of contrast ratio indicates a transparent material and a CR of one is opaque (Kingery, 1960)].

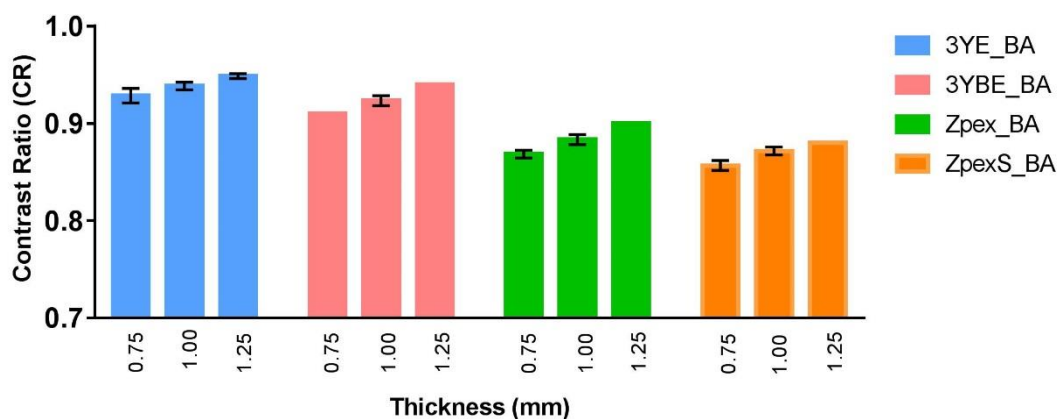


Figure 5-5 Effect of thickness on Contrast Ratio(CR). The bar chart showing clearly the significant difference in the Contrast ratio (CR) for different thickness for each material.

Following normality testing, one way ANOVA showed that the contrast ratio of 0.75 mm thickness was significantly ($p < 0.05$) lower than that of 1.25 mm (Table 5-3) which showed the highest. The contrast ratio value for all groups showed a significant linear relationship with thickness ($P < 0.0001$) and R^2 ranging from (0.88-0.98).

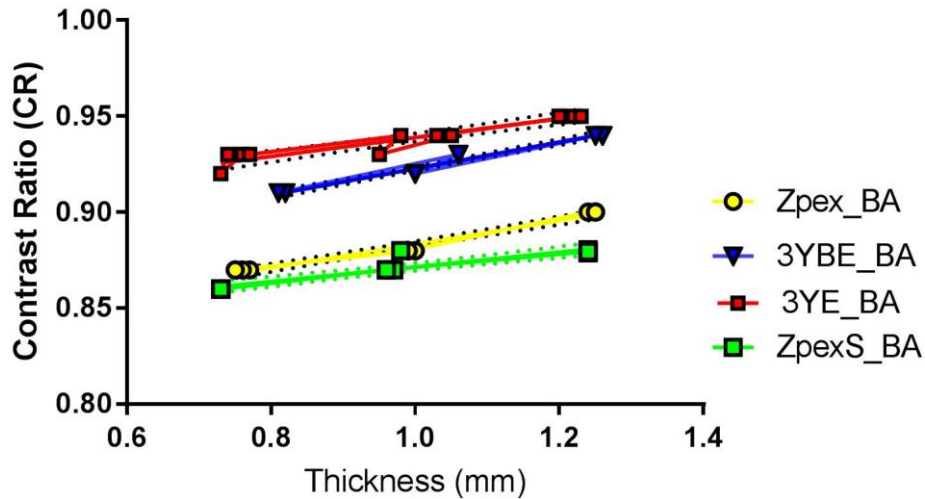


Figure 5-6 Plot of the thickness and contrast ratio (CR) of all groups before aging.

Table 5-3 Mean, SD and R^2 of Contrast ratio (CR)

Thickness (mm)	0.75	1.00	1.25	Δ CR			R^2
				0.75-1.00mm	1.00-1.25 mm	0.75-1.25mm	
Material							
3YE_BA	0.928 (0.008)	0.938 (0.004)	0.949 (0.003)	0.01	0.011	0.02	0.90
3YBE_BA	0.910 (0.000)	0.923 (0.005)	0.940 (0.004)	0.013	0.017	0.03	0.98
Zpex_BA	0.868 (0.004)	0.883 (0.004)	0.900 (0.00)	0.015	0.017	0.03	0.96
ZpexS_BA	0.857 (0.005)	0.872 (0.004)	0.880 (0.00)	0.015	0.008	0.023	0.88

Despite the fact that CR showed a statistically significant difference as a function of thickness, this was the least sensitive parameter to show the effect of thickness on translucency. The biggest difference between the thickest and thinnest sample recorded was 0.03 for 3YB and for Zpex. This difference is clinically not detectable and not perceivable as differences below 0.07 in CR are considered not detectable by the human eye. This value is based on the mean translucency perception threshold (TPT) defined by Liu et al. 2010 who tried to compare the human eye's ability to detect the changes in the translucency of ceramic measured using a spectrophotometer. They found that the mean Translucency Perception Threshold (TPT) can be affected by the type of lighting used to measure the translucency as well as the level of the experience of the observer. They concluded that the mean TPT of inexperienced groups was 0.09 and for the expert was 0.04 and overall mean TPT of all subjects was 0.07. Their conclusion was a difference in CR more than 0.06 may be perceived by 50% of the population (Liu et al., 2010a, Carrabba et al., 2017).

Pearson rank correlation between CR and TP showed a strong significant negative correlation between the two parameters where all the sample of different thicknesses of all tested groups included ($p < 0.01$) and the coefficient of correlation was -0.96. The same correlation test conducted between Tt% and CR and it showed also a significant negative strong correlation with a correlation factor of -0.91.

Even with this high statistically significant correlation, CR did not reflect what TP showed in terms of perceptibility. TP showed, in addition to the statistically significant difference in the translucency in terms of thickness, a perceptible difference in the translucency which can be clinically detectable.

The effect of thickness on the translucency of different types of dental ceramic was reported in many studies (Kingery et al., 1976, Johnston and Kao, 1989, Luo and Zhang, 2010, Nakamura et al., 2016). Antonson et al, 2001 studied how thickness can affect the contrast ratio of dental core and veneering ceramics. They concluded that the relationship between the contrast ratio of dental core and veneer ceramics and thickness was a linear relationship and an increase in the thickness showed a clear increase in the contrast ratio

(Antonson et al., 2001). Kanchanavasita et al. (2014) studied the effect of accelerated aging on translucency of monolithic zirconia and found the thickness has a clear effect on the translucency of monolithic zirconia. They claimed that the relationship between CR and thickness was not linear but rather was logarithmic as an increase in the thickness showed a non-linear drop in transmission (Kanchanavasita et al., 2014).

A significant increase in light transmission with a decrease in thickness of various dental ceramics and zirconia respectively has been reported (Rasetto et al., 2004, Cekic-Nagas et al., 2012). Awad et al. (2015) found a large decrease in translucency when the thickness of ceramic doubled (Awad et al., 2015).

Colour and translucency are two highly correlated parameters and each has an effect on the other. The appearance of natural tooth results from the reflectance of dentine modified by the absorption, scattering and the thickness of the translucent enamel (Seghi et al., 1986). The contrast ratio is unlike TP and Tt% as it does not take into consideration the value of a^* and b^* and only takes L^* value into consideration. Both a^* and b^* values when considered in the measurements of transmission and translucency parameter showed a clear contribution to the translucency value.

The effect of thickness on the translucency can be explained as follows; increasing thickness of a crystalline structure such as zirconia can result in an increase in the light-sample interactions during its passing through the sample, e.g. more light scattering and reflection as the light needs to face more grains and grain boundaries. Accordingly, increasing the thickness results in a reduced amount of light that can pass through the material, resulting in reduced translucency (Xu et al., 2015a).

Spink (2009), compared absolute translucency and relative translucency of dental ceramics using different thicknesses of a wide range of dental ceramics and found that the relationship between absolute and relative translucency is sensitive up to 50% and when this absolute translucency dropped below 50%, the contrast ratio reaching high up to one. Therefore, she suggested that the contrast ratio might be useful for ranking the translucency when the transmission is higher than 50%. She also found that the thickness can affect

the transmission but in a different manner between different materials and it was material dependant. In the same study, she found that zirconia specimens' translucency were the least affected by increasing the thickness compared to all other types of dental ceramic (Spink, 2009).

The result of the current study agree with Spink (2009) and Mohie el-Din Wahba et al. (2017) about the sensitivity of direct transmission compared to contrast ratio. It has been found that contrast ratio is a less sensitive measurement of translucency compared to both translucency parameters and direct transmission measurements. Contrast ratio might not be useful in measuring the translucency of high absorbance or high scattering materials as it would not be sensitive enough to detect the small changes in the transmission for those materials. Accordingly, direct transmission (Spink, 2009, Mohie el-Din Wahba et al., 2017) and/or translucency parameter measurements should be the gold standard to measure translucency of dental ceramics as both are more sensitive and do take into consideration all the $L^*a^*b^*$ values compared to only lightness when measuring the contrast ratio. As mentioned earlier that the colour and translucency are highly correlated parameters, therefore **all** colour parameters should be considered during measuring the translucency.

The result of translucency for the different thicknesses being tested showed that, even with a thickness of 0.75mm the materials were still predominantly opaque compared to other ceramics such as lithium disilicate (Carrabba et al., 2017). This agrees with Zhang, 2014 who reported that the commercially available, so-called 'translucent' zirconia could only show a considerable amount of translucency when the thickness was <0.5mm (Zhang, 2014).

5.2 Effect of aging on the translucency

The 1.00 mm thickness group was picked as representative to check the effect of aging. This thickness was chosen to allow the researcher to compare the result with other studies as this is one of the most commonly studied thickness for different types of dental ceramic. It is also recommended to be used for monolithic zirconia (Sun et al., 2014). Normality test showed normally distributed data for all groups and paired sample T test conducted on each

material before and after aging showed that aging had no significant effect on all of the three parameters measured including Tt%, CR and TP. This was applicable to all of the material tested, apart from Zpex which showed statistically significant changes in TP and Tt% measurements but not in CR.

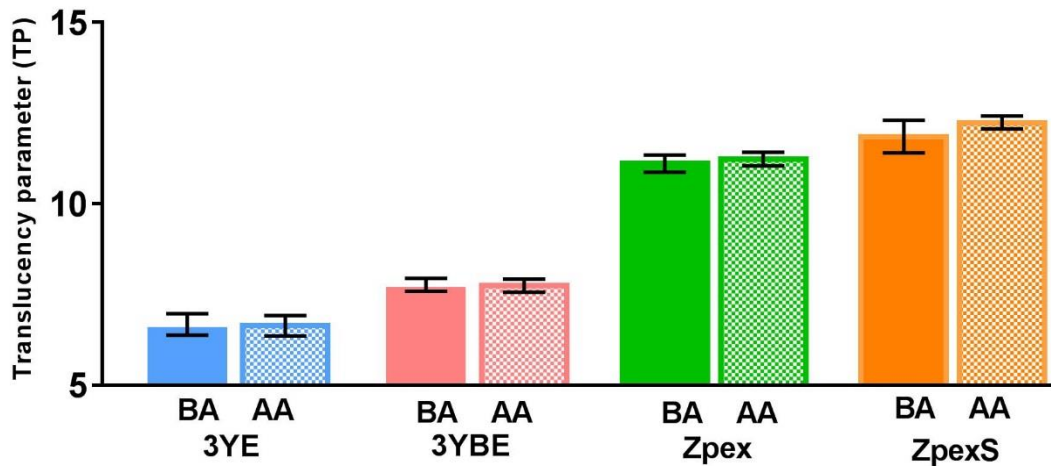


Figure 5-7 Effect of aging on Translucency Parameter(TP). The bar chart showing there is no significant changes to the TP of all groups apart from the Zpex.

5.2.1 Translucency parameter

Zpex_BA showed a TP of $11.11 \pm (0.23)$ and Zpex_AA showed a TP of $11.23 \pm (0.18)$, which means an increase in TP after aging by 0.12, however this statistically significant change is clinically not detectable as the difference in TP < 2 (Yu and Lee, 2008, Lee, 2015). With this tiny amount of increase in TP, it is extremely difficult to find a specific reason however this material showed the more monoclinic volume after aging. This result disagrees with a recent study by Abdelbary et al, 2016, who studied the effect of accelerated aging on the translucency of InCoris1 TZI translucent zirconia. They reported that the material was not affected significantly by aging at thickness of 1.00 mm and the TP was 11.49 ± 0.95 , (Abdelbary et al., 2016).

The result also does not agree with Fathy et al ,2015 who studied the effect of accelerated aging on the translucency of monolithic and core zirconia. They stated that aging had a significant reduction on TP of both types used in their study. (Zirkonzahn Prettau, Zirkonzahn GmbH, Bruneck, Italy) used as monolithic zirconia in their study showed a drop in the TP from (16.4 ± 0.316)

to 13.35 ± 0.158) before and after aging respectively while for the core, (Lava frame, 3M-ESPE, St. Paul, MN) the TP dropped from (9.38 ± 0.395) before aging to (7.05 ± 0.261) after aging (Fathy et al., 2015), however they used a different aging cycle, to the one used in this study, which lasted for 15hrs at 134° at 2 bar. This was attributed to the effect of aging on phase transformation as both monolithic and core material showed an increase in the volume of monoclinic. This increase can result in micro cracking and uplift of the grains which act as a porosity that enhanced the scattering of light and reduce the light transmission (Fathy et al., 2015). The difference in the translucency between the monolithic and the core was attributed to the grain size as core type showed a smaller grain size compared to the monolithic one (Fathy et al., 2015).

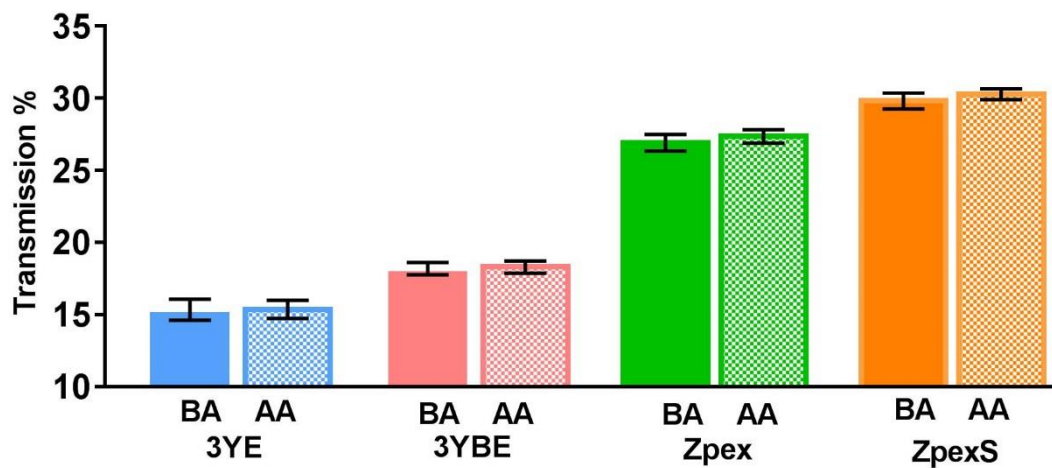


Figure 5-8 Effect of aging on Transmission %. The bar chart showing there is no significant changes to the Tt% of all groups apart from the Zpex.

5.2.2 Transmission

The Tt% for Zpex_BA was 26.91 ± 0.58 while for Zpex_AA was 27.35 ± 0.47 . this means transmission showed an increase after aging by 0.44, however this

statistically significant changes might not be detectable clinically.

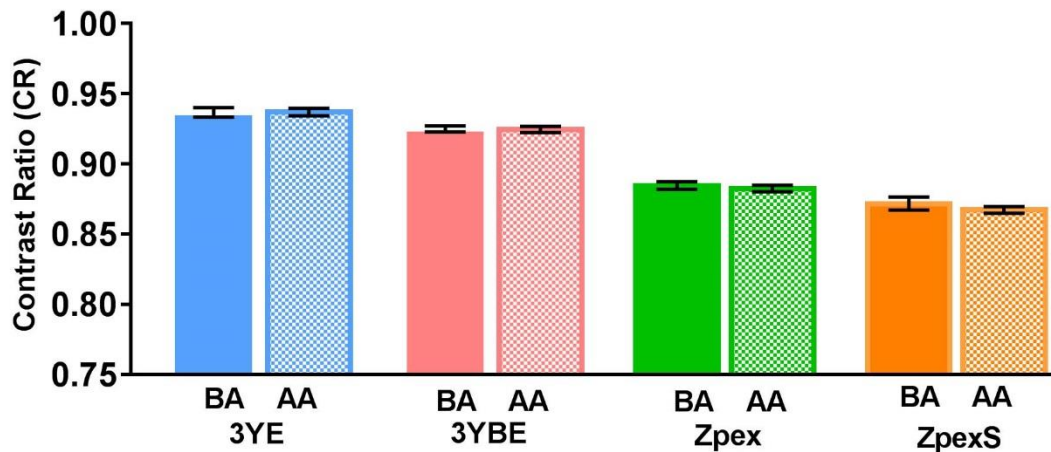


Figure 5-9 Effect of aging on Contrast ratio (CR). The bar chart showing there is no significant changes in the CR of all groups.

5.2.3 Contrast Ratio

Aging showed no statistically significant effect on the CR of all tested materials including Zpex. As mentioned earlier CR is less sensitive than other parameters and this due to the fact that only L^* value is considered and a^* and b^* who could also be affected by aging are not considered in the measurement of CR.

5.3 Effect of material on translucency

The null hypothesis that there is no difference in the translucency between different materials was rejected. Following normality testing, one way ANOVA showed a significant difference ($p < 0.05$) in the translucency parameters (TP) of the four different materials used in this study (Figure 5-10).

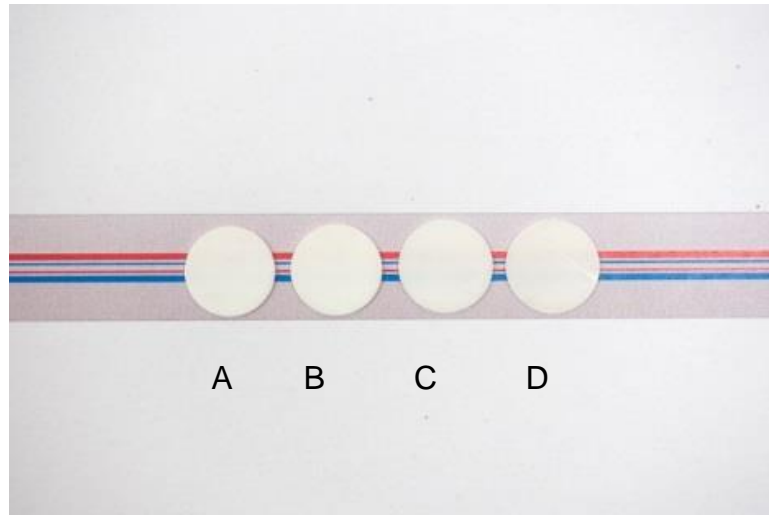


Figure 5-10 The difference in the translucency, 0.75mm thickness. (A) 3YE (B) 3YBE (C) Zpex (D) ZpexS.

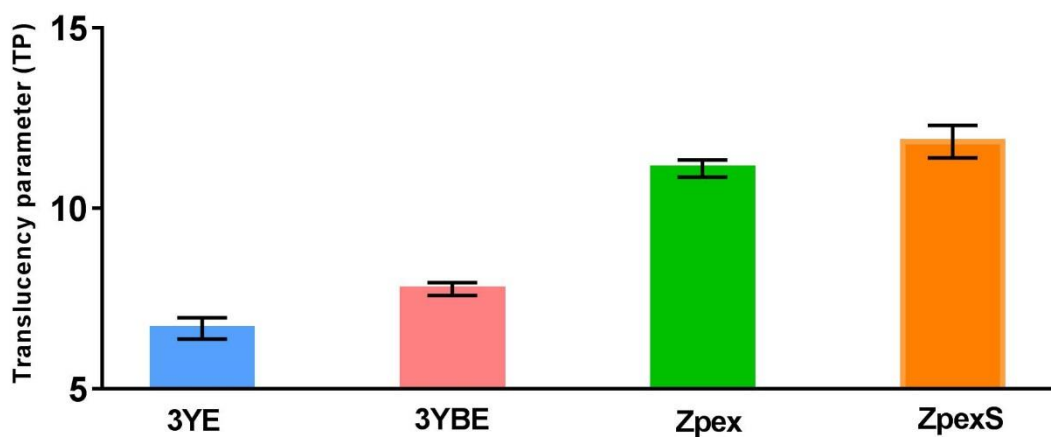


Figure 5-11 TP of the four tested groups. The bar chart showing a clear significant difference in the TP of all tested groups.

5.3.1 Translucency Parameter

The 1.00 mm thickness of the tested groups showed an average of TP from 6.67 to 11.85. ZpexS showed the highest TP of 11.85 ± 0.45 followed by Zpex 11.11 ± 0.23 , 3YBE 7.76 ± 0.18 and 3YE 6.67 ± 0.29 (Figure 5-11). According to this result, the materials can be ranked from the highest translucent to the lowest one in this order, ZpexS > Zpex > 3YBE > 3YE. The difference between all groups material is statistically significant however, according to (Yu and Lee, 2008, Liu et al., 2010a) the difference between ZpexS and Zpex was not clinically perceptible and the same applies to the difference between 3YE and 3YBE at $\Delta TP < 2$. ZpexS even with its highest translucency parameter among

other groups, is still less than that of human dentine which has a TP of 16.4 for 1.00 mm thickness and far less than that of human enamel at 1.00 mm thickness which has a TP of 18.1 (Yu et al., 2009). This means the enamel has up to 30% higher TP more than that of ZpexS.

Wang et al. (2013) studied the TP for different types of glass ceramics and zirconia at 1.00 mm thickness. The glass ceramic showed an average TP of 14.9 to 19.6 while for zirconia the range was 5.5 to 13.5 which was less than that of human enamel and dentin (Wang et al., 2013). The difference in the TP between glass ceramics and zirconia can be related to the high density microstructure compared to glass ceramics however there is still an attempt to get a zirconia with translucency comparable to that of glass ceramic.

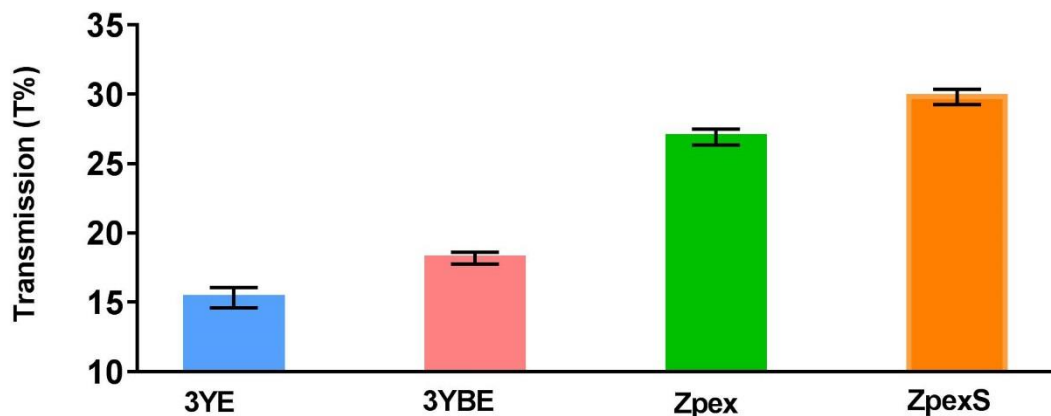


Figure 5-12 Total transmittance of the four tested groups. The bar chart showing a clear significant difference in the Tt% of all tested groups

5.3.2 Transmission

Following normality testing, one way ANOVA showed a significant difference ($p < 0.05$) in the Transmission (Tt%) of the four different materials used in this study. Tt% result followed the same trend as TP and ZpexS showed the highest Tt% while 3YE showed the lowest and the average of Transmission for 1.00 mm thickness group was from 15.34% to 29.84%. The ranking of the material from the highest Tt% to the lowest was ZpexS > Zpex > 3YBE > 3YE as can be clearly seen in (Figure 5-12).

Brodgelt, et al. (1980) studied the direct and total transmission of different types of dental porcelain; the average total transmission reported for 1.00 mm thickness sample was 26.8% which was affected by the brand, shade and

thickness. According to Spink (2009) the measurement of translucency using total transmission percentage should be the gold standard for representing translucency of dental ceramics (Spink, 2009).

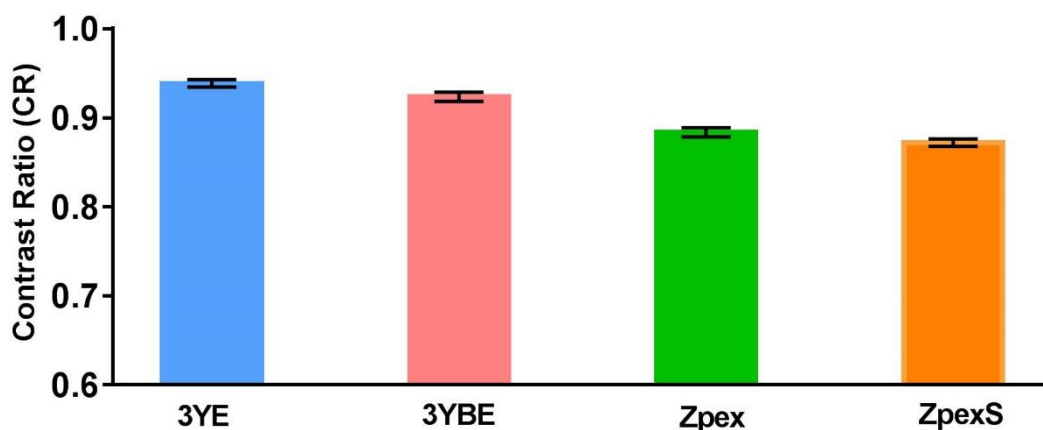


Figure 5-13 CR of the four tested groups. The bar chart showing a clear significant difference in the CR of all tested groups.

5.3.3 Contrast Ratio

Following normality testing, one way ANOVA showed a significant difference ($p < 0.05$) in the CR of the four different materials used in this study. ZpexS for all thicknesses showed the lowest contrast ratio compared to all other groups, followed by Zpex, 3YBE and 3YE respectively. Whilst the difference was *statistically* significant, there was no perceptible *clinical* difference between all groups as the maximum difference was 0.06 between 3YE and ZpexS and is not perceptible based on the mean translucency perception threshold (TPT) defined by Liu et al. 2010.

As explained earlier, this can be attributed to the less sensitivity of CR measurement as it considers only L^* during the measurement instead of all colour parameters including $L^*a^*b^*$ according to CIELAB. CR under-estimates the translucency of dental ceramics (Spink, 2009) and therefore should be avoided to represent the translucency of dental ceramics whenever possible.

ZpexS showed the highest contrast ratio between all tested groups in this study however, its translucency is still far less than different types of dental zirconia studied by Carrabba et al. (2017) who studied the CR of different

types of zirconia in addition to lithium disilicate as a control group at 1.00 mm thickness. The most opaque was Aadvia ST 0.79 and least opaque zirconia was Aadvia NT at 0.65 while for lithium disilicate (IPS e.max LT) CR was 0.56. (Carrabba et al., 2017) however, the diameter of the aperture used in this study is different to the one used in that study. They used an aperture which was 10 mm in diameter compared to 8 mm used in this study, but even with this difference in the diameter, the CR of lithium disilicate is still far less than that of ZpexS.

All the materials tested in this study showed a certain degree of translucency however their translucency is still far less than that of lithium disilicate, according to Vichi et al. (2014) who classified the material according to its contrast ratio at 1.00 mm thickness into four classes of translucency: (1) high translucency: CR up to 0.50 (2) medium translucency: CR 0.50 to 0.75 (3) low translucency: CR 0.75 to 0.90 (4) very low translucency (highly masking): CR 0.90 to 1.00. (Vichi et al., 2014). The 3YE and 3YBE can be classified into very low translucency group while Zpex and ZpexS can be categorised in low translucency group.

The difference in the translucency of different materials in this study can be attributed to many factors, including mainly compositional and processing factors. ZpexS, the material that showed the highest translucency has the least amount of Al_2O_3 and the highest amount of Y_2O_3 compared to all other material. Less amount of Al_2O_3 has a direct effect on increasing the amount of translucency, as Al_2O_3 acts as an impurity which can result in more light being scattered and internally reflected within the material rather than passing smoothly through it (Zhang, 2014). In addition, it has a different refractive index from that of zirconia; the refractive index of Al_2O_3 is 1.7–1.8 (Rakić, 1995, Landry et al., 2008) while for ZrO_2 it is 2.13–2.20 (Landry et al., 2008) and this can result in more light scattering when the light beam passes between the boundaries of the two phases. The internal scattering can also be a product of grain boundaries and therefore decreasing the grain boundaries by increasing the grain size can decrease the internal scattering resulting in more light transmission and more translucent zirconia.

This can explain why ZpexS showed the highest translucency among other material as it has, in addition to less Al_2O_3 , the biggest grains compared to all other tested materials. The higher percentage of bigger grains in this material is mainly due to the predominant cubic phase in this material as a result of higher percentage Y_2O_3 compared to all other tested material. The amount of Y_2O_3 in ZpexS was 9.26 by wt% compared to 5.25 wt% in all other used materials.

Increasing sintering temperature can result in a bigger grain size which means less grain boundaries and therefore more light transmission and an increase in the translucency. This can explain the difference in the translucency between 3YE and 3YBE where both have the same composition and the difference was in the sintering temperature. This result agrees with (Stawarczyk et al., 2013) who reported that the grain size increased with increasing the sintering temperature and contrast ratio decreased.

The translucency of ZpexS is not only attributed to the grain size, Increasing the amount of stabiliser was found to increase translucency. Using more than 9 % by weight of Y_2O_3 (corresponding to 5.5 mol%) results in a material having more cubic zirconia and changed from (PSZ) to (FSZ) (Anselmi-Tamburini et al., 2007, Sulaiman et al., 2015b, Carrabba et al., 2017). This increase in the translucency of zirconia can be explained by the fact that the cubic phase of zirconia unlike tetragonal, is isotropic in different crystallographic directions, and due to this isotropic refractive index, the light scattering occurring at grain boundaries is decreased resulting in more light transmittance (Peuchert et al., 2009, Zhang, 2014, Harada et al., 2016).

The synergistic effect of decreasing the amount of Al_2O_3 and increasing the amount of Y_2O_3 can explain the reason why ZpexS showed the highest translucency compared to the other tested materials.

The lower translucency expressed by other tested materials compared to ZpexS was due to higher percentage of Al_2O_3 and the highest amount of tetragonal phase (including that in Zpex) compared to ZpexS. In addition to the refractive index mismatch between Al_2O_3 and ZrO_2 , the tetragonal phase is known to be optically anisotropic and has a large birefringence and high

reflective index which may further explain the reduced translucency of the materials tested compared to ZpexS (Zhang, 2014).

In addition to the grain size and Al₂O₃ effect on the translucency of zirconia , the actual phase, or combinations of phases, of zirconia showed a clear effect on the translucency and played a pivotal role in improving the translucency of the material.

In this study, bigger grains corresponded to more translucency and this agrees with (Apetz and Bruggen, 2003) while disagreeing with (Casolco et al., 2008) and (Kim et al., 2013) who reported that a smaller grain size could enhance the translucency with an average of grain size located within the range of visible light. This was not the case in this study as both Zpex and ZpexS who showed higher translucencies had grain sizes ranged within the visible light wave length, 413 nm and 526 nm for Zpex and ZpexS respectively while for 3YE and 3YBE the grain size was 259 nm and 362 nm respectively.

It was reported that translucency of a polycrystalline material can be more affected by the presence of pores than by grain boundaries (Hayashi et al., 1991, Apetz and Bruggen, 2003, Alaniz et al., 2009), however this will be of less impact when the grain size falls below 1.00 µm as in the materials used in this study (Hayashi et al., 1991, Apetz and Bruggen, 2003, Anselmi-Tamburini et al., 2007, Casolco et al., 2008).

5.4 Colour Stability after Aging

The results of colour stability are presented in (Figure 5-14). Following normality testing, one way ANOVA followed by Tukey HSD post Hoc test, showed that colour changes (ΔE^*ab) as a result of aging were significantly affected by thickness of the sample for all groups ($p < 0.05$), apart from 3YE which showed no statistically significant difference in the change of colour between different thicknesses as result of aging.

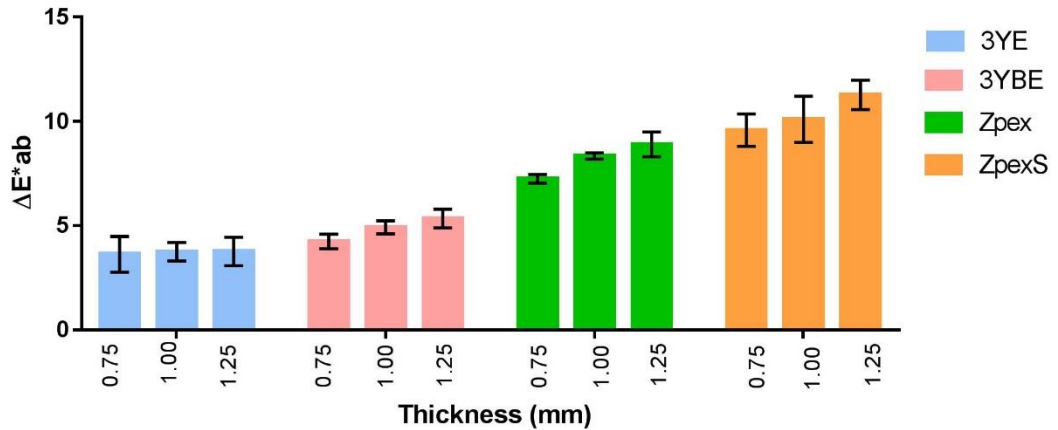


Figure 5-14 Mean +SD of ΔE^*ab for all groups.

All of the materials that showed a significant increase in ΔE^*ab with an increase in the thickness. The thicker the sample the more colour changes recorded.

In order to compare the change in colour between different materials. 1.00 mm group was picked as representative. One way ANOVA followed by Tukey HSD post Hoc test, showed that there was a significant difference ($p < 0.05$) in the mean value of ΔE^*ab between all tested materials (Figure 5-15).

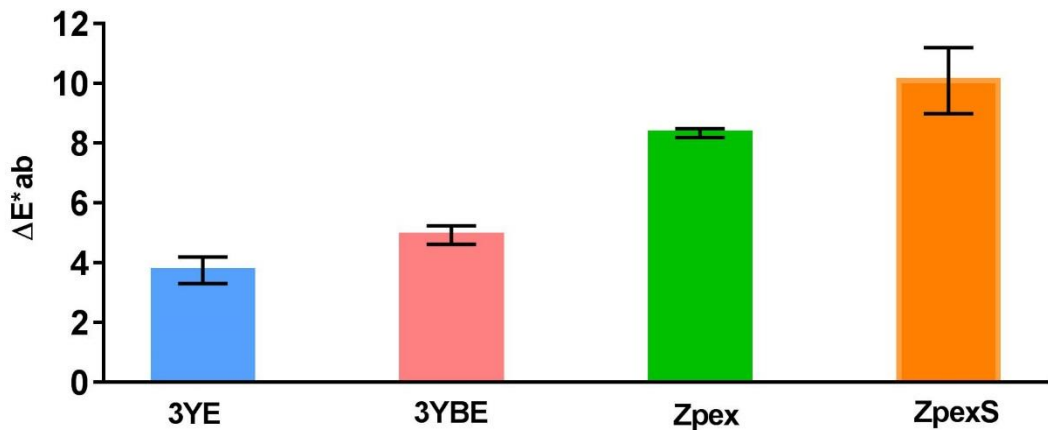


Figure 5-15 ΔE^*ab Mean +SD of 1.00 mm thickness of all tested groups.

The more the translucent groups showed more colour changes after aging, i.e. 3YE, and 3YBE showed more colour stability compared to Zpex and ZpexS. The materials were, from the highest colour changes to lowest, $ZpexS > Zpex > 3YBE > 3YE$. The difference in colour after hydrothermal aging

was a result of a significant increase in lightness (L^*) and blue-yellow coordinate (b^*) mean values of all groups. Following normality testing, paired sample T tests of L^* for all materials (Figure 5-16) showed a statistically significant increase ($p < 0.05$) after hydrothermal aging, as did the b^* mean value (Figure 5-18). This means samples after aging got brighter and moved toward a yellower colour. The a^* mean value was the only colour parameter that behaved differently between groups as it showed an increase in 3YE and Zpex but decreased for 3YBE and ZpexS (Figure 5-17).

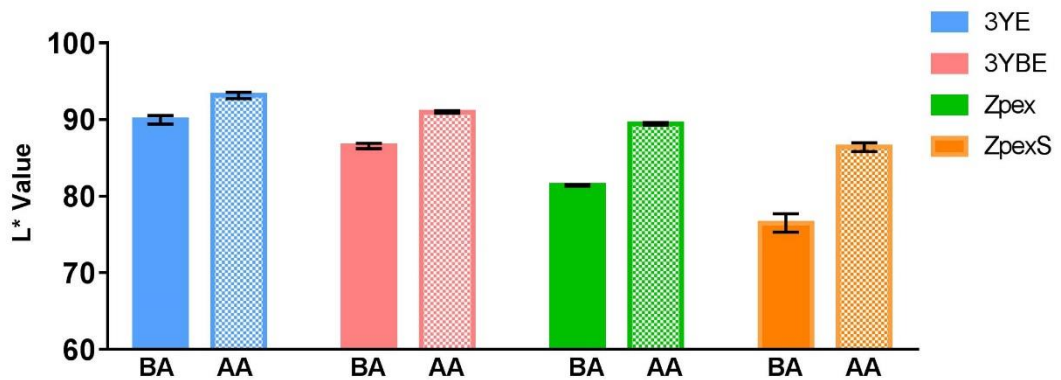


Figure 5-16 L^* mean values+ SD before and after aging.

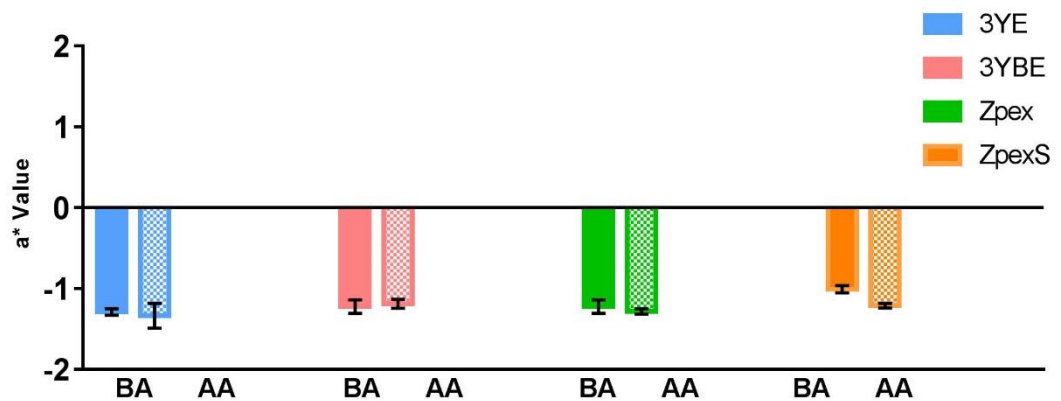


Figure 5-17 a^* mean values+ SD before and after aging.

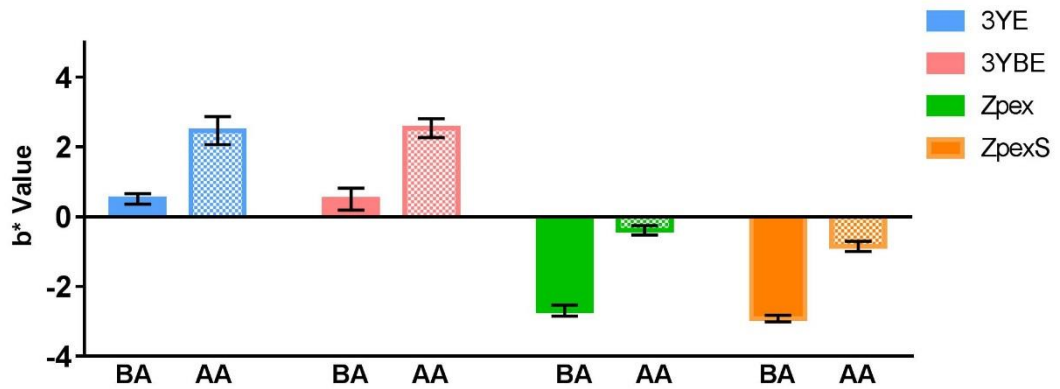


Figure 5-18 b^* mean values+ SD before and after aging.

5.4.1 Chroma

The change in the Chroma as a result of aging is presented in (Figure 5-19).

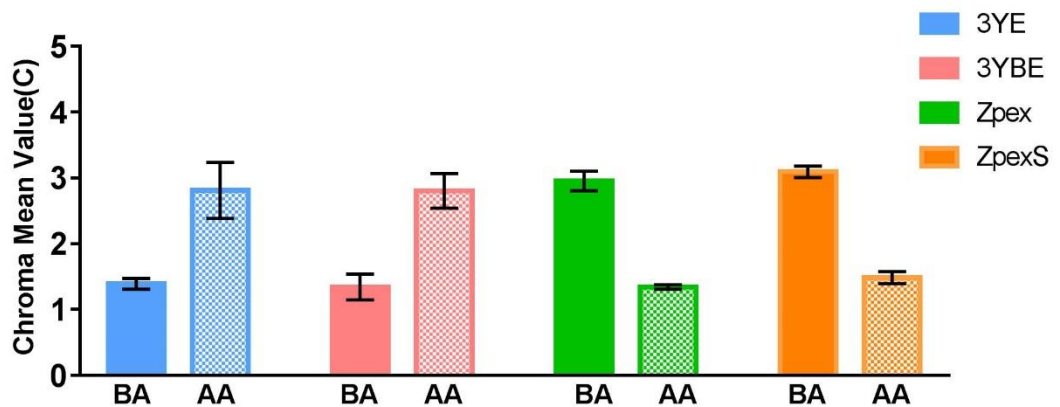


Figure 5-19 Chroma mean values \pm SD before and after aging.

Chroma is mainly determined by a^* and b^* *absolute* values. In this study chroma showed a clear significant increase for 3YE and 3YBE and a significant decrease for Zpex and ZpexS. It might be confusing why even with the increase in b^* , Zpex and ZpexS still showed a significant decrease in Chroma, however it is important to note that only the absolute value is considered.

The colour of an object is mainly determined by its surface spectral reflectance (Ghinea et al., 2011). This reflectance is highly sensitive to the surface roughness (Bennett and Porteus, 1961), and therefore the optical properties

of dental materials can be highly affected by the surface roughness (Chung, 1994, Reis et al., 2003, Paravina et al., 2004).

Different authors studied the effect of hydrothermal aging on dental zirconia and their results have shown that it can affect its mechanical properties, increase the surface roughness, produce micro-cracking, enhance wear rates, etc. (Ardlin, 2002, Chevalier, 2006, Chevalier et al., 2007, Chevalier et al., 2009, Lughì and Sergo, 2010, Cattani-Lorentè et al., 2011, Swain, 2014, Zhang et al., 2017) however there is a scarcity of studies on the effect of aging on the optical properties of dental zirconia. Volpato et al. (2016) confirmed that aging can affect the colour stability of dental zirconia, however the author could not explain the reason behind this other than assigning it to microstructural changes.

The greater colour stability of 3YE and 3YBE compared to Zpex can be mainly attributed to less transformation of *t-m* after hydrothermal aging as the transformation can result in a rougher surface (Ardlin, 2002, Roy et al., 2007, Kim et al., 2009b) due to the uplift of grains as could be clearly seen in Zpex which showed the highest amount of transformation. However, ZpexS with less amount of transformation showed the highest amount of colour changes, which is counter-intuitive. These colour changes can also contribute to the microstructural changes that can happen as a result of aging, however these changes need to be investigated further to understand what can cause this change in colour in addition to the increase in surface roughness. For example, the concentration of oxygen vacancies is much higher in cubic phase than tetragonal (Guo and He, 2003), this oxygen vacancy when trapped with electrons will form colour centres and result in yellowish brown colour of zirconia (Anselmi-Tamburini et al., 2007, Alaniz et al., 2009, Zhang et al., 2010, Zhang et al., 2011) and an increase or decrease in these vacancies can result in clear colour changes (Limarga et al., 2012). These oxygen vacancies can be depleted as a result of hydrothermal aging (Zhang et al., 2017) and this can be one of the reasons behind colour changes after aging. However, what happens to oxygen vacancy in cubic zirconia as a result of aging is not clear and there is no study to the best of author's knowledge that addressed this issue.

How relevant these colour changes are clinically, in terms of perception and clinically accepted changes is arguable, as all of the tested materials showed a change in the colour that is clinically not acceptable according to (ISO-28642, 2016) i.e. all of the materials showed a colour change more than $\Delta E^*ab = 2.7$. A preliminary study was conducted by asking five experienced restorative clinical staff at the School of Dentistry to differentiate between two pairs of samples, the first pair was 3YBE and the second was for Zpex (Figure 5-20), each pair before and after aging. Participants were not told what the samples were and samples were examined in a light box with D65 illuminant. They all confirmed that the changes were barely detectable for Zpex which showed ΔE^*ab more than 8 and were not detectable for 3YBE which showed ΔE^*ab of more than 5. This shows that values set up in ISO can be questionable and can vary depending on the device used for measurement of the colour. The diameter of aperture and the quality/ age of the white/ black standards are factors that can result in different readings of CIELab values. Holman et al. (2015) has confirmed that the size of aperture has a great effect on the values of colour measurement and the bigger the aperture the higher the colour values; therefore in order to compare results of any study to other studies, it is vital that the size of the aperture and the type of the device used to be reported clearly.

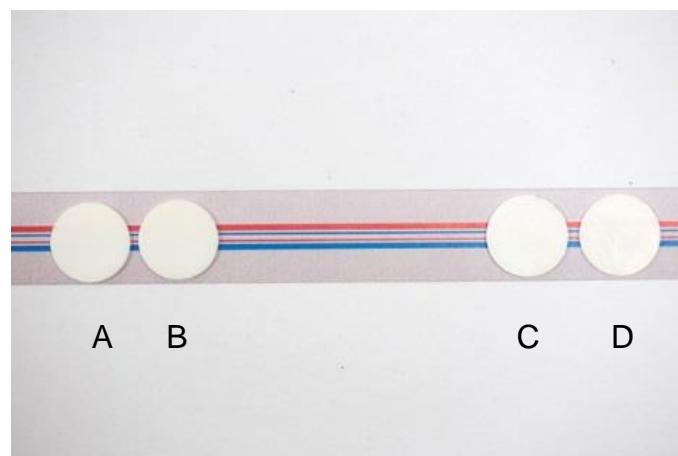


Figure 5-20 Difference in colour before and after aging. (A,B) 3YBE before and after aging,(C,D) Zpex before and after aging.

5.5 Effect of thickness and aging on light irradiance

Translucency of zirconia is not only important to achieve a high aesthetic restoration, It is also pivotal and has a direct effect on the polymerization of resin dental cement used for cementation of crowns and veneers (Rasetto et al., 2004). The thicker and the more opaque the material, the less light will be transmitted and this will have a direct effect on the critical intensity of light cure required to achieve the optimal polymerisation of the material (Myers et al., 1994).

Following normality testing, one way ANOVA showed that both thickness and hydrothermal aging have a significant effect on the measured amount of light irradiance ($p < 0.05$). Increasing thickness led to decrease in the mean value of irradiance (Figure 5-21) and aging led to increase in the amount of irradiance compared to before aging (Figure 5-22).

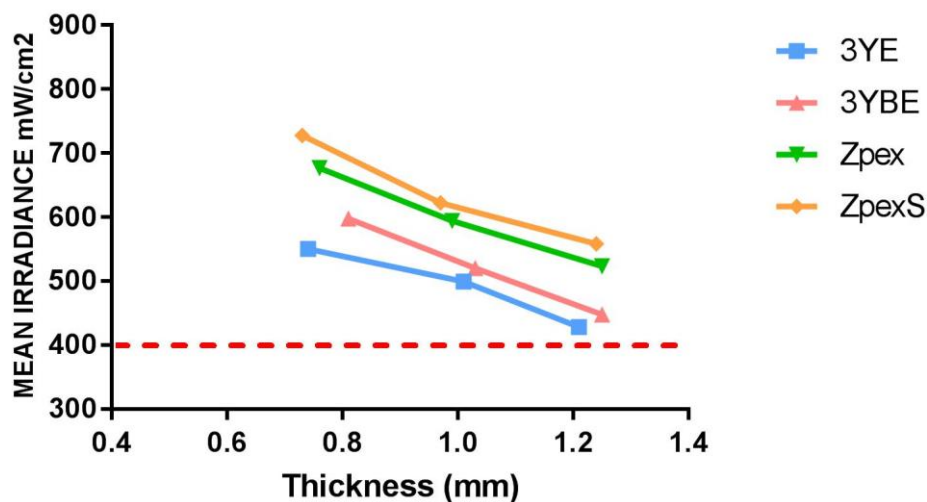


Figure 5-21 Mean light irradiance for all tested materials before aging at various thicknesses. Red line indicates minimum amount of light irradiance required to initiate polymerization.

The thicker the sample, the less light irradiance and the less the amount of total energy. In terms of materials, the result of total amount of irradiance and the total irradiance energy was consistent with the result of translucency, i.e ZpexS showed both the highest amount of irradiance and the total amount of irradiance energy followed by Zpex, 3YBE and 3YE respectively..

Rueggeberg and Caughman, 1993, in their study recommended that 400mW/cm² as adequate irradiance to initiate polymerization of resin based materials with a duration of curing of 60 seconds. In this study, the lowest irradiance value was recorded for 3YE at 1.25 mm thickness before aging and this was still higher than the amount required for initiation of polymerization (Rueggeberg and Caughman, 1993).

According to Suliman et al. (2015), total irradiant energy which can be defined as *“the mathematical product of the curing light irradiance (mW/cm²) multiplied by the exposure duration in seconds”* would be of more importance to the polymerization of resin than the mean value of irradiance (Sulaiman et al., 2015a). This can help in knowing whether certain thickness of material will allow the total energy required for polymerization or not and can be calculated by knowing the total energy from the light cure unit and the time recommended by the manufacturer to cure the resin (Sulaiman et al., 2015a). The result of this study agree with (Peixoto et al., 2007, Pazin et al., 2008, Kilinc et al., 2011) who confirmed in their study the pivotal role of thickness of the material in developing the hardness of indirectly activated dual-cured resin luting agents. The effect of thickness was also addressed by Ilie and Stawarczyk, (2014) who concluded that zirconia samples thicker than 1.5mm might not allow sufficient light required for polymerization of resin cement and therefore, they recommended less light sensitive resin cement to be used to overcome this issue with thicker restoration (Ilie and Stawarczyk, 2014).

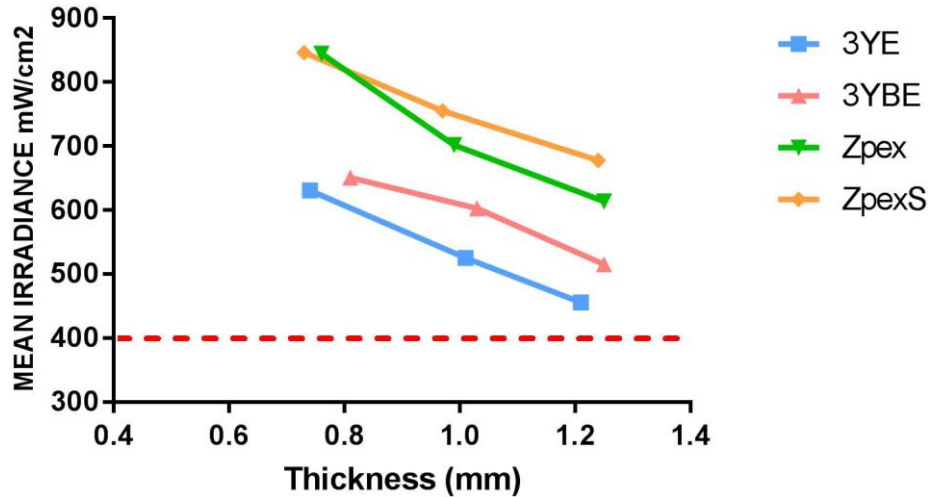


Figure 5-22 Mean light irradiance for all tested materials after aging at various thicknesses. Red line indicates minimum amount of light irradiance required to initiate polymerization.

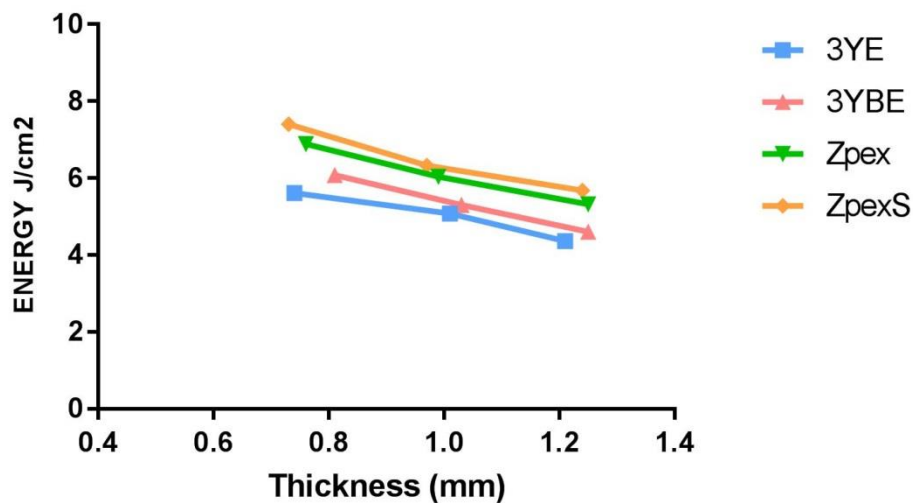


Figure 5-23 Total irradiant energy for all tested groups zirconia brands at different thicknesses and 10 s curing time.

Hydrothermal aging showed a significant increase in the amount of mean irradiance values for all tested groups apart from 3YE which showed an insignificant increase. Zpex showed the highest amount of mean value of irradiance followed by ZpexS, 3YBE and 3YE respectively (Figure 5-22, Figure 5-24).

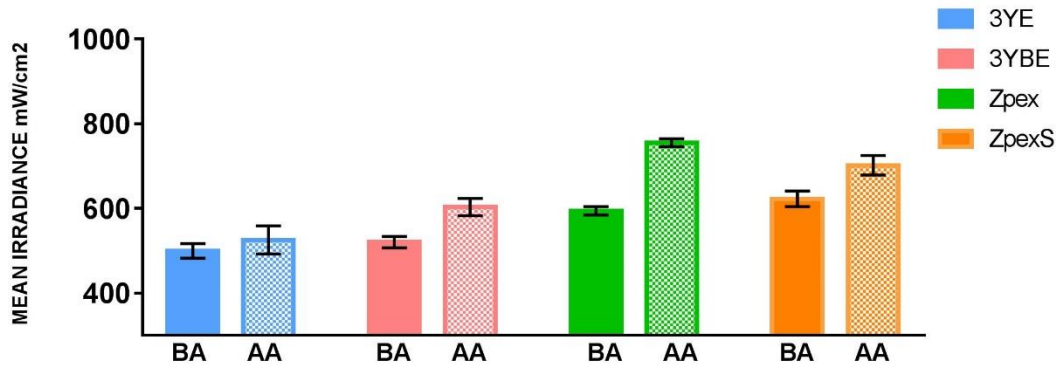


Figure 5-24 Effect of hydrothermal aging on the irradiance of all tested materials.

This increase can be attributed to the microstructural changes that aging can cause. Zpex which showed the highest amount of phase transformation showed the highest amount of increase in light transmission. It can be speculated that this can be attributed mainly to a decrease in the oxygen vacancy concentration as a result of transformation of tetragonal to monoclinic through the interaction of OH⁻ ions from water with oxygen vacancies in ZrO₂ (Guo, 2004). The concentration of oxygen vacancies was found to have a direct effect on the optical properties of zirconia (Shahmiri et al., 2017) and a decrease in oxygen vacancies can result in a decrease in absorption coefficient and an increase in light transmission (Alaniz et al., 2009), and vice versa, if there is an increase in oxygen vacancy means an increase in absorption coefficient and decrease in light transmission. Even though ZpexS showed less transformation, it still showed a significant increase in the transmission. This could be attributed to its higher amount of oxygen vacancies compared to tetragonal zirconia (Guo and He, 2003), which can be filled during aging resulting in an increase in the transmission without affecting stability of cubic zirconia.

Chapter 6 General discussion

The core materials, 3YE and 3YBE were similar in their composition apart from the binder and the sintering temperature. They behaved in a broadly similar manner. 3YE showed the highest stability of all of the tested materials in this study. It showed no significant changes in its mechanical properties and in its structure as there was no detectable phase transformation after aging. It showed the highest Weibull modulus even after aging. It had the least translucency and the smallest grain size among all the groups and was also more stable in terms of colour changes after aging. 3YBE behaved broadly similar to 3YE and showed the highest strength among all other groups. It showed a 5% of transformation after aging, however it showed no significant changes in its translucency in response to aging. The behaviour of both 3YE and 3YBE in terms of the mechanical and optical properties can be mainly attributed to the composition of the materials. The higher strength for 3YE and 3YBE can be explained by the fact that both of these materials contain a higher amount (0.25 by wt%) of Al_2O_3 compared to Zpex and ZpexS (0.05 wt%). Samodurova et al. (2015) reported that the presence of Al_2O_3 positively influenced the nucleation of zirconia and promoted strong grain boundaries increasing the zirconia strength (Samodurova et al., 2015). In addition, the presence of Al_2O_3 was found to have a clear direct influence on the grain growth and the stability of tetragonal zirconia (Rao et al., 2004) by acting as a matrix for zirconia to be dispersed in it evenly (Kurtz et al., 2014). It is also found to be responsible for tuning the amount of dopant inside zirconia lattice (Palmero et al., 2014).

Unlike the 'conventional' materials, the two translucent zirconia materials, Zpex and ZpexS behaved differently in response to hydrothermal aging. Zpex showed the highest amount of transformation after aging among all other groups and the highest amount of increase in direct light transmission which can be attributed mainly to decrease in the oxygen vacancy concentration as a result of transformation of tetragonal to monoclinic through the interaction of OH^- ions from water with oxygen vacancy in ZrO_2 (Guo, 2004), however even this level of transformation had no effect on the mechanical properties of this material. A low Al_2O_3 can be the reason behind the transformation which might

have resulted in less of the tetragonal zirconia for the same reason mentioned earlier. This material was less stable in term of colour changes in comparison with 3YE and 3YBE. It showed a considerable amount of colour changes in comparison to conventional core materials. The changes in the colour was attributed to the structural changes which resulted in rougher surface and to the occupation of oxygen vacancies as a result of aging. ZpexS showed the least strength and Weibull modulus and the highest translucency with the biggest grain size and the least colour stability after aging compared to all other groups. It showed a significant increase in direct light transmission; which can be attributed to its higher amount of oxygen vacancy associated with cubic zirconia compared to tetragonal zirconia (Guo and He, 2003), which can be filled during aging resulting in an increase in the transmission without affecting stability of cubic zirconia.

It has the least amount of Al_2O_3 and the highest amount of Y_2O_3 compared to all other material. These two components were the main players in the optical properties and mechanical properties of the studied materials in addition to the processing regimes. Al_2O_3 acted as impurities which can result in more light scattered and reflected internally within the material rather than passing smoothly therefore affecting the translucency of zirconia (Zhang, 2014). In addition to that, it has a different refractive index from that of zirconia, the refractive index of Al_2O_3 is 1.7–1.8 (Rakić, 1995, Landry et al., 2008) while for ZrO_2 is 2.13–2.20 (Landry et al., 2008) and this can result in more light scattering when the light beam passes between the boundaries of the two phases. Therefore, the less amount of Al_2O_3 in ZpexS could be regarded as an enhancing factor for the translucency in ZpexS compared to conventional core materials. Decreasing the grain boundaries by increasing the grain size can decrease the internal scattering resulting in more light transmission and more translucent zirconia. As a result of the higher percentage of Y_2O_3 in ZpexS compared to all other tested material, (the amount of Y_2O_3 in ZpexS was 9.26 wt% compared to 5.25 wt% to the rest of the materials), the material consisted predominantly of the cubic phase with bigger grains and less grain boundaries.

The cubic phase of zirconia unlike tetragonal, is isotropic in different crystallographic directions, and due to this isotropic refractive index, the light

scattering occurs at grain boundaries is decreased resulting in more light transmittance (Peuchert et al., 2009, Zhang, 2014, Harada et al., 2016). This can explain why ZpexS showed the highest translucency. This increase in the highly stable cubic phase was also responsible for the lower strength of ZpexS compared to all other tested materials, due to the loss of the advantages of stress induced *t-m* transformation surface toughening effect.

In general, any transformation effect resulting from hydrothermal aging was limited and had no significant impact on the mechanical properties of tested materials, however aging showed a significant effect on the optical properties of all tested material including a change in colour and an increase in the light transmission and a trend of an increase in translucency parameters.

According to ISO 6872:2015, ZpexS, even with its reduction in strength due the synergistic effect of reducing the amount of Al_2O_3 and increasing the amount of Y_2O_3 , resulting in the formation of the cubic phase, still fulfils the threshold strength requirement for (ISO Class 4) and accordingly, can be used for up to three-unit prostheses involving molar restoration while for the remaining tested groups as they fulfil the highest requirement for (ISO class 5), they can be used for up to four or more unit FPDs (ISO-6872, 2015). This still applies to aged Zpex with its 22% of monoclinic transformation given that according to (ISO-13356, 2015) aging in autoclave under 2 bar of pressure and 134° for 5 hours should produce less than 25% phase transformation to be biomedically accepted.

Chapter 7 Conclusions

Within the limitation of this in vitro study, it can be concluded that hydrothermal aging can result in structural changes without significant effect on the mechanical properties of zirconia, including both the strength and the hardness, even with up to 22% of tetragonal to monoclinic transformation. Aging can however affect the reliability of zirconia without affecting the characteristic strength resulting in a drop in the Weibull modulus. It is also can significantly affect the optical properties and can result in significant colour changes in zirconia, however the clinical acceptability and perceptibility of these colour changes should be further investigated. Aging can also result in an increase in the surface roughness which can be one of the reasons behind the colour changes. It can also result in significant increase in the direct transmission which means an increase in the translucency.

Direct transmission, as a measure of translucency, was found to be more sensitive measurement of translucency and contrast ratio was the least sensitive one. Thickness has a direct effect on the translucency and colour of dental zirconia; the thicker the sample the less translucent. However at small differences in thickness, the difference in translucency might not be significantly detectable. The more the translucent the material the more sensitive it was to a change in the thickness.

Reducing the amount of Al_2O_3 and increasing the amount of Y_2O_3 can improve the translucency of zirconia, by reducing the impurities and producing more cubic zirconia, however this can result in decreasing the strength of zirconia significantly.

Increasing the sintering temperature can improve the translucency of zirconia by getting a bigger grain size, however the effect of increasing sintering temperature was limited.

Hydrothermal aging can result in porosity, however this might be due to the opening of already existing pores due to internal stress that can be developed due to aging.

The presence and effect of binder in zirconia processing was assessed by comparing 3YE and 3YBE, in which the only difference was the presence of

binder. Even though it disappeared early in the sintering cycle (Abd El-Ghany and Sherief, 2016), it can be inferred that the presence of a binder can assist in holding powder particles in a better condition comparing to no binder material. In addition, the presence of binder clearly facilitated the processing of the starting powder to make a green body at the beginning of sample preparation methods (Aziz et al., 2016).

Chapter 8 Future Works

1. Detailed fractographic study for the broken samples to understand the reason behind the drop in Weibull modulus without the drop in the characteristic strength.
2. Further investigation to understand the reason behind the increase in the porosity after hydrothermal aging by using FIB-SEM on more samples and for deep sections.
3. Using different sintering temperature and different sintering regimes finding out the effect on the grain size and the translucency of the studied materials.
4. Measuring the difference in colour after hydrothermal aging using different devices and different apertures to see how this difference can affect the measurements in colour stability.
5. Comprehensive study to determine the permeability and acceptability from the patients perspective.
6. Further structural analysis to understand how oxygen vacancies can affect the optical properties of zirconia.

Chapter 9 References

- ABBAS, S., MALEKSAEEDI, S., KOLOS, E. & RUYS, A. 2015. Processing and Properties of Zirconia-Toughened Alumina Prepared by Gelcasting. *Materials*, 8, 4344-4362.
- ABD EL-GHANY, O. S. & SHERIEF, A. H. 2016. Zirconia based ceramics, some clinical and biological aspects: Review. *Future Dental Journal*, 2, 55-64.
- ABDELAAL, M. M. E. 2016. *Effect of post-processing heat treatment on flexural strength of zirconia for dental applications*, The University of Iowa.
- ABDELBARY, O., WAHSH, M., SHERIF, A. & SALAH, T. 2016. Effect of accelerated aging on translucency of monolithic zirconia. *Future Dental Journal*, 2, 65-69.
- ABI, C. B., EMRULLAHOGLU, O. F. & SAID, G. 2013. Microstructure and mechanical properties of MgO-stabilized ZrO₂-Al₂O₃ dental composites. *J Mech Behav Biomed Mater*, 18, 123-31.
- ABOUSHLIB, M. N., DE JAGER, N., KLEVERLAAN, C. J. & FEILZER, A. J. 2005. Microtensile bond strength of different components of core veneered all-ceramic restorations. *Dent Mater*, 21, 984-91.
- ABOUSHLIB, M. N., FEILZER, A. J. & KLEVERLAAN, C. J. 2009. Bridging the gap between clinical failure and laboratory fracture strength tests using a fractographic approach. *Dent Mater*, 25, 383-91.
- AFFERRANTE, L., CIAVARELLA, M. & VALENZA, E. 2006. Is Weibull's modulus really a material constant? Example case with interacting collinear cracks. *International Journal of Solids and Structures*, 43, 5147-5157.
- AHLBERG, J. P., KOVERO, O. A., HURMERINTA, K. A., ZEPA, I., NISSINEN, M. J. & KÖNÖNEN, M. H. 2003. Maximal bite force and its association with signs and symptoms of TMD, occlusion, and body mass index in a cohort of young adults. *CRANIO®*, 21, 248-252.
- AHN, J.-S. & LEE, Y.-K. 2008a. Difference in the translucency of all-ceramics by the illuminant. *Dental materials*, 24, 1539-1544.
- AHN, J. S. & LEE, Y. K. 2008b. Difference in the translucency of all-ceramics by the illuminant. *Dent Mater*, 24, 1539-44.
- AL-HIYASAT, A., SAUNDERS, W., SHARKEY, S., SMITH, G. M. & GILMOUR, W. 1998. Investigation of human enamel wear against four dental ceramics and gold. *Journal of dentistry*, 26, 487-495.
- AL-WAHADNI, A. 1999. The roots of dental porcelain: a brief historical perspective. *Dent News*, 2, 43-44.
- AL BADR, R. M. & HASSAN, H. A. 2017. Effect of immersion in different media on the mechanical properties of dental composite resins.
- ALANIZ, J., PEREZ-GUTIERREZ, F., AGUILAR, G. & GARAY, J. 2009. Optical properties of transparent nanocrystalline yttria stabilized zirconia. *Optical Materials*, 32, 62-68.
- ALBAKRY, M., GUAZZATO, M. & SWAIN, M. V. 2003. Fracture toughness and hardness evaluation of three pressable all-ceramic dental materials. *Journal of Dentistry*, 31, 181-188.
- ALGHAZZAWI, T. F., LEMONS, J., LIU, P. R., ESSIG, M. E., BARTOLUCCI, A. A. & JANOWSKI, G. M. 2012. Influence of low-temperature

- environmental exposure on the mechanical properties and structural stability of dental zirconia. *J Prosthodont*, 21, 363-9.
- ALMER, J., LIENERT, U., PENG, R. L., SCHLAUER, C. & ODÉN, M. 2003. Strain and texture analysis of coatings using high-energy x-rays. *Journal of Applied Physics*, 94, 697-702.
- AMERICAN DENTAL ASSOCIATION. 2013. *Code on Dental Procedures and Nomenclature (CDT)* [Online]. <http://www.ada.org/en/publications/cdt/glossary-of-dental-clinical-and-administrative-ter#c>: ADA. [Accessed 16 June 2017].
- ANDREIUOLO, R. F., SABROSA, C. E. & DIAS, K. R. 2013. Dual-scan technique for the customization of zirconia computer-aided design/computer-aided manufacturing frameworks. *Eur J Dent*, 7, S115-8.
- ANSELMI-TAMBURINI, U., WOOLMAN, J. N. & MUNIR, Z. A. 2007. Transparent Nanometric Cubic and Tetragonal Zirconia Obtained by High-Pressure Pulsed Electric Current Sintering. *Advanced Functional Materials*, 17, 3267-3273.
- ANSELMI-TAMBURINI, U., WOOLMAN, J. N. & MUNIR, Z. A. 2007. Transparent Nanometric Cubic and Tetragonal Zirconia Obtained by High-Pressure Pulsed Electric Current Sintering. *Advanced Functional Materials*, 17, 3267-3273.
- ANTONSON, S. A., ANUSAVICE, K. J., ANTONSON, S. & ANUSAVICE, K. 2001. Contrast ratio of veneering and core ceramics as a function of thickness. *International Journal of Prosthodontics*, 14.
- ANUSAVICE, K. J., SHEN, C. & RAWLS, H. R. 2013. *Phillips' science of dental materials*, Elsevier Health Sciences.
- APETZ, R. & BRUGGEN, M. P. 2003. Transparent Alumina: A Light-Scattering Model. *Journal of the American Ceramic Society*, 86, 480-486.
- ARANGO SANTANDER, S., PELAEZ VARGAS, A., SALDARRIAGA ESCOBAR, J., MONTEIRO, F. J. & RESTREPO TAMAYO, L. F. 2010. Ceramics for dental restorations-an introduction. *Dyna*, 77, 26-36.
- ARDLIN, B. I. 2002. Transformation-toughened zirconia for dental inlays, crowns and bridges: chemical stability and effect of low-temperature aging on flexural strength and surface structure. *Dental Materials*, 18, 590-595.
- ARNAUD, G. 2009. every thing you have ever wanted to know about zirconia. *Spécial Report-Dent. Tech. N 80/81*. French School of Industrial Ceramic.
- ASHBY, M. F. & CEBON, D. 1993. Materials selection in mechanical design. *Le Journal de Physique IV*, 3, C7-1-C7-9.
- AWAD, D., STAWARCZYK, B., LIEBERMANN, A. & ILIE, N. 2015. Translucency of esthetic dental restorative CAD/CAM materials and composite resins with respect to thickness and surface roughness. *J Prosthet Dent*, 113, 534-40.
- AZIZ, G. A., BUBB, N., HYDE, P. & WOOD, D. 2015. An Investigation of the Mechanical Properties of Different Types of Zirconia. *J Dent Res*, 94 A 3689.
- AZIZ, G. A., BUBB, N., HYDE, P. & WOOD, D. 2016. Effect of accelerated aging on two zirconia core materials. *J Dent Res*, 95 B.0859.

- BADWAL, S., BANNISTER, M. & HANNINK, R. H. 1993. Science and technology of zirconia V.
- BALDASSARRI, M., STAPPERT, C. F., WOLFF, M. S., THOMPSON, V. P. & ZHANG, Y. 2012. Residual stresses in porcelain-veneered zirconia prostheses. *Dent Mater*, 28, 873-9.
- BAN, S. 2014. Effect of Coloring on Mechanical Properties of Dental Zirconia. *Journal of Medical and Biological Engineering*, 34, 24.
- BAN, S. & ANUSAVICE, K. 1990. Influence of test method on failure stress of brittle dental materials. *Journal of Dental Research*, 69, 1791-1799.
- BARIZON, K. T. L. 2011. *Relative translucency of ceramic systems for porcelain veneers*, The University of Iowa.
- BASDRA, E., HUBER, H. & KOMPOSCH, G. 1996. Fluoride released from orthodontic bonding agents alters the enamel surface and inhibits enamel demineralization in vitro. *American Journal of Orthodontics and Dentofacial Orthopedics*, 109, 466-472.
- BENNETT, H. & PORTEUS, J. 1961. Relation between surface roughness and specular reflectance at normal incidence. *JOSA*, 51, 123-129.
- BERNS, R. 1981. Measuring Color.
- BINNIG, G., QUATE, C. F. & GERBER, C. 1986. Atomic force microscope. *Physical review letters*, 56, 930.
- BOEHLER, M., PLENK, H. & SALZER, M. 2000. Alumina Ceramic Bearings for Hip Endoprostheses. *Clinical Orthopaedics and Related Research*, 379, 85-93.
- BOLLENL, C. M., LAMBRECHTS, P. & QUIRYNEN, M. 1997. Comparison of surface roughness of oral hard materials to the threshold surface roughness for bacterial plaque retention: a review of the literature. *Dental Materials*, 13, 258-269.
- BOLT, R. A., TEN BOSCH, J. J. & COOPS, J. C. 1994. Influence of window size in small-window colour measurement, particularly of teeth. *Physics in Medicine and Biology*, 39, 1133.
- BORCHERS, L., STIESCH, M., BACH, F. W., BUHL, J. C., HUBSCH, C., KELLNER, T., KOHORST, P. & JENDRAS, M. 2010. Influence of hydrothermal and mechanical conditions on the strength of zirconia. *Acta Biomater*, 6, 4547-52.
- BOUVIER, P., DJURADO, E., LUCAZEAU, G. & LE BIHAN, T. 2000. High-pressure structural evolution of undoped tetragonal nanocrystalline zirconia. *Physical Review B*, 62, 8731-8737.
- BRAVO-LEON, A., MORIKAWA, Y., KAWAHARA, M. & MAYO, M. J. 2002. Fracture toughness of nanocrystalline tetragonal zirconia with low yttria content. *Acta Materialia*, 50, 4555-4562.
- BRODBELT, R., O'BRIEN, W. & FAN, P. 1980. Translucency of dental porcelains. *Journal of Dental Research*, 59, 70-75.
- BUNKER, B. 1994. Molecular mechanisms for corrosion of silica and silicate glasses. *Journal of Non-Crystalline Solids*, 179, 300-308.
- BUNTUSHKIN, V., ROMANOVICH, I. & TIMOFEEVA, N. 1971. HIGH-TEMPERATURE MICROHARDNESS AND CERTAIN PROPERTIES OF REFRACTORY OXIDES. *Inorg. Mater.(USSR)(Engl. Transl.)* 7: No. 9, 1456-7 (Sep 1971).
- BURKINSHAW, S. M. 2004. Colour in relation to dentistry. Fundamentals of colour science. *Br Dent J*, 196, 33-41; discussion 29.

- CALDAS, D., ALMEIDA, J., CORRER-SOBRINHO, L., SINHORETI, M. & CONSANI, S. 2003. Influence of curing tip distance on resin composite Knoop hardness number, using three different light curing units. *OPERATIVE DENTISTRY-UNIVERSITY OF WASHINGTON*, 28, 315-320.
- CALES, B., STEFANI, Y. & LILLEY, E. 1994. Long-term in vivo and in vivo aging of a zirconia ceramic used in orthopaedy. *Journal of biomedical materials research*, 28, 619-624.
- CALLISTER JR, W. 2005. Materials science and engineering: an integrated approach. *John Wiley, New York*.
- CARRABBA, M., KEELING, A. J., AZIZ, A., VICHI, A., FONZAR, R. F., WOOD, D. & FERRARI, M. 2017. Translucent zirconia in the ceramic scenario for monolithic restorations: A Flexural Strength and Translucency comparison test. *Journal of Dentistry*.
- CASOLCO, S. R., XU, J. & GARAY, J. E. 2008. Transparent/translucent polycrystalline nanostructured yttria stabilized zirconia with varying colors. *Scripta Materialia*, 58, 516-519.
- CATTANI-LORENTE, M., SCHERRER, S. S., AMMANN, P., JOBIN, M. & WISKOTT, H. W. 2011. Low temperature degradation of a Y-TZP dental ceramic. *Acta Biomater*, 7, 858-65.
- CEKIC-NAGAS, I., EGILMEZ, F. & ERGUN, G. 2012. Comparison of light transmittance in different thicknesses of zirconia under various light curing units. *The journal of advanced prosthodontics*, 4, 93-96.
- CESAR, P. F., GONZAGA, C. C., MIRANDA, W. G. & YOSHIMURA, H. N. 2007. Effect of ion exchange on hardness and fracture toughness of dental porcelains. *Journal of Biomedical Materials Research Part B: Applied Biomaterials*, 83, 538-545.
- CHEN, Y.-M., SMALES, R. J., YIP, K. H.-K. & SUNG, W.-J. 2008. Translucency and biaxial flexural strength of four ceramic core materials. *Dental Materials*, 24, 1506-1511.
- CHEVALIER, J. 2006. What future for zirconia as a biomaterial? *Biomaterials*, 27, 535-43.
- CHEVALIER, J., GREMILLARD, L. & DEVILLE, S. 2007. Low-Temperature Degradation of Zirconia and Implications for Biomedical Implants. *Annual Review of Materials Research*, 37, 1-32.
- CHEVALIER, J., GREMILLARD, L., VIRKAR, A. V. & CLARKE, D. R. 2009. The Tetragonal-Monoclinic Transformation in Zirconia: Lessons Learned and Future Trends. *Journal of the American Ceramic Society*, 92, 1901-1920.
- CHEVALIER, J., LOH, J., GREMILLARD, L., MEILLE, S. & ADOLFSON, E. 2011. Low-temperature degradation in zirconia with a porous surface. *Acta Biomater*, 7, 2986-93.
- CHEVALIER, J., OLAGNON, C. & FANTOZZI, G. 1999. Subcritical Crack Propagation in 3Y-TZP Ceramics: Static and Cyclic Fatigue. *Journal of the American Ceramic Society*, 82, 3129-3138.
- CHIEN, C.-Y. 2015. *Effects of Sintering Holding Time on the Microstructure and Mechanical Properties of Translucent Zirconia*.
- CHO, S.-H., LOPEZ, A., BERZINS, D. W., PRASAD, S. & AHN, K. W. 2015. Effect of different thicknesses of pressable ceramic veneers on polymerization of light-cured and dual-cured resin cements. *The journal of contemporary dental practice*, 16, 347.

- CHOI, B. K., HAN, J. S., YANG, J. H., LEE, J. B. & KIM, S. H. 2009. Shear bond strength of veneering porcelain to zirconia and metal cores. *J Adv Prosthodont*, 1, 129-35.
- CHRISTEL, P., MEUNIER, A., DORLOT, J. M., CROLET, J. M., WITVOET, J., SEDEL, L. & BOUTIN, P. 1988. Biomechanical compatibility and design of ceramic implants for orthopedic surgery. *Annals of the New York Academy of Sciences*, 523, 234-256.
- CHU, S. 2003. Use of a Reflectance Spectrophotometer in Evaluating Shade Change Resulting from Tooth-Whitening Products. *Journal of Esthetic and Restorative Dentistry*, 15.
- CHU, S. J., TRUSHKOWSKY, R. D. & PARAVINA, R. D. 2010. Dental color matching instruments and systems. Review of clinical and research aspects. *J Dent*, 38 Suppl 2, e2-16.
- CHUNG, K.-H. 1994. Effects of finishing and polishing procedures on the surface texture of resin composites. *Dental Materials*, 10, 325-330.
- CLARK, E. B. 1933. Tooth Color Selection*** Read before the Section on Operative Dentistry, Materia Medica and Therapeutics at the Seventy-Fourth Annual Session of the American Dental Association, Buffalo, NY, Sept. 15, 1932. *The Journal of the American Dental Association (1922)*, 20, 1065-1073.
- CLAUSSEN, N. 1976. Fracture toughness of Al₂O₃ with an unstabilized ZrO₂ Dispersed phase. *Journal of the American Ceramic society*, 59, 49-51.
- COOK, W. D. & MCAREE, D. C. 1985. Optical properties of esthetic restorative materials and natural dentition. *Journal of Biomedical Materials Research Part A*, 19, 469-488.
- CORTIZO, M. C., DE MELE, M. F. L. & CORTIZO, A. M. 2004. Metallic dental material biocompatibility in osteoblastlike cells. *Biological trace element research*, 100, 151-168.
- COTES, C., ARATA, A., MELO, R. M., BOTTINO, M. A., MACHADO, J. P. & SOUZA, R. O. 2014. Effects of aging procedures on the topographic surface, structural stability, and mechanical strength of a ZrO₂-based dental ceramic. *Dent Mater*, 30, e396-404.
- DA SILVA, J. D., PARK, S. E., WEBER, H.-P. & ISHIKAWA-NAGAI, S. 2008. Clinical performance of a newly developed spectrophotometric system on tooth color reproduction. *The Journal of Prosthetic Dentistry*, 99, 361-368.
- DAVIDGE, R. W. 1979. *Mechanical behaviour of ceramics*, CUP Archive.
- DEHESTANI, M. & ADOLFSSON, E. 2013. Phase Stability and Mechanical Properties of Zirconia and Zirconia Composites. *International Journal of Applied Ceramic Technology*, 10, 129-141.
- DENRY, I. & HOLLOWAY, J. A. 2010. Ceramics for Dental Applications: A Review. *Materials*, 3, 351-368.
- DENRY, I. & KELLY, J. R. 2008. State of the art of zirconia for dental applications. *Dent Mater*, 24, 299-307.
- DENRY, I. & KELLY, J. R. 2014. Emerging ceramic-based materials for dentistry. *J Dent Res*, 93, 1235-42.
- DEPPRICH, R., ZIPPRICH, H., OMMERBORN, M., NAUJOKS, C., WIESMANN, H. P., KIATTAVORNCHAROEN, S., LAUER, H. C., MEYER, U., KUBLER, N. R. & HANDSCHEL, J. 2008.

- Osseointegration of zirconia implants compared with titanium: an in vivo study. *Head Face Med*, 4, 30.
- DEVILLE, S., GREMILLARD, L., CHEVALIER, J. & FANTOZZI, G. 2005. A critical comparison of methods for the determination of the aging sensitivity in biomedical grade yttria-stabilized zirconia. *J Biomed Mater Res B Appl Biomater*, 72, 239-45.
- DEVILLE, S., GUÉNIN, G. & CHEVALIER, J. 2004. Martensitic transformation in zirconia. *Acta Materialia*, 52, 5709-5721.
- DING, H., VIRKAR, A. V. & LIU, F. 2012. Defect configuration and phase stability of cubic versus tetragonal yttria-stabilized zirconia. *Solid State Ionics*, 215, 16-23.
- DOZIĆ, A., KLEVERLAAN, C. J., MEEGDES, M., VAN DER ZEL, J. & FEILZER, A. J. 2003. The influence of porcelain layer thickness on the final shade of ceramic restorations. *The Journal of Prosthetic Dentistry*, 90, 563-570.
- DUWEZ, P., BROWN, F. H. & ODELL, F. 1951. The Zirconia-Yttria System. *Journal of the electrochemical society*, 98, 356-362.
- DUWEZ, P., ODELL, F. & BROWN, F. H. 1952. Stabilization of zirconia with calcia and magnesia. *Journal of the American Ceramic Society*, 35, 107-113.
- ĚASTKOVA, K., HADRABA, H. & CIHLÁĚ, J. 2004. Hydrothermal ageing of tetragonal zirconia ceramics. *transformation*, 9, 12.
- EGILMEZ, F., ERGUN, G., CEKIC-NAGAS, I., VALLITTU, P. K. & LASSILA, L. V. 2014. Factors affecting the mechanical behavior of Y-TZP. *J Mech Behav Biomed Mater*, 37, 78-87.
- ERSOY, N. M., AYDOGDU, H. M., DEGIRMENCI, B. U., COKUK, N. & SEVIMAY, M. 2015. The effects of sintering temperature and duration on the flexural strength and grain size of zirconia. *Acta Biomater Odontol Scand*, 1, 43-50.
- EVANS, A. 1982. Structural Reliability: A Processing-Dependent Phenomenon. *Journal of the American Ceramic Society*, 65, 127-137.
- EVANS, A. 1983. Toughening mechanisms in zirconia alloys. *Science and technology of zirconia II*.
- FABBRI, G., ZARONE, F., DELLIFICORELLI, G., CANNISTRARO, G., DE LORENZI, M., MOSCA, A. & SORRENTINO, R. 2014. Clinical evaluation of 860 anterior and posterior lithium disilicate restorations: retrospective study with a mean follow-up of 3 years and a maximum observational period of 6 years. *Int J Periodontics Restorative Dent*, 34, 165-77.
- FASSINA, P., ZAGHINI, N., BUKAT, A., PICONI, C., GRECO, F. & PIANTELLI, S. 1992. Yttria and calcia partially stabilized zirconia for biomedical applications. *Bioceramics and the human body*. Springer.
- FATHY, S. M., EL-FALLAL, A. A., EL-NEGOLY, S. A. & EL BEDAWY, A. B. 2015. Translucency of monolithic and core zirconia after hydrothermal aging. *Acta Biomater Odontol Scand*, 1, 86-92.
- FERNANDEZ-FAIREN, M., BLANCO, A., MURCIA, A., SEVILLA, P. & GIL, F. J. 2007. Aging of retrieved zirconia femoral heads. *Clinical orthopaedics and related research*, 462, 122-129.
- FILSER, F., KOCHER, P., WEIBEL, F., LUTHY, H., SCHARER, P. & GAUCKLER, L. 2001. Reliability and strength of all-ceramic dental

- restorations fabricated by direct ceramic machining (DCM). *International journal of computerized dentistry*, 4, 89-106.
- FUGOLIN, A., CORRER-SOBRINHO, L., CORRER, A. B., SINHORETI, M., GUIRALDO, R. D. & CONSANI, S. 2016. Influence of irradiance on Knoop hardness, degree of conversion, and polymerization shrinkage of nanofilled and microhybrid composite resins. *General dentistry*, 64, 26-31.
- GAILLARD, Y., JIMÉNEZ-PIQUÉ, E., SOLDERA, F., MÜCKLICH, F. & ANGLADA, M. 2008. Quantification of hydrothermal degradation in zirconia by nanoindentation. *Acta Materialia*, 56, 4206-4216.
- GARVIE, R., HANNINK, R. & PASCOE, R. 1975. Ceramic steel? *Nature*, 258, 703-704.
- GARVIE, R., URBANI, C., KENNEDY, D. & MCNEUER, J. 1984. Biocompatibility of magnesia-partially stabilized zirconia (Mg-PSZ) ceramics. *Journal of Materials Science*, 19, 3224-3228.
- GEISLER, T., JANSSEN, A., SCHEITER, D., STEPHAN, T., BERNDT, J. & PUTNIS, A. 2010. Aqueous corrosion of borosilicate glass under acidic conditions: a new corrosion mechanism. *Journal of Non-Crystalline Solids*, 356, 1458-1465.
- GHINEA, R., UGARTE-ALVAN, L., YEBRA, A., PECHO, O. E., PARAVINA, R. D. & PEREZ MDEL, M. 2011. Influence of surface roughness on the color of dental-resin composites. *J Zhejiang Univ Sci B*, 12, 552-62.
- GIESSIBL, F. J. 1995. Atomic Force Microscopy-(7x7) Surface by Atomic Force Microscopy. *Science*, 267, 68-71.
- GIESSIBL, F. J. 2003. Advances in atomic force microscopy. *Reviews of modern physics*, 75, 949.
- GIORDANO, R. & MCLAREN, E. A. 2010. Ceramics overview: classification by microstructure and processing methods. *Compend Contin Educ Dent*, 31, 682-684.
- GOLDBERG, M. 2008. In vitro and in vivo studies on the toxicity of dental resin components: a review. *Clin Oral Investig*, 12, 1-8.
- GRACIS, S., THOMPSON, V. P., FERENCZ, J. L., SILVA, N. R. & BONFANTE, E. A. 2015. A new classification system for all-ceramic and ceramic-like restorative materials. *International Journal of Prosthodontics*, 28.
- GREEN, D. J., HANNINK, R. H. & SWAIN, M. V. 1989. Transformation toughening of ceramics.
- GREMILLARD, L., CHEVALIER, J., EPICIER, T., DEVILLE, S. & FANTOZZI, G. 2004. Modeling the aging kinetics of zirconia ceramics. *Journal of the European Ceramic Society*, 24, 3483-3489.
- GUAZZATO, M., ALBAKRY, M., RINGER, S. P. & SWAIN, M. V. 2004. Strength, fracture toughness and microstructure of a selection of all-ceramic materials. Part II. Zirconia-based dental ceramics. *Dent Mater*, 20, 449-56.
- GUAZZATO, M., ALBAKRY, M., SWAIN, M. V. & IRONSIDE, J. 2002. Mechanical properties of In-Ceram Alumina and In-Ceram Zirconia. *International Journal of Prosthodontics*, 15.
- GUAZZATO, M., QUACH, L., ALBAKRY, M. & SWAIN, M. V. 2005. Influence of surface and heat treatments on the flexural strength of Y-TZP dental ceramic. *J Dent*, 33, 9-18.

- GUESS, P. C., KULIS, A., WITKOWSKI, S., WOLKEWITZ, M., ZHANG, Y. & STRUB, J. R. 2008. Shear bond strengths between different zirconia cores and veneering ceramics and their susceptibility to thermocycling. *Dent Mater*, 24, 1556-67.
- GUESS, P. C., SCHULTHEIS, S., BONFANTE, E. A., COELHO, P. G., FERENCZ, J. L. & SILVA, N. R. 2011. All-ceramic systems: laboratory and clinical performance. *Dent Clin North Am*, 55, 333-52, ix.
- GUESS, P. C., ZAVANELLI, R. A., SILVA, N. R., BONFANTE, E. A., COELHO, P. G. & THOMPSON, V. P. 2010. Monolithic CAD/CAM lithium disilicate versus veneered Y-TZP crowns: comparison of failure modes and reliability after fatigue. *International Journal of Prosthodontics*, 23.
- GUO, X. 2004. Property degradation of tetragonal zirconia induced by low-temperature defect reaction with water molecules. *Chemistry of materials*, 16, 3988-3994.
- GUO, X. & HE, J. 2003. Hydrothermal degradation of cubic zirconia. *Acta Materialia*, 51, 5123-5130.
- GUPTA, T., BECHTOLD, J., KUZNICKI, R., CADOFF, L. & ROSSING, B. 1977. Stabilization of tetragonal phase in polycrystalline zirconia. *Journal of Materials Science*, 12, 2421-2426.
- GUPTA, T. K., LANGE, F. & BECHTOLD, J. 1978. Effect of stress-induced phase transformation on the properties of polycrystalline zirconia containing metastable tetragonal phase. *Journal of Materials Science*, 13, 1464-1470.
- HALLMANN, L., MEHL, A., ULMER, P., REUSSER, E., STADLER, J., ZENOBI, R., STAWARCZYK, B., OZCAN, M. & HAMMERLE, C. H. 2012. The influence of grain size on low-temperature degradation of dental zirconia. *J Biomed Mater Res B Appl Biomater*, 100, 447-56.
- HANNINK, R. H. & GARVIE, R. C. 1982. Sub-eutectoid aged Mg-PSZ alloy with enhanced thermal up-shock resistance. *Journal of Materials Science*, 17, 2637-2643.
- HANNINK, R. H., KELLY, P. M. & MUDDLE, B. C. 2000. Transformation toughening in zirconia-containing ceramics. *Journal of the American Ceramic Society*, 83, 461-487.
- HARADA, K., RAIGRODSKI, A. J., CHUNG, K. H., FLINN, B. D., DOGAN, S. & MANCL, L. A. 2016. A comparative evaluation of the translucency of zirconias and lithium disilicate for monolithic restorations. *J Prosthet Dent*, 116, 257-63.
- HARAGUCHI, K., SUGANO, N., NISHII, T., MIKI, H., OKA, K. & YOSHIKAWA, H. 2001. Phase transformation of a zirconia ceramic head after total hip arthroplasty. *Bone & Joint Journal*, 83, 996-1000.
- HARIANAWALA, H. H., KHEUR, M. G., APTE, S. K., KALE, B. B., SETHI, T. S. & KHEUR, S. M. 2014. Comparative analysis of transmittance for different types of commercially available zirconia and lithium disilicate materials. *J Adv Prosthodont*, 6, 456-61.
- HARMAN, G. 1996. Explaining objective color in terms of subjective reactions. *Philosophical issues*, 7, 1-17.
- HAYASHI, K., KOBAYASHI, O., TOYODA, S. & MORINAGA, K. 1991. Transmission optical properties of polycrystalline alumina with submicron grains. *Materials Transactions, JIM*, 32, 1024-1029.

- HAYWOOD, V. B., HEYMANN, H. & SCURRIA, M. 1989. Effects of water, speed, and experimental instrumentation on finishing and polishing porcelain intra-orally. *Dental Materials*, 5, 185-188.
- HEFFERNAN, M. J., AQUILINO, S. A., DIAZ-ARNOLD, A. M., HASELTON, D. R., STANFORD, C. M. & VARGAS, M. A. 2002. Relative translucency of six all-ceramic systems. Part I: core materials. *The Journal of prosthetic dentistry*, 88, 4-9.
- HELLMANN, J. R. & STUBICAN, V. S. 1983. Phase Relations and Ordering in the Systems MgO-Y₂O₃-ZrO₂ and CaO-MgO-ZrO₂. *Journal of the American Ceramic Society*, 66, 265-267.
- HELMER, J. & DRISKELL, T. 1969. Research on Bioceramics: Symposium on Use of Ceramics as Surgical Implants. *South Carolina: Clemson University*.
- HELVEY, G. 2014. Classifying dental ceramics: numerous materials and formulations available for indirect restorations. *Compendium of continuing education in dentistry (Jamesburg, NJ: 1995)*, 35, 38-43.
- HENCH, L. & ETHRIDGE, E. 1975. Biomaterials: the interfacial problem. *Adv Biomed Eng*, 5, 35-150.
- HERRERO, J. P. 2007. *Influence of residual stresses on strength and toughness of an alumina/alumina-zirconia laminate*, na.
- HJERPPE, J., NARHI, T., FROBERG, K., VALLITTU, P. K. & LASSILA, L. V. 2008. Effect of shading the zirconia framework on biaxial strength and surface microhardness. *Acta Odontol Scand*, 66, 262-7.
- HMAIDOUCH, R., MULLER, W. D., LAUER, H. C. & WEIGL, P. 2014. Surface roughness of zirconia for full-contour crowns after clinically simulated grinding and polishing. *Int J Oral Sci*, 6, 241-6.
- HO, D. K., GHINEA, R., HERRERA, L. J., ANGELOV, N. & PARAVINA, R. D. 2015. Color Range and Color Distribution of Healthy Human Gingiva: a Prospective Clinical Study. *Sci Rep*, 5, 18498.
- HOFMANN, N., HUGO, B. & KLAIBER, B. 2002. Effect of irradiation type (LED or QTH) on photo-activated composite shrinkage strain kinetics, temperature rise, and hardness. *European Journal of Oral Sciences*, 110, 471-479.
- HOLZER, L., INDUTNYI, F., GASSER, P. H., MUNCH, B. & WEGMANN, M. 2004. Three-dimensional analysis of porous BaTiO₃ ceramics using FIB nanotomography. *J Microsc*, 216, 84-95.
- HORN, D. J., BULAN-BRADY, J. & HICKS, M. L. 1998. Sphere spectrophotometer versus human evaluation of tooth shade. *Journal of endodontics*, 24, 786-790.
- HOWARD, C. J., KISI, E. H., ROBERTS, R. B. & HILL, R. J. 1990. Neutron Diffraction Studies of Phase Transformations between Tetragonal and Orthorhombic Zirconia in Magnesia-Partially-Stabilized Zirconia. *Journal of the American Ceramic Society*, 73, 2828-2833.
- HUNTER, R. S. & HAROLD, R. W. 1987. *The measurement of appearance*, John Wiley & Sons.
- ILIE, N., HILTON, T., HEINTZE, S., HICKEL, R., WATTS, D., SILIKAS, N., STANSBURY, J., CADENARO, M. & FERRACANE, J. 2017. Academy of Dental Materials guidance—Resin composites: Part I—Mechanical properties. *Dental Materials*.

- ILIE, N. & STAWARCZYK, B. 2014. Quantification of the amount of light passing through zirconia: the effect of material shade, thickness, and curing conditions. *J Dent*, 42, 684-90.
- INOKOSHI, M., ZHANG, F., VANMEENSEL, K., DE MUNCK, J., MINAKUCHI, S., NAERT, I., VLEUGELS, J. & VAN MEERBEEK, B. 2017. Residual compressive surface stress increases the bending strength of dental zirconia. *Dental Materials*, 33, e147-e154.
- ISGRÒ, G., PALLAV, P., VAN DER ZEL, J. M. & FEILZER, A. J. 2003. The influence of the veneering porcelain and different surface treatments on the biaxial flexural strength of a heat-pressed ceramic. *The Journal of prosthetic dentistry*, 90, 465-473.
- ISO-843-4 2015. Advanced technical ceramics — Mechanical properties of monolithic ceramics at room temperature — Vickers, Knoop and Rockwell superficial hardness. International Standards Organization
- ISO-6872 2015. Dentistry — Ceramic materials. Geneva: International Standards Organization.
- ISO-10650 2015. Dentistry-Powered polymerization activators. Geneva: International Standards Organization.
- ISO-13356 2015. Implants for surgery - Ceramic materials based on yttria-stabilized tetragonal zirconia (Y-TZP). Geneva: International Organization for Standardization.
- ISO-14705 2016. Fine ceramics (advanced ceramics, advanced technical ceramics) *Test method for hardness of monolithic ceramics at room temperature*. Geneva: International Standards Organization.
- ISO-28642 2016. Dentistry — Guidance on colour measurement. Geneva: International Standards Organization.
- JAMES, S. A., POWELL, L. C. & WRIGHT, C. J. 2016. Atomic Force Microscopy of Biofilms—Imaging, Interactions, and Mechanics.
- JANABI, A. U. 2014. *The Mechanical Properties of Full-Contour Zirconia*.
- JANDA, R., ROULET, J. F., KAMINSKY, M., STEFFIN, G. & LATTA, M. 2004. Color stability of resin matrix restorative materials as a function of the method of light activation. *European journal of oral sciences*, 112, 280-285.
- JANG, G. W., KIM, H. S., CHOE, H. C. & SON, M. K. 2011. Fracture Strength and Mechanism of Dental Ceramic Crown with Zirconia Thickness. *Procedia Engineering*, 10, 1556-1560.
- JANNEY, M. A., CALHOUN, C. L. & KIMREY, H. D. 1992. Microwave Sintering of Solid Oxide Fuel Cell Materials: I, Zirconia-8 mol% Yttria. *Journal of the American Ceramic Society*, 75, 341-346.
- JENKINS, R. 2000. X-Ray Techniques: Overview. *Encyclopedia of analytical chemistry*.
- JIANG, L., LIAO, Y., WAN, Q. & LI, W. 2011a. Effects of sintering temperature and particle size on the translucency of zirconium dioxide dental ceramic. *Journal of Materials Science: Materials in Medicine*, 22, 2429-2435.
- JIANG, L., LIAO, Y., WAN, Q. & LI, W. 2011b. Effects of sintering temperature and particle size on the translucency of zirconium dioxide dental ceramic. *J Mater Sci Mater Med*, 22, 2429-35.

- JOHNSTON, W., HESSE, N., DAVIS, B. & SEGHI, R. 1996. Analysis of edge-losses in reflectance measurements of pigmented maxillofacial elastomer. *Journal of dental research*, 75, 752-760.
- JOHNSTON, W. M. & KAO, E. C. 1989. Assessment of appearance match by visual observation and clinical colorimetry. *J Dent Res*, 68, 819-22.
- JOHNSTON, W. M., MA, T. & KIENLE, B. H. 1995. Translucency parameter of colorants for maxillofacial prostheses. *International Journal of Prosthodontics*, 8.
- JOHNSTON, W. M. & REISBICK, M. 1997. Color and translucency changes during and after curing of esthetic restorative materials. *Dental Materials*, 13, 89-97.
- JUM'AH, A. A. H. A. 2015. *An In Vitro Investigation of a Novel, Two-Piece Zirconia Dental Implant System*. University of Leeds.
- KANAT, B., COMLEKOGLU, E. M., DUNDAR-COMLEKOGLU, M., HAKAN SEN, B., OZCAN, M. & ALI GUNGOR, M. 2014. Effect of various veneering techniques on mechanical strength of computer-controlled zirconia framework designs. *J Prosthodont*, 23, 445-55.
- KANCHANAVASITA, W., TRIWATANA, P., SUPUTTAMONGKOL, K., THANAPITAK, A. & CHATCHAIGANAN, M. 2014. Contrast ratio of six zirconia-based dental ceramics. *J Prosthodont*, 23, 456-61.
- KATZ, G. 1971. X-Ray Diffraction Powder Pattern of Metastable Cubic ZrO₂. *Journal of the American Ceramic Society*, 54, 531-531.
- KAWAI, Y., MOTOHIRO, U. & WATARI, F. 2010. Microstructure evaluation of the interface between dental zirconia ceramics and veneering porcelain. *Nano Biomedicine*, 2, 31-36.
- KEUPER, M., EDER, K., BERTHOLD, C. & NICKEL, K. G. 2013. Direct evidence for continuous linear kinetics in the low-temperature degradation of Y-TZP. *Acta Biomater*, 9, 4826-35.
- KHAMVERDI, Z. & MOSHIRI, Z. 2012. Zirconia: An up-to-date literature review. *Avicenna Journal of Dental Research*, 4, 1-15.
- KHURANA, R., TREDWIN, C., WEISBLOOM, M. & MOLES, D. 2007. A clinical evaluation of the individual repeatability of three commercially available colour measuring devices. *British Dental Journal*, 203, 675-680.
- KIELBASSA, A. M., BEHEIM-SCHWARZBACH, N. J., NEUMANN, K. & ZANTNER, C. 2009. In vitro comparison of visual and computer-aided pre-and post-tooth shade determination using various home bleaching procedures. *The Journal of prosthetic dentistry*, 101, 92-100.
- KILINC, E., ANTONSON, S. A., HARDIGAN, P. C. & KESERCIOGLU, A. 2011. The effect of ceramic restoration shade and thickness on the polymerization of light- and dual-cure resin cements. *Oper Dent*, 36, 661-9.
- KIM, B., ZHANG, Y., PINES, M. & THOMPSON, V. P. 2007. Fracture of porcelain-veneered structures in fatigue. *J Dent Res*, 86, 142-6.
- KIM, H.-K. & KIM, S.-H. 2014. Effect of the number of coloring liquid applications on the optical properties of monolithic zirconia. *Dental Materials*, 30, e229-e237.
- KIM, H.-T., HAN, J.-S., YANG, J.-H., LEE, J.-B. & KIM, S.-H. 2009a. The effect of low temperature aging on the mechanical property & phase

- stability of Y-TZP ceramics. *The journal of advanced prosthodontics*, 1, 113-117.
- KIM, H. T., HAN, J. S., YANG, J. H., LEE, J. B. & KIM, S. H. 2009b. The effect of low temperature aging on the mechanical property & phase stability of Y-TZP ceramics. *J Adv Prosthodont*, 1, 113-7.
- KIM, I.-J., LEE, Y.-K., LIM, B.-S. & KIM, C.-W. 2003. Effect of surface topography on the color of dental porcelain. *Journal of Materials Science: Materials in Medicine*, 14, 405-409.
- KIM, M. J., AHN, J. S., KIM, J. H., KIM, H. Y. & KIM, W. C. 2013. Effects of the sintering conditions of dental zirconia ceramics on the grain size and translucency. *J Adv Prosthodont*, 5, 161-6.
- KINGERY, W., BOWEN, H. & UHLMANN, D. 1976. Introduction to ceramics, 1976. *Jhon Willey & Sons, New York*.
- KINGERY, W. D. 1960. Introduction to ceramics.
- KIRSTEIN, A. & WOOLLEY, R. 1967. Symmetrical bending of thin circular elastic plates on equally spaced point supports. *J. Res. Natl. Bur. Stand. C*, 71, 1-10.
- KISI, E. H. & HOWARD, C. J. 1998. Crystal Structures of Zirconia Phases and their Inter-Relation. *Key Engineering Materials*, 153-154, 1-36.
- KLEIN, C. A. 2009. Characteristic strength, Weibull modulus, and failure probability of fused silica glass. *Optical Engineering*, 48, 113401-113401-10.
- KLIMKE, J., TRUNEC, M. & KRELL, A. 2011. Transparent Tetragonal Yttria-Stabilized Zirconia Ceramics: Influence of Scattering Caused by Birefringence. *Journal of the American Ceramic Society*, 94, 1850-1858.
- KNOOP, F., PETERS, C. G. & EMERSON, W. B. 1939. A sensitive pyramidal-diamond tool for indentation measurements. *Journal of Research of the National Bureau of standards*, 23, 39-61.
- KOBAYASHI, E., MATSUMOTO, S., YONEYAMA, T. & HAMANAKA, H. 1995. Mechanical properties of the binary titanium-zirconium alloys and their potential for biomedical materials. *Journal of Biomedical Materials Research Part A*, 29, 943-950.
- KOBAYASHI, K., KUWAJIMA, H. & MASAKI, T. 1981. Phase change and mechanical properties of ZrO₂-Y₂O₃ solid electrolyte after ageing. *Solid State Ionics*, 3, 489-493.
- KOHORST, P., BORCHERS, L., STREMPER, J., STIESCH, M., HASSEL, T., BACH, F.-W. & HÜBSCH, C. 2012. Low-temperature degradation of different zirconia ceramics for dental applications. *Acta Biomaterialia*, 8, 1213-1220.
- KOMINE, F., BLATZ, M. B. & MATSUMURA, H. 2010. Current status of zirconia-based fixed restorations. *Journal of Oral Science*, 52, 531-539.
- KONDO, S., KATOH, Y., KIM, J. & SNEAD, L. 2010. VALIDATION OF EQUIBIAXIAL FLEXURAL TEST FOR MINIATURIZED CERAMIC SPECIMENS.
- KORSUNSKY, A. M., SEBASTIANI, M. & BEMPORAD, E. 2010. Residual stress evaluation at the micrometer scale: Analysis of thin coatings by FIB milling and digital image correlation. *Surface and Coatings Technology*, 205, 2393-2403.

- KUEHNI, R. G. 2002. The early development of the Munsell system. *Color Research & Application*, 27, 20-27.
- KURTZ, S. M., KOCAGOZ, S., ARNHOLT, C., HUET, R., UENO, M. & WALTER, W. L. 2014. Advances in zirconia toughened alumina biomaterials for total joint replacement. *J Mech Behav Biomed Mater*, 31, 107-16.
- L'ECLAIRAGE, C. I. D. 2004. *Colorimetry: Technical Report*, Central Bureau of the CIE.
- L'ECLAIRAGE, C. C. I. 1986. Colorimetry–technical report. *CIE Publication*, 2.
- LANDRY, V., RIEDL, B. & BLANCHET, P. 2008. Alumina and zirconia acrylate nanocomposites coatings for wood flooring: Photocalorimetric characterization. *Progress in Organic Coatings*, 61, 76-82.
- LANGFORD, R. & CLINTON, C. 2004. In situ lift-out using a FIB-SEM system. *Micron*, 35, 607-611.
- LAWN, B. R., DENG, Y. & THOMPSON, V. P. 2001. Use of contact testing in the characterization and design of all-ceramic crownlike layer structures: a review. *The Journal of prosthetic dentistry*, 86, 495-510.
- LEE, Y.-K. 2015. Translucency of Dental Ceramic, Post and Bracket. *Materials*, 8, 7241-7249.
- LEE, Y.-K., YU, B., LIM, H.-N. & LIM, J. I. 2011. Difference in the color stability of direct and indirect resin composites. *Journal of Applied Oral Science*, 19, 154-160.
- LEE, Y. K., LIM, B. S., KIM, C. W. & POWERS, J. M. 2001. Color characteristics of low-chroma and high-translucence dental resin composites by different measuring modes. *J Biomed Mater Res*, 58, 613-21.
- LEE, Y. K., YU, B., LEE, S. H., CHO, M. S., LEE, C. Y. & LIM, H. N. 2010. Variation in instrument-based color coordinates of esthetic restorative materials by measurement method-A review. *Dent Mater*, 26, 1098-105.
- LESSA, F. C. R., ENOKI, C., ITO, I. Y., FARIA, G., MATSUMOTO, M. A. N. & NELSON-FILHO, P. 2007. In-vivo evaluation of the bacterial contamination and disinfection of acrylic baseplates of removable orthodontic appliances. *American Journal of Orthodontics and Dentofacial Orthopedics*, 131, 705. e11-705. e17.
- LIM, H.-N., YU, B. & LEE, Y.-K. 2010. Spectroradiometric and spectrophotometric translucency of ceramic materials. *The Journal of Prosthetic Dentistry*, 104, 239-246.
- LIMARGA, A. M., SHIAN, S., BARAM, M. & CLARKE, D. R. 2012. Effect of high-temperature aging on the thermal conductivity of nanocrystalline tetragonal yttria-stabilized zirconia. *Acta Materialia*, 60, 5417-5424.
- LIN, C., GAN, D. & SHEN, P. 1988. Stabilization of zirconia sintered with titanium. *Journal of the American Ceramic Society*, 71, 624-629.
- LIU, M. C., AQUILINO, S. A., LUND, P. S., VARGAS, M. A., DIAZ-ARNOLD, A. M., GRATTON, D. G. & QIAN, F. 2010a. Human perception of dental porcelain translucency correlated to spectrophotometric measurements. *J Prosthodont*, 19, 187-93.

- LIU, Q., SHAO, L. Q., WEN, N. & DENG, B. 2010b. Surface Microhardness and Flexural Strength of Colored Zirconia. *Advanced Materials Research*, 105-106, 49-50.
- LIU, Y., FENG, H., BAO, Y., QIU, Y., XING, N. & SHEN, Z. 2010c. Fracture and interfacial delamination origins of bilayer ceramic composites for dental restorations. *Journal of the European Ceramic Society*, 30, 1297-1305.
- LUGHI, V. & SERGO, V. 2010. Low temperature degradation -aging- of zirconia: A critical review of the relevant aspects in dentistry. *Dent Mater*, 26, 807-20.
- LUO, H., TANG, X., DONG, Z., TANG, H., NAKAMURA, T. & YATANI, H. 2016. The influences of accelerated aging on mechanical properties of veneering ceramics used for zirconia restorations. *Dent Mater J*, 35, 187-93.
- LUO, X.-P., SILIKAS, N., ALLAF, M., WILSON, N. & WATTS, D. 2001. AFM and SEM study of the effects of etching on IPS-Empress 2 TM dental ceramic. *Surface Science*, 491, 388-394.
- LUO, X. P. & ZHANG, L. 2010. Effect of Veneering Techniques on Color and Translucency of Y-TZP. *Journal of Prosthodontics*, 19, 465-470.
- MACCAURO, G., BIANCHINO, G., SANGIORGI, S., MAGNANI, G., MAROTTA, D., MANICONE, P. F., RAFFAELLI, L., IOMMETTI, P. R., STEWART, A. & CITTADINI, A. 2009. Development of a new zirconia-toughened alumina: promising mechanical properties and absence of in vitro carcinogenicity. *International journal of immunopathology and pharmacology*, 22, 773-779.
- MAGNE, P., OH, W.-S., PINTADO, M. R. & DELONG, R. 1999. Wear of enamel and veneering ceramics after laboratory and chairside finishing procedures. *The Journal of prosthetic dentistry*, 82, 669-679.
- MALKONDU, Ö., TINASTEPE, N., AKAN, E. & KAZAZOĞLU, E. 2016. An overview of monolithic zirconia in dentistry. *Biotechnology & Biotechnological Equipment*, 30, 644-652.
- MANICONE, P. F., ROSSI IOMMETTI, P. & RAFFAELLI, L. 2007. An overview of zirconia ceramics: basic properties and clinical applications. *J Dent*, 35, 819-26.
- MASSIMI, F., MERLATI, G., SEBASTIANI, M., BATTAINI, P., MENGHINI, P. & BEMPORAD, E. 2012. FIB/SEM and SEM/EDS microstructural analysis of metal-ceramic and zirconia-ceramic interfaces. *Bulletin du Groupement International pour la Recherche Scientifique en Stomatologie et Odontologie*, 50, 1-10.
- MATINLINNA, J. P. 2014. *Handbook of oral biomaterials*, Pan Stanford Publishing.
- MCLAREN, E., LAWSON, N., CHOI, J., KANG, J. & TRUJILLO, C. 2017. New High-Translucent Cubic-Phase-Containing Zirconia: Clinical and Laboratory Considerations and the Effect of Air Abrasion on Strength. *Compendium of continuing education in dentistry (Jamesburg, NJ: 1995)*, 38, e13.
- MCLEAN, J. 1965. A higher strength porcelain for crown and bridge work. *Br Dent J*, 119, 268-272.
- MCLEAN, J. W. 1979. The science and art of dental ceramics. *The nature of dental ceramics and their clinical use*, 79-82.

- MECHOLSKY, J. J. 1995. Fracture mechanics principles. *Dental Materials*, 11, 111-112.
- MEHTA, D. & SHETTY, R. 2010. Bonding to zirconia: elucidating the confusion. *Int Dent SA*, 12, 46-52.
- MIJOSKA, A. & POPOVSKA, M. 2015. Evaluation of Different in Vitro Testing Methods for Mechanical Properties of Veneer Ceramics/Евалуација На Тестовите In Vitro За Одредување На Механичките Особини На Порцеланските Маси За Фасетирање. *prilozi*, 36, 225-230.
- MILLEDING, P., KARLSSON, S. & NYBORG, L. 2003. On the surface elemental composition of non-corroded and corroded dental ceramic materials in vitro. *Journal of Materials Science: Materials in Medicine*, 14, 557-566.
- MITRA, S. B., WU, D. & HOLMES, B. N. 2003. An application of nanotechnology in advanced dental materials. *The Journal of the American Dental Association*, 134, 1382-1390.
- MIYAGAWA, Y., POWERS, J. & O'BRIEN, W. 1981. Optical properties of direct restorative materials. *Journal of Dental Research*, 60, 890-894.
- MIYAZAKI, T., NAKAMURA, T., MATSUMURA, H., BAN, S. & KOBAYASHI, T. 2013. Current status of zirconia restoration. *J Prosthodont Res*, 57, 236-61.
- MOHIE EL-DIN WAHBA, M., EL-ETREBY, A. S. & MORSI, T. S. 2017. Effect of core/veneer thickness ratio and veneer translucency on absolute and relative translucency of CAD-On restorations. *Future Dental Journal*, 3, 8-14.
- MUNOZ, E. M., LONGHINI, D., ANTONIO, S. G. & ADABO, G. L. 2017. The effects of mechanical and hydrothermal aging on microstructure and biaxial flexural strength of an anterior and a posterior monolithic zirconia. *J Dent*.
- MUNZ, D. & FETT, T. 2013. *Ceramics: mechanical properties, failure behaviour, materials selection*, Springer Science & Business Media.
- MYERS, M. L., CAUGHMAN, W. F. & RUEGGERBERG, F. A. 1994. Effect of restoration composition, shade, and thickness on the cure of a photoactivated resin cement. *Journal of Prosthodontics*, 3, 149-157.
- NAKAMURA, K. 2015. *Mechanical and Microstructural Properties of Monolithic Zirconia*.
- NAKAMURA, T., NAKANO, Y., USAMI, H., WAKABAYASHI, K., OHNISHI, H., SEKINO, T. & YATANI, H. 2016. Translucency and low-temperature degradation of silica-doped zirconia: A pilot study. *Dent Mater J*, 35, 571-7.
- O'BRIEN, W. 1985. Double layer effect and other optical phenomena related to esthetics. *Dental Clinics of North America*, 29, 667-672.
- O'BRIEN, W. J. 2008. Dental materials and their selection.
- O'KEEFE, K., PEASE, P. & HERRIN, H. 1991. Variables affecting the spectral transmittance of light through porcelain veneer samples. *The Journal of prosthetic dentistry*, 66, 434-438.
- OH, W.-S., DELONG, R. & ANUSAVICE, K. J. 2002. Factors affecting enamel and ceramic wear: a literature review. *The journal of prosthetic dentistry*, 87, 451-459.

- OHMACHI, N., KAMIOKA, K., MATSUI, K. & OHGAI, M. 1999. Phase transformation of zirconia ceramics by annealing in hot water. *Journal of the Ceramic Society of Japan*, 107, 128-133.
- ØILO, M., GJERDET, N. R. & TVINNEREIM, H. M. 2008. The firing procedure influences properties of a zirconia core ceramic. *dental materials*, 24, 471-475.
- OYAGUE, R. C., MONTICELLI, F., TOLEDANO, M., OSORIO, E., FERRARI, M. & OSORIO, R. 2009. Effect of water aging on microtensile bond strength of dual-cured resin cements to pre-treated sintered zirconium-oxide ceramics. *Dent Mater*, 25, 392-9.
- ÖZKURT-KAYAHAN, Z. 2016. Monolithic zirconia: A review of the literature. *Biomedical Research*, 27, 1427-1436.
- OZTURK, O., ULUDAG, B., USUMEZ, A., SAHIN, V. & CELIK, G. 2008. The effect of ceramic thickness and number of firings on the color of two all-ceramic systems. *The Journal of Prosthetic Dentistry*, 100, 99-106.
- PALMERO, P., MONTANARO, L., REVERON, H. & CHEVALIER, J. 2014. Surface Coating of Oxide Powders: A New Synthesis Method to Process Biomedical Grade Nano-Composites. *Materials*, 7, 5012-5037.
- PARAVINA, R., ROEDER, L., LU, H., VOGEL, K. & POWERS, J. 2004. Effect of finishing and polishing procedures on surface roughness, gloss and color of resin-based composites. *American Journal of Dentistry*, 17, 262-266.
- PARAVINA, R. D. 2004. *Esthetic color training in dentistry*, Mosby.
- PARAVINA, R. D., GHINEA, R., HERRERA, L. J., BONA, A. D., IGIEL, C., LINNINGER, M., SAKAI, M., TAKAHASHI, H., TASHKANDI, E. & PEREZ MDEL, M. 2015. Color difference thresholds in dentistry. *J Esthet Restor Dent*, 27 Suppl 1, S1-9.
- PASHCHENKO, V., NESTEROV, A., BROVKINA, G., MIKHAILENKO, G. P., KLOCHAI, I. & LISOVSKII, A. 1995. Influence of the forming process and sintering conditions on the structure and properties of powder ferrite materials. *Powder Metallurgy and Metal Ceramics*, 33, 620-622.
- PASSERINI, L. 1939. Isomorphism among oxides of different tetravalent metals: CeO₂-ThO₂; CeO₂-ZrO₂; CeO₂-HfO₂. *Gazzet Chim Ital*, 60, 762-76.
- PASSOS, S. P., KIMPARA, E. T., BOTTINO, M. A., SANTOS, G. C., JR. & RIZKALLA, A. S. 2013. Effect of ceramic shade on the degree of conversion of a dual-cure resin cement analyzed by FTIR. *Dent Mater*, 29, 317-23.
- PAUL, S., PETER, A., PIETROBON, N. & HAMMERLE, C. H. 2002. Visual and spectrophotometric shade analysis of human teeth. *J Dent Res*, 81, 578-82.
- PAUL, S. J., PETER, A., RODONI, L. & PIETROBON, N. 2004. Conventional visual vs spectrophotometric shade taking for porcelain-fused-to-metal crowns: a clinical comparison. *The Journal of Prosthetic Dentistry*, 92, 577.
- PAZIN, M. C., MORAES, R. R., GONÇALVES, L. S., BORGES, G. A., SINHORETI, M. A. & CORRER-SOBRINHO, L. 2008. Effects of ceramic thickness and curing unit on light transmission through

- leucite-reinforced material and polymerization of dual-cured luting agent. *Journal of oral science*, 50, 131-136.
- PECHO, O. E., GHINEA, R., IONESCU, A. M., CARDONA JDE, L., PARAVINA, R. D. & PEREZ MDEL, M. 2012. Color and translucency of zirconia ceramics, human dentine and bovine dentine. *J Dent*, 40 Suppl 2, e34-40.
- PEELEN, J. & METSELAAR, R. 1974. Light scattering by pores in polycrystalline materials: Transmission properties of alumina. *Journal of Applied Physics*, 45, 216-220.
- PEIXOTO, R. T., PAULINELLI, V. M. F., SANDER, H. H., LANZA, M. D., CURY, L. A. & POLETTO, L. T. A. 2007. Light transmission through porcelain. *Dental Materials*, 23, 1363-1368.
- PEREIRA, P., INOKOSHI, S., YAMADA, T. & TAGAMI, J. 1998. Microhardness of in vitro caries inhibition zone adjacent to conventional and resin-modified glass ionomer cements. *Dental Materials*, 14, 179-185.
- PEUCHERT, U., OKANO, Y., MENKE, Y., REICHEL, S. & IKESUE, A. 2009. Transparent cubic-ZrO₂ ceramics for application as optical lenses. *Journal of the European Ceramic Society*, 29, 283-291.
- PICONI, C. & MACCAURO, G. 1999. Zirconia as a ceramic biomaterial. *Biomaterials*, 20, 1-25.
- PICONI, C., MACCAURO, G., MURATORI, F. & PREVER, E. 2003. Alumina and zirconia ceramics in joint replacements. *Journal of Applied Biomaterials & Biomechanics*, 1, 19-32.
- PILATHADKA, S., VAHALOVÁ, D. & VOSÁHLO, T. 2007. The Zirconia: a new dental ceramic material. An overview. *Prague Med Rep*, 108, 5-12.
- PILO, R. & CARDASH, H. 1992. Post-irradiation polymerization of different anterior and posterior visible light-activated resin composites. *Dental Materials*, 8, 299-304.
- PIRES, J. A. F., CVITKO, E., DENEHY, G. E. & SWIFT JR, E. J. 1993. Effects of curing tip distance on light intensity and composite resin microhardness. *Quintessence International*, 24.
- PITTAYACHAWAN, P. 2009. *Comparative study of physical properties of zirconia based dental ceramics*. UCL (University College London).
- PIWOWARCZYK, A., OTTL, P., LAUER, H. C. & KURETZKY, T. 2005. A clinical report and overview of scientific studies and clinical procedures conducted on the 3M ESPE Lava All-Ceramic System. *J Prosthodont*, 14, 39-45.
- POWERS, J. M., DENNISON, J. B. & LEPEAK, P. J. 1978. Parameters that affect the color of direct restorative resins. *Journal of Dental Research*, 57, 876-880.
- PREIS, V., BEHR, M., KOLBECK, C., HAHNEL, S., HANDEL, G. & ROSENTRITT, M. 2011. Wear performance of substructure ceramics and veneering porcelains. *Dent Mater*, 27, 796-804.
- PREIS, V., SCHMALZBAUER, M., BOUGEARD, D., SCHNEIDER-FEYRER, S. & ROSENTRITT, M. 2015. Surface properties of monolithic zirconia after dental adjustment treatments and in vitro wear simulation. *Journal of dentistry*, 43, 133-139.

- QUEIROZ, J. R., BENETTI, P., MASSI, M., JUNIOR, L. N. & DELLA BONA, A. 2012. Effect of multiple firing and silica deposition on the zirconia-porcelain interfacial bond strength. *Dent Mater*, 28, 763-8.
- QUINN, G. 1998. Hardness testing of ceramics. *Adv Mater Process* 154, 8-23.
- QUINN, J. B. & QUINN, G. D. 2010. A practical and systematic review of Weibull statistics for reporting strengths of dental materials. *Dent Mater*, 26, 135-47.
- RAGHAVAN, R. N. 2012. *Ceramics in Dentistry*, INTECH Open Access Publisher.
- RAIGRODSKI, A. J. 2004. Contemporary materials and technologies for all-ceramic fixed partial dentures: A review of the literature. *The Journal of Prosthetic Dentistry*, 92, 557-562.
- RAIGRODSKI, A. J., HILLSTEAD, M. B., MENG, G. K. & CHUNG, K.-H. 2012. Survival and complications of zirconia-based fixed dental prostheses: A systematic review. *The Journal of Prosthetic Dentistry*, 107, 170-177.
- RAKIĆ, A. D. 1995. Algorithm for the determination of intrinsic optical constants of metal films: application to aluminum. *Applied optics*, 34, 4755-4767.
- RANDALL, D. 1997. Instruments for the measurement of color. *Color Technology in the Textile Industry, Second Edition*, AATCC, 9-17.
- RAO, P., IWASA, M., WU, J., YE, J. & WANG, Y. 2004. Effect of Al₂O₃ addition on ZrO₂ phase composition in the Al₂O₃-ZrO₂ system. *Ceramics International*, 30, 923-926.
- RASETTO, F. H., DRISCOLL, C. F., PRESTIPINO, V., MASRI, R. & VON FRAUNHOFER, J. A. 2004. Light transmission through all-ceramic dental materials: a pilot study. *The Journal of Prosthetic Dentistry*, 91, 441-446.
- RAVISHANKAR, N. & CARTER, C. 1999. Application of SEM to the study of ceramic surfaces. *Revista Latinoamericana de Metalurgia y Materiales(Venezuela)*, 19, 7-12.
- REICH, S., WICHMANN, M., NKENKE, E. & PROESCHEL, P. 2005. Clinical fit of all-ceramic three-unit fixed partial dentures, generated with three different CAD/CAM systems. *European journal of oral sciences*, 113, 174-179.
- REIS, A. F., GIANNINI, M., LOVADINO, J. R. & AMBROSANO, G. M. 2003. Effects of various finishing systems on the surface roughness and staining susceptibility of packable composite resins. *Dental Materials*, 19, 12-18.
- RICHERSON, D. W. Modern ceramic engineering: properties, processing, and use in design, 1992. *There is no corresponding record for this reference*, 378.
- RICHERSON, D. W. 2005. *Modern ceramic engineering: properties, processing, and use in design*, CRC press.
- RIEDEL, R. & CHEN, I.-W. 2011. *Ceramics Science and Technology, Materials and Properties*, John Wiley & Sons.
- RIZKALLA, A. 2004. Indentation fracture toughness and dynamic elastic moduli for commercial feldspathic dental porcelain materials. *Dental Materials*, 20, 198-206.

- RODRIGUES, S. A., JR., FERRACANE, J. L. & DELLA BONA, A. 2008. Flexural strength and Weibull analysis of a microhybrid and a nanofill composite evaluated by 3- and 4-point bending tests. *Dent Mater*, 24, 426-31.
- ROSENTRITT, M., PREIS, V., BEHR, M., HAHNEL, S., HANDEL, G. & KOLBECK, C. 2012. Two-body wear of dental porcelain and substructure oxide ceramics. *Clin Oral Investig*, 16, 935-43.
- ROUFS, J. 1978. Light as a true visual quantity: principles of measurement.
- ROY, M. E., WHITESIDE, L. A., KATERBERG, B. J. & STEIGER, J. A. 2007. Phase transformation, roughness, and microhardness of artificially aged yttria- and magnesia-stabilized zirconia femoral heads. *J Biomed Mater Res A*, 83, 1096-102.
- RUEGGERBERG, F. & CAUGHMAN, W. F. 1993. The influence of light exposure on polymerization of dual-cure resin cements. *Operative Dentistry*, 18, 48-55.
- RUFF, O., EBERT, F. & STEPHEN, E. 1929. Contributions to the ceramics of highly refractory materials: li. System zirconia-lime. *Z Anorg Allg Chem*, 180, 215-24.
- SAKAGUCHI, R. L. & POWERS, J. M. 2012. *Craig's restorative dental materials*, Elsevier Health Sciences.
- SAMODUROVA, A., KOCJAN, A., SWAIN, M. V. & KOSMAC, T. 2015. The combined effect of alumina and silica co-doping on the ageing resistance of 3Y-TZP bioceramics. *Acta Biomater*, 11, 477-87.
- SANON, C., CHEVALIER, J., DOUILLARD, T., KOHAL, R. J., COELHO, P. G., HJERPPE, J. & SILVA, N. R. 2013. Low temperature degradation and reliability of one-piece ceramic oral implants with a porous surface. *Dent Mater*, 29, 389-97.
- SCHERRER, S. S., QUINN, G. D. & QUINN, J. B. 2008. Fractographic failure analysis of a Procera AllCeram crown using stereo and scanning electron microscopy. *Dent Mater*, 24, 1107-13.
- SCHMAUDER, S. & SCHUBERT, H. 1986. Significance of Internal Stresses for the Martensitic Transformation in Yttria-Stabilized Tetragonal Zirconia Polycrystals During Degradation. *Journal of the American Ceramic Society*, 69, 534-540.
- SCHMITTER, M., MUSSOTTER, K., RAMMELSBERG, P., STOBBER, T., OHLMANN, B. & GABBERT, O. 2009. Clinical performance of extended zirconia frameworks for fixed dental prostheses: two-year results. *J Oral Rehabil*, 36, 610-5.
- SCOTT, H. 1975. Phase Relationships in the ZrO₂-Y₂O₃ System. *J. Mater. Sci*, 10, 1527-35.
- SEGHI, R. R., JOHNSTON, W. M. & O'BRIEN, W. J. 1986. Spectrophotometric analysis of color differences between porcelain systems. *The Journal of Prosthetic Dentistry*, 56, 35-40.
- SHAH, K., HOLLOWAY, J. A. & DENRY, I. L. 2008. Effect of coloring with various metal oxides on the microstructure, color, and flexural strength of 3Y-TZP. *J Biomed Mater Res B Appl Biomater*, 87, 329-37.
- SHAHMIRI, R., STANDARD, O. C., HART, J. N. & SORRELL, C. C. 2017. Optical properties of zirconia ceramics for esthetic dental restorations: A systematic review. *J Prosthet Dent*.
- SHEN, J. 2013. *Advanced ceramics for dentistry*, Butterworth-Heinemann.

- SHINKAI, R., CURY, A. & CURY, J. 2001. In vitro evaluation of secondary caries development in enamel and root dentin around luted metallic restoration. *Oper Dent*, 26, 52-9.
- SHOKRY, T. E., SHEN, C., ELHOSARY, M. M. & ELKHODARY, A. M. 2006. Effect of core and veneer thicknesses on the color parameters of two all-ceramic systems. *The Journal of prosthetic dentistry*, 95, 124-129.
- SIARAMPI, E., KONTONASAKI, E., ANDRIKOPOULOS, K. S., KANTIRANIS, N., VOYIATZIS, G. A., ZORBA, T., PARASKEVOPOULOS, K. M. & KOIDIS, P. 2014. Effect of in vitro aging on the flexural strength and probability to fracture of Y-TZP zirconia ceramics for all-ceramic restorations. *Dent Mater*, 30, e306-16.
- SILVA, N. R., BONFANTE, E. A., ZAVANELLI, R. A., THOMPSON, V. P., FERENCZ, J. L. & COELHO, P. G. 2010. Reliability of metaloceramic and zirconia-based ceramic crowns. *J Dent Res*, 89, 1051-6.
- SOLDERA, F. A., GAILLARD, Y., GOMILA, M. A. & MUECKLICH, F. 2007. FIB-Tomography of Nanoindentation Cracks in Zirconia Polycrystals. *Microscopy and Microanalysis*, 13.
- SPINK, L. 2009. A Comparison of Absolute Translucency and Relative Translucency of Dental Ceramics.
- SPINK, L. S., RUNGRUANGANUT, P., MEGREMIS, S. & KELLY, J. R. 2013. Comparison of an absolute and surrogate measure of relative translucency in dental ceramics. *Dental Materials*, 29, 702-707.
- SPROULL, R. C. 1973a. Color matching in dentistry. Part I. The three-dimensional nature of color. *The Journal of prosthetic dentistry*, 29, 416-424.
- SPROULL, R. C. 1973b. Color matching in dentistry. Part II. Practical applications of the organization of color. *The Journal of prosthetic dentistry*, 29, 556-566.
- SPROULL, R. C. 1974. Color matching in dentistry. Part III. Color control. *The Journal of prosthetic dentistry*, 31, 146-154.
- SRIAMPORN, T., THAMRONGANANSKUL, N., BUSABOK, C., POOLTHONG, S., UO, M. & TAGAMI, J. 2014. Dental zirconia can be etched by hydrofluoric acid. *Dental Materials Journal*, 33, 79-85.
- STAWARCZYK, B., OZCAN, M., HALLMANN, L., ENDER, A., MEHL, A. & HAMMERLET, C. H. 2013. The effect of zirconia sintering temperature on flexural strength, grain size, and contrast ratio. *Clin Oral Investig*, 17, 269-74.
- STOBER, T., BERMEJO, J. L., RAMMELSBERG, P. & SCHMITTER, M. 2014. Enamel wear caused by monolithic zirconia crowns after 6 months of clinical use. *J Oral Rehabil*, 41, 314-22.
- STOKES, D. 2008. *Principles and practice of variable pressure: environmental scanning electron microscopy (VP-ESEM)*, John Wiley & Sons.
- SUBASI, M. G. & INAN, O. 2012. Evaluation of the topographical surface changes and roughness of zirconia after different surface treatments. *Lasers Med Sci*, 27, 735-42.
- SUBBARAO, E., MAITI, H. & SRIVASTAVA, K. 1974. Martensitic transformation in zirconia. *Physica status solidi (a)*, 21, 9-40.
- SUCCARIA, F. & MORGANO, S. M. 2011. Prescribing a dental ceramic material: Zirconia vs lithium-disilicate. *Saudi Dent J*, 23, 165-6.

- SUKUMARAN, V. & BHARADWAJ, N. 2006. Ceramics in dental applications. *Trends in Biomaterials and Artificial Organs*, 20, 7-11.
- SULAIMAN, T. A., ABDULMAJEED, A. A., DONOVAN, T. E., RITTER, A. V., VALLITTU, P. K., NARHI, T. O. & LASSILA, L. V. 2015a. Optical properties and light irradiance of monolithic zirconia at variable thicknesses. *Dent Mater*, 31, 1180-7.
- SULAIMAN, T. A., ABDULMAJEED, A. A., DONOVAN, T. E., VALLITTU, P. K., NARHI, T. O. & LASSILA, L. V. 2015b. The effect of staining and vacuum sintering on optical and mechanical properties of partially and fully stabilized monolithic zirconia. *Dent Mater J*, 34, 605-10.
- SULAIMAN, T. A., DELGADO, A. J. & DONOVAN, T. E. 2015c. Survival rate of lithium disilicate restorations at 4 years: A retrospective study. *J Prosthet Dent*, 114, 364-6.
- SUN, T., ZHOU, S., LAI, R., LIU, R., MA, S., ZHOU, Z. & LONGQUAN, S. 2014. Load-bearing capacity and the recommended thickness of dental monolithic zirconia single crowns. *Journal of the mechanical behavior of biomedical materials*, 35, 93-101.
- SUNDH, A. & SJÖGREN, G. 2006. Fracture resistance of all-ceramic zirconia bridges with differing phase stabilizers and quality of sintering. *Dental materials*, 22, 778-784.
- SUTTOR, D., BUNKE, K., HOESCHELER, S., HAUPTMANN, H. & HERTLEIN, G. 2001. LAVA--the system for all-ceramic ZrO₂ crown and bridge frameworks. *International journal of computerized dentistry*, 4, 195-206.
- SWAIN, M. V. 2009. Unstable cracking (chipping) of veneering porcelain on all-ceramic dental crowns and fixed partial dentures. *Acta Biomater*, 5, 1668-77.
- SWAIN, M. V. 2014. Impact of oral fluids on dental ceramics: what is the clinical relevance? *Dental Materials*, 30, 33-42.
- TAN, J. P., SEDERSTROM, D., POLANSKY, J. R., MCLAREN, E. A. & WHITE, S. N. 2012. The use of slow heating and slow cooling regimens to strengthen porcelain fused to zirconia. *The Journal of Prosthetic Dentistry*, 107, 163-169.
- TANDON, R., GUPTA, S. & AGARWAL, S. K. 2010. Denture base materials: From past to future. *Indian J Dent Sci*, 2, 33-39.
- TANOUE, N., KOISHI, Y., ATSUTA, M. & MATSUMURA, H. 2003. Properties of dual-curable luting composites polymerized with single and dual curing modes. *Journal of oral rehabilitation*, 30, 1015-1021.
- TAYLOR, J. A. 1922. *History of dentistry: A practical treatise for the use of dental students and practitioners*, Lea & Febiger.
- THOLEY, M. J., SWAIN, M. V. & THIEL, N. 2009. SEM observations of porcelain Y-TZP interface. *Dent Mater*, 25, 857-62.
- THOMPSON, J. Y., STONER, B. R., PIASCNIK, J. R. & SMITH, R. 2011. Adhesion/cementation to zirconia and other non-silicate ceramics: where are we now? *Dent Mater*, 27, 71-82.
- TINSCHERT, J., NATT, G., MAUTSCH, W., SPIEKERMANN, H. & ANUSAVICE, K. 2001. Marginal fit of alumina-and zirconia-based fixed partial dentures produced by a CAD/CAM system. *Operative dentistry*, 26, 367-374.

- TINSCHERT, J., ZWEZ, D., MARX, R. & ANUSAVICE, K. 2000. Structural reliability of alumina-, feldspar-, leucite-, mica- and zirconia-based ceramics. *Journal of dentistry*, 28, 529-535.
- TSUKUMA, K., YAMASHITA, I. & KUSUNOSE, T. 2008. Transparent 8 mol% Y₂O₃-ZrO₂(8Y) Ceramics. *Journal of the American Ceramic Society*, 91, 813-818.
- UHL, A., MILLS, R. W. & JANDT, K. D. 2003. Photoinitiator dependent composite depth of cure and Knoop hardness with halogen and LED light curing units. *Biomaterials*, 24, 1787-1795.
- UHL, A., MILLS, R. W., VOWLES, R. W. & JANDT, K. D. 2002. Knoop hardness depth profiles and compressive strength of selected dental composites polymerized with halogen and LED light curing technologies. *Journal of Biomedical Materials Research Part A*, 63, 729-738.
- UMERI, A. 2010. Study of Zirconia's ageing for applications in dentistry.
- VAGKOPOULOU, T., KOUTAYAS, S. O., KOIDIS, P. & STRUB, J. R. 2009. Zirconia in dentistry: Part 1. Discovering the nature of an upcoming bioceramic. *European Journal of Esthetic Dentistry*, 4.
- VANASUPA, L., JOO, Y.-C., BESSER, P. R. & PRAMANICK, S. 1999. Texture analysis of damascene-fabricated Cu lines by x-ray diffraction and electron backscatter diffraction and its impact on electromigration performance. *Journal of Applied Physics*, 85, 2583-2590.
- VAREZ, A., GARCIA-GONZALEZ, E., JOLLY, J. & SANZ, J. 2007. Structural characterization of Ce_{1-x}Zr_xO₂ (0 ≤ x ≤ 1) samples prepared at 1650 °C by solid state reaction. *Journal of the European Ceramic Society*, 27, 3677-3682.
- VATALI, A., KONTONASAKI, E., KAVOURAS, P., KANTIRANIS, N., PAPADOPOULOU, L., PARASKEVOPOULOS, K. K. & KOIDIS, P. 2014. Effect of heat treatment and in vitro aging on the microstructure and mechanical properties of cold isostatic-pressed zirconia ceramics for dental restorations. *Dent Mater*, 30, e272-82.
- VICHI, A., CARRABBA, M., PARAVINA, R. & FERRARI, M. 2014. Translucency of ceramic materials for CEREC CAD/CAM system. *J Esthet Restor Dent*, 26, 224-31.
- VICHI, A., FERRARI, M. & DAVIDSON, C. L. 2004. Color and opacity variations in three different resin-based composite products after water aging. *Dent Mater*, 20, 530-4.
- VICHI, A., LOUCA, C., CORCIOLANI, G. & FERRARI, M. 2011. Color related to ceramic and zirconia restorations: a review. *Dent Mater*, 27, 97-108.
- VOLPATO, C., PHILIPPI, A., PETTER, C. & FREDEL, M. 2010. *Ceramic materials and color in dentistry*, INTECH Open Access Publisher.
- VOLPATO, C. Â. M., ALTOÉ GARBELOTTO, L. G. D., FREDEL, M. C. & BONDIOLI, F. 2011. Application of zirconia in dentistry: biological, mechanical and optical considerations. *Advances in ceramics-electric and magnetic ceramics, bioceramics, ceramics and environment*. InTech.
- WACHTMAN, J. B., CANNON, W. R. & MATTHEWSON, M. J. 2009. *Mechanical properties of ceramics*, John Wiley & Sons.

- WANG, F., TAKAHASHI, H. & IWASAKI, N. 2013. Translucency of dental ceramics with different thicknesses. *The Journal of Prosthetic Dentistry*, 110, 14-20.
- WANG, H., ABOUSHELIB, M. N. & FEILZER, A. J. 2008. Strength influencing variables on CAD/CAM zirconia frameworks. *Dent Mater*, 24, 633-8.
- WANG, J., LI, S. & STEVENS, R. 1992. Effects of organic binders on the sintering of isostatically compacted zirconia powders. *Journal of materials science*, 27, 63-67.
- WANG, L., D'ALPINO, P. H. P., LOPES, L. G. & PEREIRA, J. C. 2003. Mechanical properties of dental restorative materials: relative contribution of laboratory tests. *Journal of Applied Oral Science*, 11, 162-167.
- WANG, Y. 2014. *Use of confinement and additives to control inorganic crystallization*, University of Leeds.
- WATTS, A. & ADDY, M. 2001. Tooth discolouration and staining: Tooth discolouration and staining: a review of the literature. *British dental journal*, 190, 309-316.
- WEIBULL, W. 1939. A statistical theory of the strength of materials. *Ingeniors Vetenskaps Akademien*.
- WEIBULL, W. 1951. Wide applicability. *Journal of applied mechanics*, 103, 293-297.
- WHITEHEAD, S., SHEARER, A., WATTS, D. & WILSON, N. 1995. Comparison of methods for measuring surface roughness of ceramic. *Journal of Oral Rehabilitation*, 22, 421-427.
- WONGKAMHAENG, K. 2016. *Effect of chairside surface treatments on biaxial flexural strength and subsurface damage in monolithic zirconia for dental applications*. The University of Iowa.
- WURST, J. & NELSON, J. 1972. Lineal Intercept Technique for Measuring Grain Size in Two-Phase Polycrystalline Ceramics. *Journal of the American Ceramic Society*, 55, 109-109.
- X-RITE 2016. A Guide to Understanding Color. In: LTD, X.-R. C. (ed.) *X-Rite PANTONE*. USA: X-Rite .com.
- XU, X. F., PARKINSON, A., BATES, P. J. & ZAK, G. 2015a. Effect of part thickness, glass fiber and crystallinity on light scattering during laser transmission welding of thermoplastics. *Optics & Laser Technology*, 75, 123-131.
- XU, Y., HAN, J., LIN, H. & AN, L. 2015b. Comparative study of flexural strength test methods on CAD/CAM Y-TZP dental ceramics. *Regen Biomater*, 2, 239-44.
- YAMASHITA, I., NAGAYAMA, H. & TSUKUMA, K. 2008. Transmission Properties of Translucent Polycrystalline Alumina. *Journal of the American Ceramic Society*, 91, 2611-2616.
- YAMASHITA, I. & TSUKUMA, K. 2011. Light scattering by residual pores in transparent zirconia ceramics. *Journal of the Ceramic Society of Japan*, 119, 133-135.
- YASHIMA, M., SASAKI, S., KAKIHANA, M., YAMAGUCHI, Y., ARASHI, H. & YOSHIMURA, M. 1994. Oxygen-induced structural change of the tetragonal phase around the tetragonal-cubic phase boundary in ZrO₂-YO_{1.5} solid solutions. *Acta Crystallographica Section B: Structural Science*, 50, 663-672.

- YILMAZ, H., AYDIN, C. & GUL, B. E. 2007. Flexural strength and fracture toughness of dental core ceramics. *The Journal of Prosthetic Dentistry*, 98, 120-128.
- YOSHIMURA, M., NOMA, T., KAWABATA, K. & SŌMIYA, S. 1987. Role of H₂O on the degradation process of Y-TZP. *Journal of Materials Science Letters*, 6, 465-467.
- YU, B., AHN, J.-S. & LEE, Y.-K. 2009. Measurement of translucency of tooth enamel and dentin. *Acta Odontologica Scandinavica*, 67, 57-64.
- YU, B. & LEE, Y.-K. 2008. Translucency of varied brand and shade of resin composites. *Am J Dent*, 21, 229-32.
- ZALEWSKI, E. F. 1995. Radiometry and photometry. *Handbook of optics*, 2, 24.1-24.51.
- ZHANG, F., CHEVALIER, J., OLAGNON, C., BATUK, M., HADERMANN, J., VAN MEERBEEK, B. & VLEUGELS, J. 2017. Grain-Boundary Engineering for Aging and Slow-Crack-Growth Resistant Zirconia. *J Dent Res*, 96, 774-779.
- ZHANG, F., INOKOSHI, M., BATUK, M., HADERMANN, J., NAERT, I., VAN MEERBEEK, B. & VLEUGELS, J. 2016. Strength, toughness and aging stability of highly-translucent Y-TZP ceramics for dental restorations. *Dent Mater*, 32, e327-e337.
- ZHANG, F., VANMEENSEL, K., BATUK, M., HADERMANN, J., INOKOSHI, M., VAN MEERBEEK, B., NAERT, I. & VLEUGELS, J. 2015. Highly-translucent, strong and aging-resistant 3Y-TZP ceramics for dental restoration by grain boundary segregation. *Acta Biomater*, 16, 215-22.
- ZHANG, H., KIM, B.-N., MORITA, K., YOSHIDA, H., LIM, J.-H. & HIRAGA, K. 2010. Optimization of high-pressure sintering of transparent zirconia with nano-sized grains. *Journal of Alloys and Compounds*, 508, 196-199.
- ZHANG, H., KIM, B. N., MORITA, K., KEIJIRO HIRAGA, H. Y. & SAKKA, Y. 2011. Effect of sintering temperature on optical properties and microstructure of translucent zirconia prepared by high-pressure spark plasma sintering. *Sci Technol Adv Mater*, 12, 055003.
- ZHANG, H., LI, Z., KIM, B.-N., MORITA, K., YOSHIDA, H., HIRAGA, K. & SAKKA, Y. 2012. Effect of Alumina Dopant on Transparency of Tetragonal Zirconia. *Journal of Nanomaterials*, 2012, 1-5.
- ZHANG, N. & ASLE ZAEEM, M. 2017. Effects of specimen size and yttria concentration on mechanical properties of single crystalline yttria-stabilized tetragonal zirconia nanopillars. *Journal of Applied Physics*, 122, 014302.
- ZHANG, Y. 2014. Making yttria-stabilized tetragonal zirconia translucent. *Dent Mater*, 30, 1195-203.